TURKEY-ADJUSTED NEXT GENERATION ATTENUATION MODELS

A THESIS SUBMITTED TO
THE GRADUATE SCHOOL OF NATURAL AND APPLIED SCIENCES
OF
MIDDLE EAST TECHNICAL UNIVERSITY

BY

BAHADIR KARGIOĞLU

IN PARTIAL FULFILLMENT OF THE REQUIREMENTS
FOR
THE DEGREE OF THE MASTER OF SCIENCE
IN
CIVIL ENGINEERING

SEPTEMBER 2012

Approval of the thesis:

TURKEY-ADJUSTED NEXT GENERATION ATTENUATION MODELS

submitted by **BAHADIR KARGIOĞLU** in partial fulfillment of the requirements for the degree of **Master of Science in Civil Engineering Department, Middle East Technical University** by,

Prof. Dr. Canan Özgen _____
Dean, Graduate School of **Natural and Applied Science**

Prof. Dr. Güney Özcebe _____
Head of Department, **Civil Engineering**

Asst. Prof. Dr. Zeynep Gülerce _____
Supervisor, **Civil Engineering Dept., METU**

Examining Committee Members:

Prof. Dr. Erdal Çokça _____
Civil Engineering Dept., METU

Asst. Prof. Dr. Zeynep Gülerce _____
Civil Engineering Dept., METU

Prof. Dr. Kemal Önder Çetin _____
Civil Engineering Dept., METU

Prof. Dr. Sinan Akkar _____
Civil Engineering Dept., METU

Dr. Nazan Kılıç _____
Disaster and Emergency Management Presidency
(AFAD)

Date: **12.09.2012**

I hereby declare that all information in this document has been obtained and presented in accordance with academic rules and ethical conduct. I also declare that, as required by these rules and conduct, I have fully cited and referenced all material and results that are not original to this work.

Name, Last name : Bahadır Kargıoğlu

Signature :

ABSTRACT

TURKEY-ADJUSTED NEXT GENERATION ATTENUATION MODELS

Kargıoğlu, Bahadır

M.S., Department of Civil Engineering

Supervisor: Asst. Prof. Dr. Zeynep Gülerce

September 2012, 127 pages

The objective of this study is to evaluate the regional differences between the worldwide based NGA-W1 ground motion models and available Turkish strong ground motion dataset and make the required adjustments in the NGA-W1 models. A strong motion dataset using parameters consistent with the NGA ground motion models is developed by including strong motion data from Turkey. Average horizontal component ground motion is computed for response spectral values at all available periods using the $GMRotI_{50}$ definition consistent with the NGA-W1 models. A random-effects regression with a constant term only is used to evaluate the systematic differences in the average level of shaking. Plots of residuals are used to evaluate the differences in the magnitude, distance, and site amplification scaling between the Turkish dataset and the NGA-W1 models. Model residuals indicated that the ground motions are overestimated by all 5 NGA-W1 models significantly, especially for small-to-moderate magnitude earthquakes. Model residuals relative to distance measures plots suggest that NGA-W1 models slightly underestimates the ground motions for rupture distances within 100-200 km range. Models including the aftershocks over-predict the ground motions at stiff soil/engineering rock sites. The misfit between the actual data and model predictions are corrected with adjustments functions for each scaling term.

Turkey-Adjusted NGA-W1 models proposed in this study are compatible with the Turkish strong ground motion characteristics and preserve the well-constrained features of the global models. Therefore these models are suitable candidates for ground motion characterization and PSHA studies conducted in Turkey.

Keywords: Probabilistic seismic hazard assessment, ground motion prediction models, ground motion characterization, regional tectonic effects, Turkish strong ground motions

ÖZ

GLOBAL YENİ NESİL TAHMİN DENKLEMLERİNİN TÜRKİYE'YE UYARLANMASI

Kargıoğlu, Bahadır
Yüksek Lisans, İnşaat Mühendisliği Bölümü
Tez Yöneticisi: Yrd. Doç. Dr. Zeynep Gülerce

Eylül 2012, 127 sayfa

Bu çalışmanın amacı global bir veri tabanına dayalı yeni nesil kuvvetli yer hareketi tahmin denklemleri ile Türkiye'de kaydedilen kuvvetli yer hareketi kayıtlarını karşılaştırarak olası bölgesel farklılıkları belirlemek ve modellere gerekli düzeltmeleri uygulamaktır. Türkiye'de gerçekleşen depremlerden alınan kayıtlar kullanılarak, yeni nesil tahmin denklemleri veri tabanı ile aynı parametreleri içeren bir veri tabanı hazırlanmıştır. Ortalama yatay yer hareketleri, G_{mrotI} yöntemi kullanılarak davranış spektrumunda mevcut tüm devir (periyot) değerleri için hesaplanmıştır. Gelişigüzel (random) etkiler çoklu regresyon yöntemi kullanılarak Türk deprem veri tabanı ile yeni nesil tahmin denklemleri arasındaki olası farklılıklar istatistiksel değerlendirmeye tabi tutulmuştur. Türk deprem veri tabanı ile yeni nesil tahmin denklemleri arasındaki farklar, deprem büyüklüğü, fay uzaklığı ve zemin büyütme parametreleri ile karşılaştırılmıştır. Yeni nesil tahmin denklemlerinin tamamı, özellikle küçük ve orta ölçekli depremlerde, normalden yüksek ivme değerleri hesaplamıştır. Model farkları ile fay uzaklığı ilişki grafiği incelenmiş olup, yeni nesil tahmin denklemlerinin, yalnızca fay uzaklığı 100 ile 200 kilometre arasında eğilim barındırdığı gözlemlenmiştir. Artçı depremleri veri tabanında barındıran tahmin denklemleri, özellikle kaya türü zeminlerde, beklenenden

daha yüksek değerler hesaplamaktadır. Gözlemlenen model farkları, her parametre için düzeltme fonksiyonu kullanarak giderilmiştir. Türk deprem veri tabanı ile uyumlu hale getirilen bu tahmin denklemlerinin, Türkiye'de yapılacak olasılıksal sismik tehlike analizi için uygun olduğu kanaatine varılmıştır.

Anahtar Kelimeler: Olasılıksal sismik tehlike analizi, yer hareketi tahmin denklemleri, yer hareketi tanımlamaları, bölgesel tektonik etkiler, Türk deprem veri tabanı

To My Beloved Family

ACKNOWLEDGEMENTS

I would like to thank my advisor Asst. Prof. Dr. Zeynep Gülerce for her guidance and support throughout the preparation of this thesis. I would also like to thank Dr. Norman Abrahamson, for his invaluable guidance in residual analysis and providing the comparison code.

I respectfully commemorate my grandmother Hatice Kaçar who we have lost during the study of my Master's degree.

At last for this study but not the least for my life, sincere thanks to my beloved family Fatma Kargıoğlu, Ali Kargıoğlu and Onur Kargıoğlu grow me up until now and who do not avoid their help, support, guidance, understanding and protection at any time during my life.

TABLE OF CONTENTS

LIST OF TABLES

TABLES

LIST OF FIGURES

FIGURES

CHAPTER 1

INTRODUCTION

Turkey's national border is located in one of the world's most active tectonic regions. Strain energy accumulating along the major fault systems of Turkey due to the westward-moving Anatolian Block resulted in many large and destructive earthquakes in the past and future large earthquakes to relieve this continually accumulating strain are a certainty. Increasing number of special projects such as nuclear power plants, bridges and high-rise structures in the past decade calls for comprehensive evaluation of the seismic hazard and risk in Turkey. Slowly, prevalent method for conducting seismic hazard assessment has shifted from deterministic approach to the probabilistic one around the globe. Probabilistic seismic hazard assessment (PSHA) approach allows the experts to consider the uncertainties in the size, location and rate of recurrence of earthquakes and in the variation of ground motion characteristics explicitly in the evaluation of seismic hazards (Kramer, 1996). These aspects make the PSHA studies a more complete and reliable way of assessing the seismic hazard.

PSHA methodology and the main components of the PSHA framework are rapidly evolving with the increasing number of ground motion characterization efforts for special structures and awareness of earthquake risk reduction around the world. The ground motion prediction equations (GMPEs) are used to estimate the ground motion parameters for the earthquake scenarios from each source in PSHA. These equations use statistical models based on

physical characteristics of ground motions to predict the ground motion intensities in terms of source (magnitude, depth, style-of faulting, etc.), path (distance, etc.) and site (site conditions, basin effects, etc.) parameters. The uncertainty introduced by the ground motion prediction models is significantly higher than any other parameter model included in the hazard integral; therefore selection of proper GMPEs for the region have a significant effect on the total hazard calculated at the site.

Next Generation Attenuation (NGA-W1) models are new and improved in terms of additional prediction parameters (such as depth of the source, basin effects, magnitude dependent standard deviations, etc.), statistical approach, and a well constrained global database. The applicability of the advances in these fields, especially the NGA-W1 models developed for California (US), is a controversial topic for PSHA studies conducted in Turkey mainly due to the lack of local information on parameters used in these models. Recently, an extensive project on Turkish strong motion recordings was performed and the established database of Turkish strong motions published by this project make it possible to check the compatibility of Turkish strong ground motion characteristics with global prediction models.

1.1 Research Statement and Motivation

The objective of this study is to evaluate the regional differences between the worldwide based NGA-W1 ground motion model predictions and Turkish strong ground motion dataset. Turkish strong ground motion data may show a divergence from the NGA model predictions since the ground motions recorded in the events occurred in Turkey were poorly represented in NGA-W1 database. Differences between the comparison dataset and NGA-W1 model predictions are evaluated in terms of magnitude, distance and site effect terms and these terms are modified when necessary to validate the applicability of the NGA-W1 models in the probabilistic seismic hazard assessment (PSHA) studies conducted in Turkey. Adjusting the global models according to the regional tectonic characteristics allow the user to

keep the well-constrained features of the global models such as large magnitude, distance and hanging wall scaling while reflecting the regional ground motion characteristics.

Compiling a high quality and well-constrained dataset of Turkish ground motions is the most vital part of this study. Largest project on the Turkish seismic catalogue and strong motion database in the last 50 years, “Compilation of Turkish strong motion network according to the international standards” (abbreviated as TSMD from now on) project, was finalized in 2008, providing a precious starting point for any ground motion characterization study in Turkey. TSMD database is selected and used as the preliminary dataset, however many efforts are made to estimate the missing parameters required for comparison with the NGA-W1 predictive models, to screen the ground motion waveforms for data quality and to calculate the orientation-independent intensity measures.

The preferred methodology for evaluating the differences between the model predictions and actual data is the analysis of model residuals. Using the random-effects regression with a constant term, model residuals between the actual strong motion data and NGA-W1 model predictions are calculated for each recording in the comparison dataset. Plots of the residuals are used to evaluate the differences in the magnitude, distance, and site amplification scaling between the Turkish data set and the NGA-W1 models. Model residuals indicated that the ground motions in the dataset are overestimated by all 5 NGA-W1 models especially for small-to-moderate magnitude earthquakes. The misfit between the actual data and model predictions are corrected with adjustments functions preserving the well-constrained large magnitude parameters of the models. Model residuals relative to distance measures plots suggest no trend within the applicability range of the NGA-W1 models for tectonic regions other than Western US (100 kilometers, Power et al., 2008), however NGA-W1 models slightly underestimates the ground motions in the comparison dataset for rupture distances within 100-

200 km range. Adjustment functions are added to the large distance terms of Abrahamson and Silva (2008) and Chiou and Youngs (2008) models since other models do not consider large distance effects. Models including the aftershocks under-predicts the ground motions in the comparison dataset at stiff soil/engineering rock sites but this effect diminishes as Vs30 decreases, therefore site effects terms of these models are modified. Reason of these trends is attributed to inclusion of aftershock events from Taiwan in these models.

The work described here is the first study that adjusts global GMPEs to Turkey. Similar studies are conducted within last 5 years for various tectonic regions. It is expected that this study will set a precedent for the adjustment works that will conducted for different regions. Result of this study, is expected to provide suitable candidates for ground motion characterization and PSHA studies conducted in Turkey.

1.2 Scope

The scope of this thesis can be summarized as follows;

In the first chapter general information about the concepts reviewed in this study are revisited. Research statement, motivation and the scope of this study is presented.

In Chapter 2, the previous ground motion prediction modeling efforts in global and regional scale are reviewed. Recent studies on the regional compatibility of NGA-W1 models are summarized.

In Chapter 3, a comprehensive summary of the changes on the initial TSMD dataset, efforts on estimating the missing parameters required for comparison with the NGA-W1 predictive models, calculation of the orientation-independent intensity measures, and final comparison dataset is presented.

In Chapter 4, presents the applied methodology for checking the compatibility of magnitude scaling, distance scaling and site effects scaling of NGA-W1 models with that of Turkish strong motion comparison dataset.

Chapter 5 encloses the thesis by presenting the final forms of the Turkey-Adjusted models and comparing the proposed models with original NGA-W1 models and Turkish GMPEs.

CHAPTER 2

PREVIOUS EFFORTS ON GROUND MOTION PREDICTION EQUATIONS IN GLOBAL AND REGIONAL SCALE

In probabilistic seismic hazard assessment framework, the ground motion prediction equations (GMPEs) are used to estimate the ground motion intensity measures for the earthquake scenarios. GMPEs introduce the biggest uncertainty in the hazard calculations so they have a significant effect on the total hazard at the site. Many GMPEs are available in the literature, global ground motion models representing the shallow crustal earthquakes in active tectonic regions and local ground motion models developed for specific areas. Choosing the ground motion model from one of these groups is a controversial topic since both groups has its own advantages and disadvantages.

The local ground motion prediction equations are developed from the regional databases therefore they reflect the regional tectonic differences better than the global models. However, since they are based on limited and small datasets, regional models may not constrain some important features represented in global models effectively. Global GMPEs based on large and well-constrained datasets but they may require adjustments to represent the local tectonic characteristics. One way to facilitate the use of global GMPEs in specific regions is to check the compatibility of these models with regional

datasets. For this purpose, applicability of the NGA-W1 models has been studied extensively since these models were proposed in 2008; however general consensus on this matter was not reached yet.

This chapter starts with general information on the main features of ground motion prediction modeling, and then previous models proposed by NGA model developing teams were introduced. Next Generation Attenuation (NGA-W1) project and NGA-W1 models are discussed briefly in the following section. Turkish practice in ground motion prediction modeling and Turkish ground motion models are included to this chapter for comparison. Finally, recent studies on the regional compatibility of NGA-W1 models are summarized.

2.1 Early-Stage Attenuation Models of North America Developed for Shallow Crustal Earthquakes in Active Tectonic Regions

GMPEs use physical-based statistical models to predict the ground motion intensities in terms of source (magnitude, depth, style-of faulting, etc.), path (distance, etc.) and site (site conditions, basin effects, etc.) parameters. Typical formulation of early-stage (before the year 2000) GMPEs are:

$$Ln\,Y = c_1 + c_2 M + c_3 M^2 + c_4 \ln(R + c_5) + c_6 F + c_7 S \qquad (2.1)$$

where c_1-c_7 are model constants calculated during the regression analysis, M is the magnitude, R is distance, F and S are dummy variables representing the style-of-faulting and site effects. Y represents the ground motion intensity measure which is defined by the peak ground acceleration or spectral acceleration of the largest horizontal component or geometric mean of the two-horizontal components. In early-stage models, no data selection criteria were applied to the dataset, simply because the number of recordings was not sufficient. Parallel to increase in number of recordings, the weights of different events in terms of number of recordings were found to have a significant effect in regression analysis. Two different weighing procedures were proposed to take care of this hitch: two-stage regression procedure

(Joyner and Boore, 1993) and the random effects model (Abrahamson and Youngs, 1992) which based on the regression method developed by Brillinger and Priesler (1984, 1985). Today more than hundreds of GMPEs are available for shallow crustal earthquakes in active tectonic regions. Only the GMPEs developed by the NGA model developers in the past are introduced here to stand for the early-stage predictive models.

Abrahamson and Silva (1997) used 655 recordings obtained from 58 earthquakes occurred mainly in Western US. Moment magnitude and closest distance to the rupture (R_{rup}) were used in the basic model for strike-slip earthquakes. To characterize the site effects, Geomatrix site class definitions were modified and reduced into 2 different site categories: rock site and deep soil site. Random effects model proposed by Abrahamson and Youngs (1992) was employed in regression. In addition to the basic model (f_1 in Equation 2.2), style-of-faulting, hanging wall and site response effects were included using dummy variables as:

$$\ln Sa = f_1(M, r_{rup}) + F\, f_3(M) + HW f_4\big(M, r_{rup}\big) + S\, f_5(\widehat{pga}_{rock}) \qquad (2.2)$$

where Sa is spectral acceleration, M is moment magnitude, R_{rup} is rupture distance, F is style of faulting, HW is dummy for hanging wall site, S is dummy for site class, f_1 is the basic functional form of attenuation relation, $f_3 and f_5$ represent the functional form for style of faulting and site effects, $f_{HW}(M)$ and $f_{HW}\big(R_{rup}\big)$ are the models to account for the systematic increase in the ground motions recorded over the hanging wall.

Boore et al. (1997) derived their prediction equation using 112 recordings obtained from 14 earthquakes. The recordings obtained from instruments stationed at three stories or higher structures, dam abutments or base of bridge columns were excluded from the dataset. To represent the site effects, continuous function of average shear wave velocity at the upper 30 m (V_{S30}) is used. Moment magnitude and Joyner Boore distance (R_{jb}) were used to define the earthquake size and source-to-site distance. Two-stage regression

procedure defined by Joyner and Boore (1993) were employed in regression. The median ground motion model is given by;

$$\log Y = b_1 + b_2(M-6) + b_3(M-6)^2 + b_5 \ln r + b_v \ln\left(\frac{V_S}{V_A}\right) \quad (2.3)$$

where Y is spectral acceleration, M is moment magnitude, r is the function for distance term, V_S is average shear wave velocity at the upper 30 m, b_1 - b_5 and V_A are coefficients calculated in regression analysis.

Campbell and Bozorgnia (2003) updated the Campbell (1997) model using 960 unprocessed recordings obtained from 49 earthquakes and 443 processed recordings obtained from 36 earthquakes. Four different categories were used for local site classification: firm soil, very firm soil, soft rock and firm rock. Moment magnitude (M_w) was used for defining the size of earthquake and shortest distance between the station and zone of seismogenic energy release (r_{seis}) was used for defining source-to-site distance. Recordings were included in the database only if their r_{seis} was less than 60 km to avoid the complications related to arrival of multiple reflections from lower crust. Non-linear least squares method was used to determine the coefficients of the equation. Median ground motion is given as;

$$\ln Y = c_1 + f_1(M_w) + c_4 ln\sqrt{f_2(M_w, r_{seis}, S} + f_3(F) + f_4(S) + f_5(HW, F, M_w, r_{seis}) \quad (2.4)$$

where Y is spectral acceleration, M_w is moment magnitude, r_{seis} is the closest distance to seismogenic rupture in kilometers, F is dummy term for faulting style, S is dummy term for local site conditions, c_1 and c_4 are regression coefficients, f_1 is functional form defining magnitude scaling, f_2 is functional form for source to site distance effects, f_3 is functional form for faulting style, f_4 is functional form for local site effects and f_5 is functional form for hanging wall effects. The hanging wall model of this model was adopted from Abrahamson and Silva (1997) model with a few modifications

Sadigh et al. (1997) derived their formula using the earthquakes spanning from 1952 to 1994 occurred in Western US. Only 4 foreign events were included in their database. Moment magnitude (M_w) was used for characterizing the earthquake size and closest distance to the rupture (R_{rup}) was used for characterizing source-to-site distance. Two site categories, namely rock and deep soil, was used for defining local site conditions. Two different ground motion models were defined for deep soil (Equation 2.5) and for rock sites (Equation 2.6):

$$\ln y = C_1 + C_2 M - C_3 \ln\left(r_{rup} + C_4 e^{C_5 M}\right) + C_6 + C_7 (8.5 - M)^{2.5} \tag{2.5}$$

$$\ln y = C_1 + C_2 M + C_3 (8.5 - M)^{2.5} + C_4 \ln\left(r_{rup} + \exp(C_5 + C_6 M)\right) + C_7 \ln\left(r_{rup} + 2\right) \tag{2.6}$$

where y is median spectral acceleration, M is the moment magnitude, r_{rup} is the rupture distance and C_1-C_7 are regression coefficients.

Idriss (1991) used 572 individual horizontal components of recordings from rock sites for developing the prediction model. For earthquake size, he used local magnitude (M_L) for M smaller than 6 and surface wave magnitude (M_S) for M is equal or greater than 6. As the distance parameter, closest distance to the source was used, but for small magnitude earthquakes (M smaller than 6), hypocentral distance was incorporated. Idriss (1991) prediction equation is given by;

$$\ln(Y) = [\alpha_0 + \exp(\alpha_1 + \alpha_2 M)] + [\beta_0 - \exp(\beta_1 + \beta_2 M)]\ln(R + 20) + aF \tag{2.7}$$

where M is magnitude variable, R is closest distance to the rupture in kilometer, F is dummy variable for faulting style, a and α_0-α_2 and β_0-β_2 are coefficients calculated in regression analysis.

The authors of early-stage empirical ground motion models often set limits on their applicability based on the dataset used to derive the models. Spectral

period range for Abrahamson and Silva (1997) and Campbell and Bozorgnia (2003) was 0-5 seconds, whereas, Sadigh et al. (1997) relations were limited to 0-4 seconds. Sadigh et al. (1997) relationship is only applicable to earthquakes of magnitude 4 to 8 at distances of up to 100 km for rock sites; however, these limits are typically ignored in the application of models in probabilistic seismic hazard assessment (PSHA) since the PSHA needs to have the ground motion estimates for all relevant sources (Abrahamson and Silva, 2008).

2.2 Next Generation Attenuation Models

GMPEs are improved in time from basic formulas provided in the previous section to today's more comprehensive and accurate equations. In 2005, PEER initiated the Next Generation Attenuation (NGA) relation project incorporating a number of attenuation relationship developer teams to model their own sets of NGA relationships in a systematic process using the improved resources. Most prominent of these improvements is the increase in the number of strong motion recordings, the NGA-W1 dataset includes 3551 recordings from 173 shallow crustal earthquakes. Most of the recordings are processed by using PEER processing procedure (Chiou et al., 2008) and the remaining ones are added to the database without additional processing. Each team screened the NGA-W1 database based on their discretion and used their version of the dataset in the regression analysis. It is notable that the main portion of this database consists of California earthquakes and number of earthquakes from Turkey is rather sparse; Turkish ground motions were represented by only 67 recordings among the total number of 3551 recordings. The definition of average horizontal ground motion was also altered for the new project and the orientation-independent ground motion intensity measures (explained in Chapter 3) were used. Ground motion models for shallow crustal earthquakes that cover all relevant sources in California for the average horizontal component were developed by five attenuation relationship developer teams (Abrahamson and Silva

(2008), Boore and Atkinson (2008), Chiou and Youngs (2008), Campbell and Bozorgnia (2008), and Idriss (2008)). The NGA project required the developers to extrapolate their model to be applicable to the ranges shown below in Table 2.1.

Table 2.1 NGA-W1 model requirements

Style of Faulting:	Strike-slip, Reverse, Normal
Distance Range:	0-200 km
Magnitude Range (for Strike-slip):	5.0-8.5
Magnitude Range (for Reverse and Normal):	5.0-8.0
Ground Motion Parameters:	PGA, PGV, PGD, Sa (5% damping) for average horizontal, fault normal and fault parallel
Spectral Period Range:	0.0 to 10.0 seconds.

Abrahamson and Silva (2008) (AS08) used 2754 recordings obtained from 135 earthquakes but the earthquakes were classified into two main categories; aftershock events which produce systematically lower ground motions than the other category including the mainshock, foreshock or swarm events. Instead of the site dummies, two parameters were used to define the site effects; V_{S30} and depth to engineering rock $Z_{1.0}$ ($Z_{1.0}$ is defined as the depth from surface to V_S = 1000 m/s) and the non-linear site effects were included. For defining fault geometry, depth-to-top of rupture (Z_{TOR}), fault dip in degrees (δ) and down-dip rupture width (W) were used in addition to the rupture distance. Two other source-to-site distance metrics, R_{jb} and R_x (horizontal distance from top edge of rupture) were included in hanging wall effects model. Instead of two, three categories for defining fault type were used (normal fault type was introduced). For regression analysis, random

effects model proposed by Abrahamson and Youngs (1992) was employed as the previous model. Equation for the new median ground motion is more complicated than the Abrahamson and Silva (1997) model as:

$$\ln Sa(g) = f_1\left(M, R_{rup}\right) + a_{12}F_{RV} + a_{13}F_{NM} + a_{15}F_{AS} + f_5\left(P\hat{G}A_{1100}, V_{S30}\right) + F_{HW}f_4\left(R_{jb}, R_{rup,}R_{x,}W, \delta, Z_{TOR}, M\right) + f_6(Z_{TOR}) + f_8\left(R_{rup}, M\right) + f_{10}(Z_{1.0}, V_{S30}) \quad (2.8)$$

where Sa is median spectral acceleration, M is moment magnitude, R_{rup} is rupture distance, F_{RV} and F_{NM} are dummy variables for faulting style, $P\hat{G}A_{1100}$ is the rock peak ground acceleration, V_{S30} is the average shear wave velocity for the top 30 meters, R_{jb} is Joyner-Boore distance, R_{rup} is rupture distance, R_x is the horizontal distance from top edge of rupture, W is fault width, δ is dip angle of the fault plane, Z_{TOR} is depth to top of rupture value in kilometer, $Z_{1.0}$ is depth to V_S=1.0 km/s in kilometers, a_{12}, a_{13} and a_{15} are regression coefficients. In the new model, f_1 represents the functional form for magnitude scaling which remained the same as the previous model, f_4 and f_5 define hanging wall and site effects which were modified significantly from the previous version, f_6, f_8, and f_{10} are the new terms that model the rupture depth effects, large distance effects (gamma term) and basin effects. Also the standard deviations of the new model include the nonlinear site response effects.

Boore and Atkinson (2008) (BA08) used the NGA-W1 database after eliminating the aftershocks as these recordings might result in different ground motion scaling when compared to the mainshock recordings. Boore and Atkinson (2008) used the functional form of Boore et al. (1997) model as the starting point and added further complexity when necessary. Parameters used for defining magnitude and source-to-site were the same as the previous model. V_{S30} was used for site characterization and non-linear site effects were included. They used 3 different categories for defining style of faulting; strike-slip, reverse and normal. The new model did not include

depth-to-top of rupture, hanging wall/footwall or basin depth effects since the analysis of residuals indicated that inclusion of these factors would not result in improvement in predictive capability of the formula as stated by the authors. Same statistical approach (two-stage regression introduced by Joyner and Boore, 1993, 1994) were used. The median ground motion prediction equation is given by:

$$\ln Y = F_M(M) + F_D\left(R_{JB}, M\right) + F_S\left(V_{S30}, R_{JB}, M\right) \tag{2.9}$$

where y is spectral acceleration, M is moment magnitude, R_{JB} is Joyner and Boore distance, V_{S30} is the average shear wave velocity of upper 30 m of soil strata, F_M, F_D and F_S are functional form for magnitude scaling, distance scaling and site effects respectively.

Campbell and Bozorgnia (2008) (CB08) used 1561 recordings from 64 earthquakes (aftershocks were excluded) to develop the new model. Two site parameters, V_{S30} and $Z_{2.5}$ (depth to 2.5 km/s shear wave velocity) were used for characterizing local site conditions instead of the site dummies in the previous version. Three different categories for defining style of faulting; reverse or reverse-oblique, normal or normal-oblique and strike slip was used and the categorization was done by using rake angle intervals. Previous model used shortest distance between the station and zone of seismogenic energy release (r_{seis}), which was replaced by the closest distance to the rupture (R_{rup}) in this version. Previous model was developed for a maximum of 60 km distance; a magnitude-dependent slope in the distance term was added to the new formula to provide for the model requirements given in Table 2.1. Depth-to-top of rupture (Z_{TOR}) and fault dip in degrees (δ) were also used for defining fault geometry. Hanging-wall effects for normal-faulting and non-vertical strike-slip earthquakes were included in the new model. The authors used two-stage regression procedure proposed by Joyner and Boore (1993) in regression analysis. The median prediction equation is formulated as;

$$\ln \hat{Y} = f_{mag} + f_{dis} + f_{flt} + f_{hng} + f_{site} + f_{sed} \tag{2.10}$$

where $\hat{Y}$ is median spectral acceleration, f_{mag}, f_{dis}, f_{flt}, f_{hng}, f_{site} and f_{sed} are functional forms for magnitude term, distance term, style-of-faulting term, hanging wall term, site conditions term and basin response term respectively.

Chiou and Youngs (2008) (CY08) developed an NGA model as the update of Sadigh et al. (1997) model, with a dataset of 1950 recordings obtained from 125 earthquakes. Similar to Abrahamson and Silva (2008) model, aftershock events were included using a separate scaling. One of the differences from the earlier formula was the site effects parameters, V_{S30} and $Z_{1.0}$ were used for defining local site conditions instead of site dummies. Same magnitude and distance measures as the previous model were used. Distance scaling formulations of these two equations are quite different, which results in a difference in the shape of attenuation curves, especially beyond 70 km and long period motions. The new model includes hanging wall effect, therefore a more robust equation for sites located in hanging wall side were developed. Similar to Abrahamson and Silva (2008) R_x is used in the hanging wall term. The regressed coefficients were determined by using mixed effects regression model (Abrahamson and Youngs, 1992). The median ground motion is defined by:

$$\begin{aligned}\ln(y_{ij}) = \ln\left(y_{ref_{ij}}\right) &+ \emptyset_1 * \min\left(\ln\left(\frac{V_{S30j}}{1130}\right), 0\right) \\ &+ \emptyset_2\left(e^{\emptyset_3(\min(V_{S30j},1130)-360)} - e^{\emptyset_3(1130-360)}\right) * \ln\left(\frac{y_{ref_{ij}} e^{\eta_i} + \emptyset_4}{\emptyset_4}\right) \\ &+ \emptyset_5\left(1 - \frac{1}{\cosh(\emptyset_6 * \max(0, Z_{1.0} - \emptyset_7))}\right) \\ &+ \frac{\emptyset_8}{\cosh(0.15 * max(0, Z_{1.0} - 15)}\end{aligned} \tag{2.11}$$

where y_{ij} is spectral acceleration, $y_{ref_{ij}}$ is spectral acceleration for reference site condition, V_{S30j} shear wave velocity in kilometers, η_i is random variable,

$Z_{1.0}$ is depth to V_S=1.0 km/s in kilometers and $\emptyset_1$-$\emptyset_8$ are regression coefficients.

Idriss (2008) (ID08) model dataset consist of 3179 recordings obtained from 114 earthquakes (aftershocks were excluded). Local site conditions were defined by two site classes: rock sites with 900 m/s < V_{S30} and soil sites with 450 < V_{S30} <900 m/s. Idriss (2008) model used V_{S30} bins instead of a continuous function of V_{S30}, since it is more appropriate from a geotechnical engineering perspective as stated by the author. For defining source mechanism, two different categories, namely strike slip and reverse were used. Local magnitude (M_L) and surface wave magnitude (M_S) were used for defining earthquake size in the previous model, which were replaced by the moment magnitude (M_w). Similarly, hypocentral distance (R_{hyp}) of the previous model was replaced by the closest distance to the rupture (R_{rup}). The median prediction equation is given by;

$$\ln\big(PSA(T)\big) = \alpha_1(T) + \alpha_2(T)M - (\beta_1(T) + \beta_2(T)M)\ln\big(R_{rup} + 10\big) + \gamma(T)R_{rup} + \varphi(T)F \quad (2.12)$$

where $PSA(T)$ is spectral acceleration, M is moment magnitude, R_{rup} is rupture distance, F is the dummy variable for faulting style and $\alpha_1(T)$, $\alpha_2(T)$, $\beta_1(T)$, $\beta_2(T)$, $\gamma(T)$ and $\varphi(T)$ are coefficients calculated from regression analysis.

2.3 Ground Motion Prediction Equations Developed for Turkey

In Turkey, many authors attempted to develop GMPEs especially after the well-recorded 1999 Kocaeli and Düzce earthquakes. One of the first efforts on developing predictive models for peak ground acceleration (PGA) and response spectral ordinates using recordings from earthquakes occurred in Turkey was **Gülkan and Kalkan (2002)** model. The model's functional form was similar to that of Boore et al. (1997) equation. For characterizing the earthquake size, moment magnitude (M_w) was used and source-to-site

distance was defined by Joyner and Boore distance (R_{jb}). The median prediction model is shown in Equation 2.13:

$$\ln Y = b_1 + b_2(M - 6) + b_3(M - 6)^2 + b_5 \ln r + b_v \ln\left(\frac{V_S}{V_A}\right) \quad (2.13)$$

where Y is spectral acceleration, M is the moment magnitude, R is the Joyner-Boore distance, Vs is the average shear wave velocity on the top 30 meters, V_A, b_1-b_5 and b_v are the model coefficients determined by regression.

Gülkan and Kalkan (2002) used a dataset containing 47 recordings obtained during 14 earthquakes occurred in Turkey after eliminating the aftershocks. Recordings are selected from the earthquakes with moment magnitude equal or greater than 5. As the authors stated, used dataset was not of high quality due to limited and poorly distributed data, lack of knowledge of local geology and the possible distortions in the recordings due to the effects of buildings which houses the strong motion stations.

Kalkan and Gülkan (2004) and (**2005)** models used the same functional form (as given in Equation 2.13) but an improved dataset when compared to their previous model. The updated dataset contains 112 strong motion recordings obtained from 57 earthquakes. The number of the recordings were increased by adding smaller magnitude events to the dataset (Mw>4) and for those smaller events, due to absence of information about rupture surface, epicentral distance (R_{epi}) is used as source-to-site distance parameter. The authors claimed that the new models are applicable for a moment magnitude range between 4.0 and 7.5 and for distances (Rjb) up to 250 km.

Özbey et al. (2004) prediction model was based on 1188 ground motions recorded from 392 events. The majority of the recordings are obtained during the 1999 Kocaeli and Düzce Earthquakes at the Northwestern part of Turkey with source-to-site distance less than 100 km. Recordings from events with magnitude greater than 5 were included in the dataset. Moment magnitude values for events larger than 6 were included, however, for smaller events,

local magnitude (M_L) values are directly used without any conversion assuming that the variations between the magnitude scales are insignificant for magnitudes smaller than 6. Proposed model for the median ground motion was similar to Boore et al. (1997) and Kalkan and Gülkan (2004) models as shown in Equation 2.3:

$$\log(Y) = a + b(M - 6) + c(M - 6)^2 + \mathrm{d} * \log\sqrt{\mathrm{R}^2 + \mathrm{h}^2} + \mathrm{eG}_1 + \mathrm{fG}_2 \quad (2.14)$$

where Y is spectral acceleration, M is moment magnitude, R is the closest distance to rupture and a-f are model coefficients determined by mixed effects regression. Site effects were represented by site dummies (G1 and G2), and three site classes were formed: B (360 m/s < V_s), C (180 m/s < V_s < 360 m/s) and D (V_s < 180 m/s). The authors recommended that the proposed prediction equation should only be used for northwestern part of Turkey.

Ulusay et al. (2004) proposed a predictive model for peak ground acceleration based on a dataset composed of 221 recordings obtained from 122 events occurred in Turkey. Recordings obtained from events with moment magnitude greater than 4 within 100 km distance were included in the dataset. To define the local site conditions, three different site categories, namely rock, soil and soft soil were used. The authors used epicentral distance (R_{epi}) as source-to-site distance measure since they believed that the rupture surface of most of the events was not defined with accuracy and there was the lack of consensus between the agencies about focal depth values. Fault mechanism effects were not included in the model since the information about focal mechanism solutions was not available for most of the earthquakes at the time. The median model for PGA is given as;

$$PGA = a_1 * e^{a_2*(a_3 M_w - R_e + a_4 S_A + a_5 S_B)} \quad (2.15)$$

where M_w is moment magnitude, R_e is distance to epicenter in kilometers, a_1-a_5 are the model coefficients, S_A and S_B are dummy variables for defining local site conditions.

Akkar and Çağnan (2010) used 433 recording obtained from 137 earthquakes to derive their equation. Recordings were taken from recently compiled Turkish strong-motion database (the TSMD database, details provided in Chapter 3). Functional form of Abrahamson and Silva (1997, 2008) was used for modeling the basic form of the prediction equation except that the Joyner and Boore distance (R_{jb}) was used for defining source-to-site distance. Local site conditions were defined as a continuous function of V_{S30}. Site response model of Boore and Atkinson (2008) was adopted for defining linear and nonlinear site effects as this function form is compatible with the model database and it is simpler than other functional forms as stated by the authors. For modeling source mechanism, three different faulting style categories namely normal, strike-slip and reverse/thrust were used. The median ground motion prediction equation is formulized as:

$$\ln(Y) = a_1 + a_2(M - c_1) + a_4(8.5 - M)^2 + \left(a_5 + a_6(M - c_1)\right) ln\sqrt{{R_{jb}}^2 + {a_7}^2} + a_8F_N + a_9F_R + F_S \quad for \quad M \leq c_1 \tag{2.16}$$

$$\ln(Y) = a_1 + a_3(M - c_1) + a_4(8.5 - M)^2 + \left(a_5 + a_6(M - c_1)\right) ln\sqrt{{R_{jb}}^2 + {a_7}^2} + a_8F_N + a_9F_R + F_S \quad for \quad M > c_1 \tag{2.17}$$

where Y is spectral acceleration, M is moment magnitude, R_{jb} is Joyner-Boore distance, F_N and F_R are dummy variables used for defining style-of-faulting, F_S is site response function and a_1-a_9 are the model coefficients calculated in regression analysis. Akkar and Cagnan (2010) model is applicable for moment magnitudes between 5.0 and 7.6 and Joyner and Boore distances up to 200 km.

2.4 Compatibility of Regional Datasets with NGA Models

NGA-W1 models depend on a global database which contains ground motions recorded during earthquakes from many active tectonic regions. Still, applicability of the NGA-W1 models to other tectonic regions has been

studied since these models were proposed in 2008; especially in regions with an established ground motion database like Taiwan and Italy. These studies are briefly summarized below:

Lin et al. (2007) studied the applicability of NGA-W1 models in Taiwan even before the models were published. The authors used a large dataset containing 7722 recordings obtained form 71 shallow crustal earthquakes for comparison. The geometric mean of the two horizontal components was used rather than the GMRotI50 incorporated by NGA-W1 developers stating that difference between these two measures are insignificant for comparison purposes. The model residuals were calculated by subtracting the natural logarithm of GMPE median values (predictions) from natural logarithm of recorded intensity measure (actual data). Inter-event and intra-event residuals were separated and residual plots with respect to model parameters such as; magnitude, distance, and V_{S30} were examined for possible trends. Results of the study showed that the magnitude, distance and site effects scaling of NGA-W1 models were compatible with the Taiwan database. A significant trend was observed in inter-event residuals vs. depth to top of rupture plots; however the models were not adjusted to capture the difference. The authors also stated that the NGA-W1 models without crustal damping (kappa term) resulted in over prediction of short-period data at distances larger than 150 km.

Stafford et al. (2008) tested the compatibility of NGA models to the Euro-Mediterranean strong motion database compiled by Akkar and Bommer (2007). Both analysis of model residuals method and the log-likelihood approach proposed by Scherbaum et al. (2004) were used for comparison. One setback of this study was the number of models used in comparison; the authors selected Boore and Atkinson (2008) model as the representative prediction equation for NGA-W1 models and assumed that the results of this model were valid for all other models. Results of the study indicated that Boore and Atkinson (2008) model is highly compatible with the Euro-

Mediterranean strong motion database, therefore NGA-W1 models can be used in earthquake hazard studies conducted in Europe. The authors stated that using NGA-W1 models in PSHA will provide constraints on the features that cannot be offered by current European models and these models cover the spectral ordinates up to 10 seconds whereas European models can only be used for spectral ordinates up to 4 seconds. One negative aspect noted regarding the NGA-W1 models was the damping ratio; NGA-W1 models were formulated only for 5% critical damping that creates an important limitation.

Scasserra et al. (2009) studied the compatibility of magnitude, distance and site effects scaling of the NGA-W1 models to that of Italian strong motion database (ITACA database) which contains 247 recordings obtained during 81 events. Model residuals between the intensity measures of recordings (actual data) and NGA-W1 predictions were calculated and inter-event and intra-event residuals were separated using mixed effects regression. Initially, performance of NGA GMPEs' distance scaling was tested by plotting intra-event residuals with distance measures and a statistically significant trend was observed at short periods due to the faster attenuation of Italian data at these periods. The models were adjusted by changing constant, magnitude-dependent slope, and fictitious depth terms of the functional forms at PGA, T=0.2 sec and T=1 sec spectral periods. The model residuals of the adjusted GMPEs were examined for magnitude and site effects scaling. No statistically significant trends were found in inter-event residuals vs. magnitude plots, indicating that the NGA-W1 models capture the magnitude scaling of Italian database with high precision. Similarly, no significant trends were observed in intra-event residuals vs. V_{S30} graphs concluding that NGA-W1 models provide compatible site scaling with respect to Italian data.

Shojo-Taheri et al. (2009) conducted the test of applicability of NGA-W1 in Iran using a database that contains 863 strong motion recordings obtained during 166 earthquakes. Only Boore and Atkinson (2008), Campbell and Bozorgnia (2008), and Chiou and Youngs (2008) prediction equations were

used in comparison as the representative prediction equations for NGA-W1 models and the authors assumed that the results of these models were valid for other two models. Similar to the other studies, model residuals between the intensity measures of recordings (actual data) and NGA-W1 predictions were calculated, and inter-event and intra-event residuals were separated. Residual plots vs. distance and magnitude were examined for possible trends. No significant trend was observed in Boore and Atkinson (2008) and Campbell and Bozorgnia (2008) prediction equations. In Chiou and Youngs (2008) model residual plots, a significant underestimation was observed for PGA and spectral period of T=0.2 sec but the model was not adjusted to capture the difference. The authors concluded that NGA-W1 models are applicable in seismic hazard studies conducted in Iran with reasonable errors.

CHAPTER 3

COMPILATION OF COMPARISON DATASET

The primary objective of this study is to compare the magnitude, distance and site effects scaling of ground motions recorded in Turkey to these features of the NGA-W1 models; therefore compiling a high quality and well-constrained dataset of Turkish ground motions was the most substantial part of this study. Luckily, the largest project on the Turkish seismic catalogue and strong motion database in the last 50 years, the TSMD project, was finalized in 2008, providing a precious starting point for any ground motion characterization study in Turkey. TSMD database was selected and used as the preliminary dataset, however finalization of the comparison dataset had taken almost two years to be completed, and still some aspects of the dataset require expert evaluation. This chapter starts with a brief summary of the efforts on Turkish Strong Motion Network and Acceleometric Database before the TSMD project. Statistics of the TSMD database with the emphasis of available earthquake, station and ground motion parameters are also provided within this chapter. Finally, a comprehensive summary of the changes on the initial TSMD dataset, efforts on estimating the missing parameters required for comparison with the NGA-W1 predictive models, calculation of the orientation-independent intensity measures, and final comparison dataset is presented. Last sub-section is devoted to delineating the comparison dataset used in this study in terms of earthquake and recording station parameters and ground motion intensity measures.

3.1 Previous Efforts on Turkey's Strong Ground Motion Database

The practice of recording strong ground motions during earthquakes occurred in Turkey dates back to 1970's. First strong ground motion was recorded at Denizli Station by an analog, SMA-1 type accelerograph during 19 August 1976 Denizli earthquake (Ateş and Bayülke, 1982). From this date on, nationwide strong motion network has expanded, reaching a total number of 327 strong motion stations by the year 2009. As stated by Gülkan (2010), deployment of the national earthquake recording network was achieved through several phases. First strong motion network was established by funding of Earthquake Research Institute (ERI) at 1971 including 20 stations nationwide. In 1985, the total number of instruments was 65, all of them being SMA-1 type, and this number increased to 69 at 1990. From 1990 to 1996, network was improved to a state where it included 73 SMA-1 type, 19 digital SIG-SA type and one single Kinemetrics SSA-1 type instrument (Gülkan, 2010).

The year 1999 marked as a milestone in Turkey's earthquake engineering history, with two large magnitude earthquakes striking the industrial heartland of Turkey on August 17 and November 12. The strong motion network at that time was not capable of capturing these important earthquakes efficiently and the number of records and record quality were found to be unsatisfactory. These events initiated Turkey to expand its strong motion recording network and from this date on, several projects were realized to increase the number of digital instruments in the network (Gülkan, 2010). Currently, the strong ground motion network is operated by Earthquake Department of the Disaster of Emergency Management Presidency (AFAD) and all strong motion stations have digital recorders. Geographic locations of these strong ground motion stations are presented in Figure 3.1.

Ground motion characterization studies benefit from having a high quality regional strong motion database, therefore, various researches attempted to assemble the strong ground motion database of Turkey since 1984 (Erdik

1984; Ambraseys et al. 1993; İnan et al. 1996; Aydan and Hasgür 1997; Durukal et al. 1998; Çelebi et al. 2001; Erdik and Durukal 2001; Zaré and Bard 2002; Rathje et al. 2003; Yunatcı 2010). Only specific earthquakes (1999 Kocaeli and Düzce Earthquakes) were included in Çelebi et al. (2001); Erdik and Durukal (2001); Zaré and Bard (2002); Rathje et al. (2003), thus these datasets do not represent the nationwide database. Within those studies, only study that compiled a database representing nationwide seismic activity is Yunatcı (2010).

Figure 3.1 Active strong motion recording stations in Turkey by the year 2009

For almost all of studies mentioned above, the database either lack the recording site information of the strong motion or the site conditions were solely based on “expert opinion” without in-situ geotechnical or geophysical tests (Akkar et al., 2010). Only for the stations located in Marmara Region (14 permanent stations), in-situ geotechnical and geophysical tests were conducted by Rathje et al. (2003) to determine the site classification.

To provide the need for a compact and high quality nationwide strong motion database for Turkey, Earthquake Research Department of General Directorate of Disaster Affairs and Earthquake Engineering Research Center

(EERC) of Middle East Technical University (METU) launched the project entitled “Compilation of Turkish strong motion network according to the international standards” (TSMD) in 2005. The objectives of TSMD project includes; providing a seismic catalog for strong ground motions recorded in Turkish nationwide network, classification of these records according to “waveform quality” and its “uniform processing”, and conducting in-situ geotechnical or geophysical site tests to obtain site characterization (Akkar et al. 2010). The TSMD Database includes 2996 events occurred in Turkey and 4607 recordings obtained from these events between years 1976-2007. Detailed information about these records is published online and can be obtained at http://daphne.deprem.gov.tr. According to Akkar et al. (2010) the data collected during the course of the TSMD project can be summarized under three subsections:

1. **“*Earthquake information*”** which includes date, epicentral coordinates, magnitude, depth, and faulting type of the events,

2. **“*Record information*”** which includes trigger times, peak ground motion amplitudes and spectral values for each component, record type, various source-to-site distance metrics, as well as low- and high-cut filter values used in the processing of each waveform of the records,

3. **“*Station information*”** which includes coordinates, location, ID, altitude, P- and S-wave profiles, and corresponding soil conditions of the recording site.

To collect earthquake information, event date, epicentral coordinates, earthquake magnitude in various scales, and depth data from 18 different seismic agencies both international and national was harvested by Akkar et al. (2010). Still, only 75% of the events in the final TSMD database possess complete epicentral location, origin time, and depth information. Magnitude conversion relationships developed on this database by Akkar et al. (2010)

were used to homogenize the magnitude information. Approximately 80% of the strong motions in the database were recorded during events with magnitude less than 5 as shown in Figure 3.2.

To determine the style-of-faulting, Frohlich and Apperson (1992) criteria were used for the records associated with well-known faults. If the fault geometry solution was not available, rake angle intervals were used as proposed by Boore et al. (1997), Campbell (1997), and Sadigh et al. (1997). For some of the remaining events, epicentral coordinates were associated with the location of the known faults to estimate the faulting style. Akkar et al. (2010) stated that nearly 60% of the records have strike-slip or normal type fault mechanisms and a small number, approximately 1% of the records have thrust or reverse-type fault mechanism in TSMD database. The authors could not estimate style-of-faulting for the remaining records due to the absence of the fault mechanism solutions. Also some of the fault locations are not within the "*well-known faulting zones*" therefore they did not able to assign faulting styles of those strong motion records.

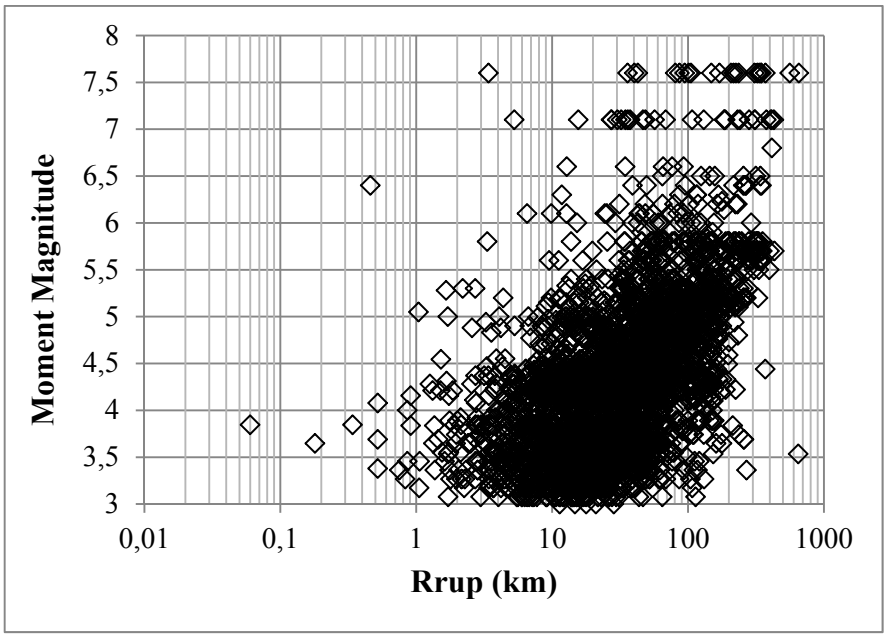

Figure 3.2 Magnitude vs. distance distribution of the recordings in TSMD database

Peak ground motion amplitudes, response spectral values, low-cut and high-cut filter values for the processed records, and the source-to-site distance metrics were included in the TSMD dataset as record information. Not all the recordings were processed in the database; the records with local magnitude less than 3.5 were excluded since smaller events are insignificant in engineering calculations. Also, the recordings that include non-standardization and digitization errors were defined and excluded using the method proposed by Douglas (2003). Remaining 1301 records were processed using bidirectional (acausal), fourth order Butterworth filter (Akkar et al., 2010). Fault geometry solutions obtained through seismological agencies were used to determine the distance metrics such as; epicentral distance (R_{epi}), hypocentral distance (R_{hyp}), Joyner and Boore distance (R_{jb}) and closest distance to rupture (R_{rup}). For the cases where no rupture parameters were available, empirical formulas proposed by Wells and Coppersmith (1994) were implied to obtain relevant fault geometry parameters, which were then used in the R_{jb} and R_{rup} calculations.

Within the course of TSMD project, local site conditions for 241 stations were obtained using field tests including multi-channel analysis of surface waves (MASW), standard penetration test, and geotechnical laboratory tests (Yılmaz et al., 2008). Average shear wave velocity in the upper 30m and NEHRP soil classification information of these strong ground motion stations were provided in the TSMD database. According to Akkar et al. (2010), 82% of the recording stations were classified as NEHRP C or NEHRP D and only a small number, 1% of the stations, were classified as NEHRP B. For the remaining 17% of the stations, the authors were not able to conduct site tests, as these stations are stationary type, temporarily installed for monitoring aftershocks of the main events.

3.2 Compilation of the Comparison Dataset

Considering the large number of processed strong motion recordings, completeness and quality of the earthquake metadata and other

seismological features, and availability of precious site classification information for the recording stations, TSMD project database was the natural choice as the starting point for the comparison dataset to be used for this study. All the events (with a total number of 2996) and 4607 sets of recordings (processed or unprocessed) from these events were included in the initial comparison dataset to preserve all valuable data.

3.2.1 Changes on the Initial TSMD Project Database Flatfile

Almost 80% of the TSMD database was composed of recordings from small magnitude events (M_w<5), however, the applicable magnitude range of the NGA models is 5.0<M_w<8.5 for strike slip earthquakes and 5.0<M_w<8.0 for reverse and normal earthquakes (Power et al. 2008). To make the comparison more meaningful, all 173 earthquakes in the database with magnitude 5 or bigger and 685 recordings from these events were preserved. Remaining 2823 small magnitude earthquakes were included in the dataset only if 3 or more recordings were available from these events. After this preliminary elimination, the size of the dataset was reduced to 414 events and 1868 recordings. No magnitude information was available for 37 of the remaining earthquakes so these events (with 151 recordings) were discarded from the dataset. The moment magnitudes for 119 earthquakes were not available; these values were estimated from local magnitude (M_L) values using regional magnitude conversion relationships proposed by Akkar et al. (2010) and Ulusay et al. (2004).

Unfortunately, no site information (V_{S30} or site classification) could be found for 431 of the recordings obtained from 50 different strong motion recording stations. Coordinates of these stations were compared to the station coordinates in NGA-W1 (Chiou et al., 2008) and NGA-W2 (Abrahamson, 2012) datasets to search for the closest match. V_{S30} values of 9 stations (49 recordings) were estimated from these datasets, assuming that small errors (±0.001°) in latitude and longitude of recording stations might occur due to measurement errors (such as Station ID# 8102 in Table 3.1) and some

stations might be duplicated or moved (such as Station ID# 303-307 in Table 3.1). The station ID numbers, coordinates and estimated V_{S30} values of the recording stations are summarized in Table 3.1. Remaining 382 records with no V_{S30} values or no site class information were removed from the database.

One of the remaining earthquakes in the dataset was missing focal depth information; therefore this event was removed from the database. Also, style of faulting for 47 events, which have 106 recordings, was missing. For 30 of these earthquakes, style-of-faulting was estimated by associating the event with other events in the sequence or dominant fault mechanism in the region. The earthquake ID numbers, coordinates and estimated fault mechanism of these 30 events are listed in Table 3.2. Spatial distribution of the estimated events with the closest earthquake epicenters in the dataset is presented in Figure 3.3. 68 recordings from these 30 events were preserved in the dataset but the remaining 38 records were removed.

Table 3.1 Stations with estimated local site conditions (V_{S30})

Station ID	Station Province, City Town and Location	Station Latitude	Station Longitude	Estimated V_{S30} (m/s)
0303	Afyon Dinar Dinar Cezaevi	38.075	30.161	219.8
0304	Afyon Dinar Dinar Devlet Hastanesi	38.067	30.171	219.8
0305	Afyon Dinar Dinar Jandarma Karakolu	38.069	30.160	219.8
0306	Afyon Dinar Koy Hizmetleri	38.053	30.139	219.8
0307	Afyon Dinar Devlet Su Is.	38.076	30.178	219.8
1004	Balikesir Merkez Bay. ve Iskan Md. Loj.	39.660	27.860	338.6
2402	Erzincan Merkez Met. Md.	39.752	39.487	274.5
6002	Tokat Merkez Bay. ve Iskan Md.	40.300	36.570	323.8
8102	Duzce Merkez Verem Savas Dispanseri Bastabipligi Bh.	40.834	31.164	276.0

Table 3.2 Events with estimated style-of-faulting

EQ ID	Mw	Depth (km)	Epicenter Latitude	Epicenter Longitude	Estimated Faulting Style
6	5.33	44.0	39.120	43.910	Strike Slip
15	5.05	8.9	36.97	28.852	Normal
34	5.40	10.0	38.716	26.589	Normal
48	5.05	10.0	37.032	28.938	Normal
49	5.05	25.0	36.949	29.058	Normal
58	4.66	10.0	40.803	27.773	Strike Slip
89	5.05	5.1	38.067	30.147	Normal
90	5.00	11.3	38.068	30.198	Normal
95	5.28	28.4	38.046	30.160	Normal
99	5.00	11.8	38.000	30.143	Normal
389	4.77	22.7	37.777	29.618	Normal
396	4.94	5.0	39.591	27.452	Normal
458	4.60	57.0	36.833	35.483	Strike Slip
464	4.44	21.6	36.878	35.525	Strike Slip
657	5.33	10.0	40.741	29.970	Strike Slip
2676	5.40	10.0	39.380	40.850	Strike Slip
2680	4.94	6.0	38.844	27.782	Normal
2771	3.50	13.0	35.913	35.695	Normal
2807	3.55	4.5	39.764	30.552	Strike Slip
2860	5.11	5.2	38.306	39.247	Strike Slip
2864	4.99	5.0	39.040	40.433	Strike Slip
2880	4.47	5.4	37.845	28.142	Normal
2895	4.66	28.0	38.139	37.439	Strike Slip
2912	4.77	27.3	39.365	40.757	Strike Slip
2913	3.65	12.0	39.342	40.820	Strike Slip
2914	4.21	7.0	37.889	29.567	Normal
2915	4.44	10.5	38.978	41.121	Strike Slip

Table 3.2 (Cont'd)

EQ ID	Mw	Depth (km)	Epicenter Latitude	Epicenter Longitude	Estimated Faulting Style
2932	4.33	28.7	38.767	25.580	Strike Slip
2934	4.42	13.2	38.266	26.533	Strike Slip
2961	4.42	21.4	38.781	27.742	Normal

Considering the applicable distance range of the NGA predictive models, 118 records with rupture distance (R_{rup}) or Joyner-Boore distance (R_{jb}) larger than 200 km were discarded from the dataset. Source-to-site distance metrics for 96 remaining records were missing. Fortunately, these ground motions were recorded during small magnitude earthquakes, therefore the R_{rup} and R_{jb} were estimated from the hypocentral distance and epicentral distance, respectively. At this stage, dataset was composed of 288 earthquakes and 1179 strong motion records.

Some of the parameters required for the NGA-W1 predictive models were missing in the TSMD database such as; depth to the engineering rock (denoted by $Z_{1.0}$ and $Z_{2.5}$) and depth to the top of the rupture (Z_{top}). These values were estimated by using empirical formulas proposed by Chiou and Youngs (2008), Campbell and Bozorgnia (2007) and Wells and Coppersmith (1994). These formula are shown in Equations 3.1 to 3.3 respectively as:

$$\ln(Z_{1.0}) = 28.5 - 0.4775 * \ln(V_{S30}^{8} + 378.7^{8}) \quad (3.1)$$

$$Z_{2.5} = 0.519 + 3.595 Z_{1.0} \quad (3.2)$$

$$Z_{top} \approx Z_{hyp} - \frac{W}{2} * \sin(\delta) \quad (3.3)$$

where $Z_{1.0}$ and $Z_{2.5}$ are basin depth terms which represents depths to the 1.0 km/s and 2.5 km/s shear wave velocities in the soil profile, respectively. Z_{hyp} is the hypocentral depth, W is fault width and δ is fault dip angle.

The mainshock and aftershock declustering of the earthquakes in the dataset were performed by using plane rupture geometries in NGA-W1 database for Erzincan (1992), Dinar (1995), Kocaeli (1999), and Düzce (1999) earthquakes, and Gardner-Knopoff (1974) methodology for other small-to-moderate magnitude earthquakes (Woddell, 2012).

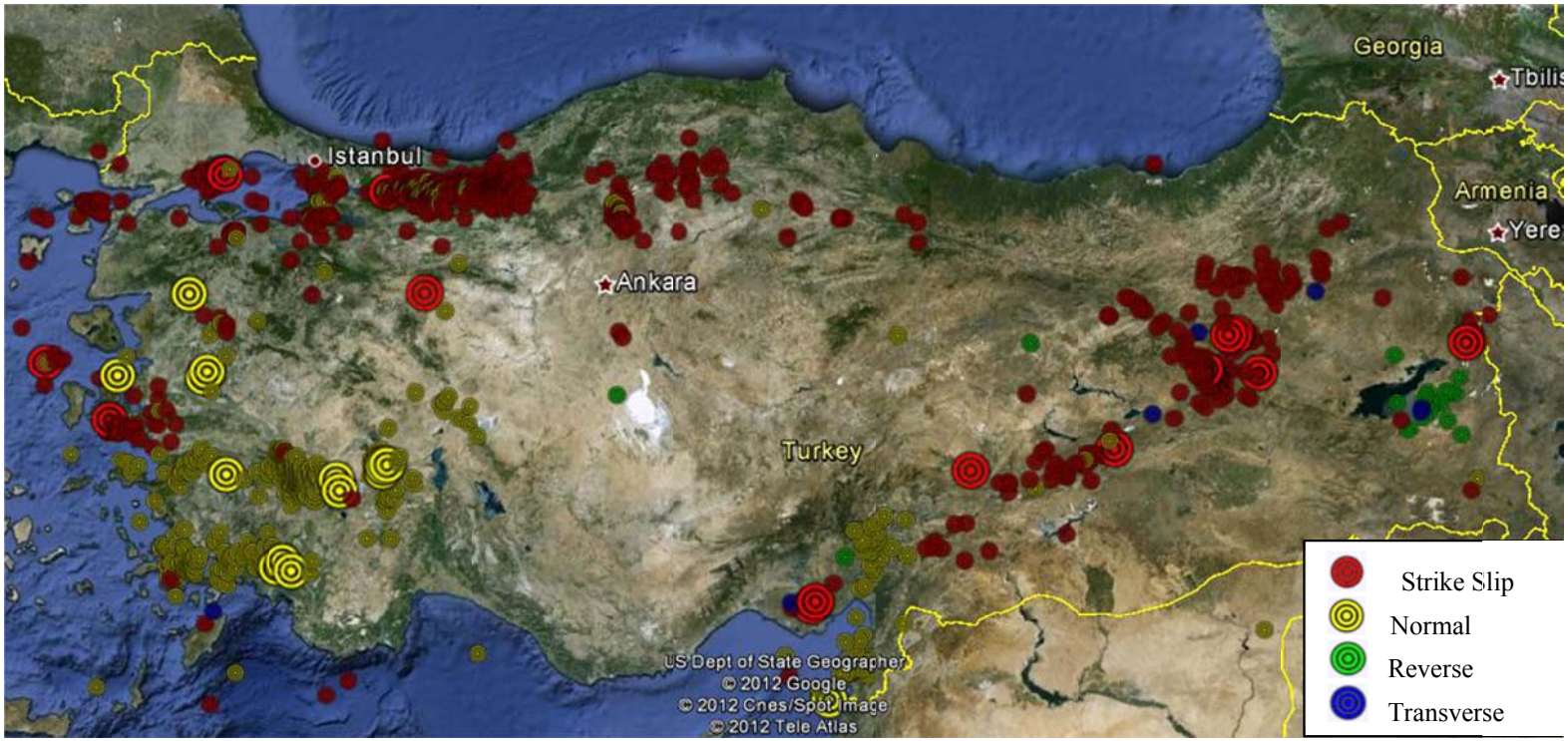

Figure 3.3 Spatial distributions of events according to fault style. Events with known fault style are shown with small dark circles whereas events with fault style assessed are shown with large bright circles

3.2.2 Time History Screening

Majority of the recordings in the remaining dataset were processed by Akkar et al. (2010). We aimed to preserve as much data as possible to obtain a representative dataset; therefore 284 unfiltered recordings were not excluded from the dataset. The waveform data of all ground motion recordings were checked for data quality and 37 unfiltered recordings were eliminated from the dataset due to spike, insufficient digitizer resolution, multi-event or S-wave trigger problems. A sample waveform from the discarded recordings with North-South, East-West and vertical ground motion components is shown in Figure 3.4 and list of removed records is given Table 3.3. After this evaluation, size of the dataset was reduced to 288 events and 1142 records.

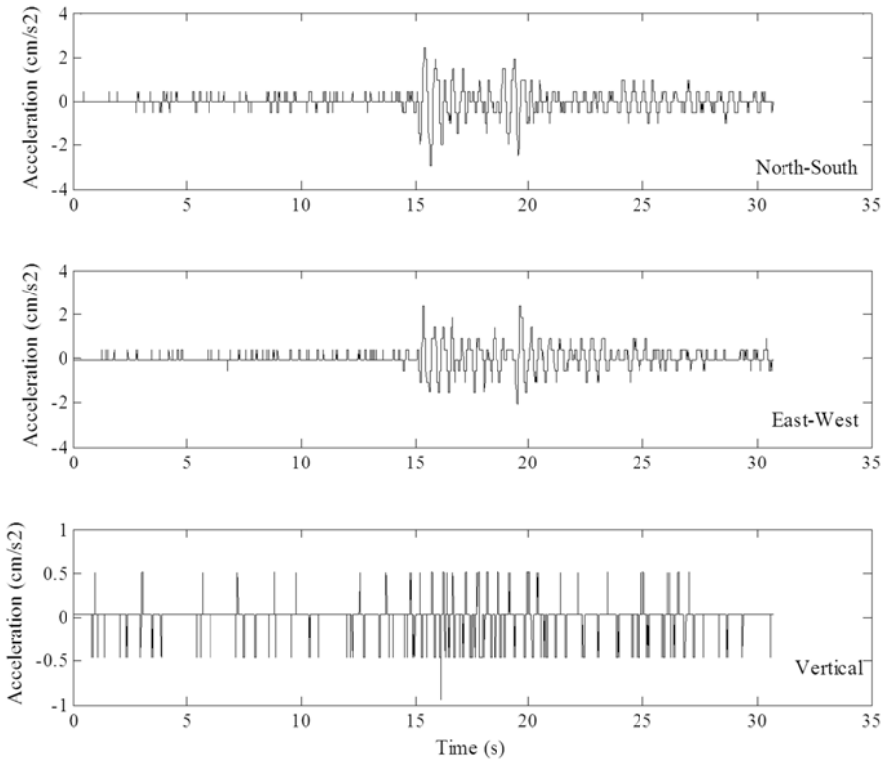

Figure 3.4 Sample record (with NS, EW and Vertical components) that was discarded due to low digitizer resolution (Record name: 19981008204912_2401).

Table 3.3 Records removed from dataset after the waveform check.

EQ ID	Record ID	File Name	Station Province, City Town and Location	Moment Magnitude (M_w)
2	2	19771005053443_1801.pad	Cankiri Cerkes Met. Ist. Md.	5.80
19	25	19880420035008_6502.pad	Van Muradiye Met. Md.	5.50
46	60	19941113065601_2002.pad	Denizli Merkez Bay. ve Iskan Md.	5.30
56	72	19950129041657_2501.pad	Erzurum Merkez Bay. ve Iskan Md.	5.20
75	94	19950413040801_3401.pad	Istanbul Merkez Bay. ve Iskan Md.	5.00
77	98	19950418053603_3401.pad	Istanbul Merkez Bay. ve Iskan Md.	4.99
162	249	19951205184932_2501.pad	Erzurum Merkez Bay. ve Iskan Md.	5.80
162	250	19951205184932_4901.pad	Mus Merkez Bay. ve Iskan Md.	5.80
240	340	19970122175720_4604.pad	Kahramanmaras Andirin Tufan Pasa Ilkogretim Okulu	5.70
243	347	19970122182510_4603.pad	Kahramanmaras Merkez Bay. ve Iskan Md.	5.10
350	462	19971025003842_1705.pad	Canakkale Gelibolu Karayollari 13. Sube Sefligi	4.11
380	499	19980123123250_7601.pad	Igdir Merkez Met. Md.	5.17
395	522	19980305014540_4501.pad	Manisa Merkez Bay. ve Iskan Md.	4.80
405	541	19980404161710_0301.pad	Afyon Merkez Bay. ve Iskan Md.	5.20
410	554	19980413151432_4901.pad	Mus Merkez Bay. ve Iskan Md.	5.20
470	695	19980709173646_4501.pad	Manisa Merkez Bay. ve Iskan Md.	5.00
544	971	19981008204827_1208.pad	Bingol Solhan Ogretmen Evi	4.60
544	973	19981008204912_2401.pad	Erzincan Merkez Bay. ve Iskan Md.	4.60
645	1092	19990725065718_4501.pad	Manisa Merkez Bay. ve Iskan Md.	5.20
1353	2240	20000512030203_0104.pad	Adana Ceyhan Ptt Md.	4.76
1353	2242	20000512030208_4603.pad	Kahramanmaras Merkez Bay. ve Iskan Md.	4.76
1959	2906	20010625132913_0104.pad	Adana Ceyhan Ptt Md.	5.40
2026	2981	20011031123415_0104.pad	Adana Ceyhan Ptt Md.	5.16
2336	3425	20030713014819_4603.pad	Kahramanmaras Merkez Bay. ve Iskan Md.	5.50
2340	3437	20030723045605_4501.pad	Manisa Merkez Bay. ve Iskan Md.	5.30
2351	3454	20030726083610_0301.pad	Afyon Merkez Bay. ve Iskan Md.	5.40
2414	3538	20040325193122_2401.pad	Erzincan Merkez Bay. ve Iskan Md.	5.60

Table 3.3 (Cont'd)

EQ ID	Record ID	File Name	Station Province, City Town and Location	Moment Magnitude (M_w)
2583	3764	20050312073610_2401.pad	Erzincan Merkez Bay. ve Iskan Md.	5.60
2587	3771	20050314015557_2401.pad	Erzincan Merkez Bay. ve Iskan Md.	5.80
2587	3775	20050314015702_4901.pad	Mus Merkez Bay. ve Iskan Md.	5.80
2592	3780	20050323214452_2401.pad	Erzincan Merkez Bay. ve Iskan Md.	5.60
2594	3784	20050323234356_1208.pad	Bingol Solhan Ogretmen Evi	5.09
2650	3871	20051017095954_4501.pad	Manisa Merkez Bay. ve Iskan Md.	5.05
2689	3927	20060126184214_3107.pad	Hatay Iskenderun Meyvecilik Uretme Ist. Md. Bh.	4.66
2689	3926	20060126184230_0104.pad	Adana Ceyhan Ptt Md.	4.66
2760	4023	20060702193939_4901.pad	Mus Merkez Bay. ve Iskan Md.	5.00
2782	4058	20061020181558_1006.pad	Balikesir Bandirma Met. Md.	5.11

During the data quality check for the waveforms, it is observed that the initial excitation times of the three orthogonal components were not consistent for a large number of processed records. This time lag results from the separate a-causal low-cut filtering applied to the individual components of the record by adding zero pads in different lengths. Figure 3.5 shows a sample record with two orthogonal horizontal components shifted with added zero pads during processing.

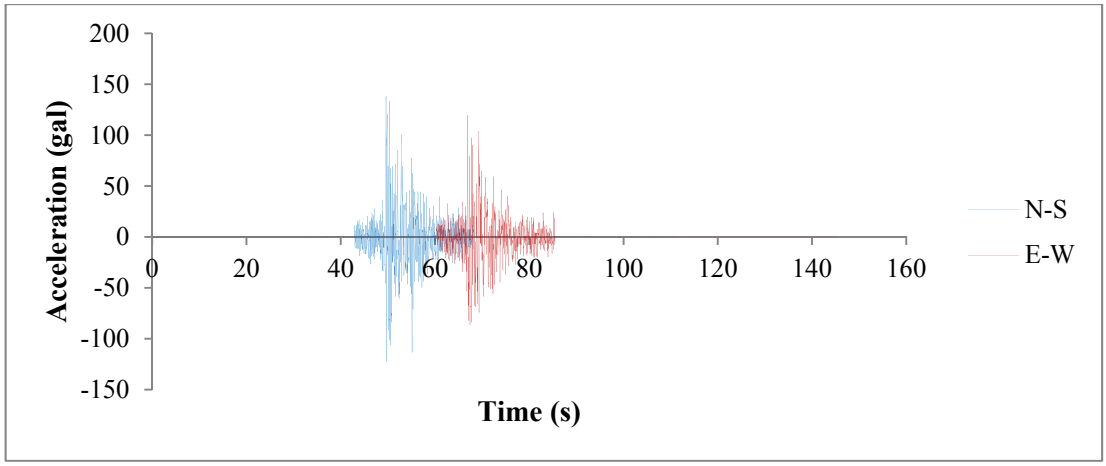

Figure 3.5 Waveform of the processed recording showing the time lag due to separate zero pads added to horizontal components (Record name: 19990817000139_1404)

To calculate the orientation-independent ground motion intensity measures, two horizontal components of the records should have the same excitation time. Boore et al. (2012) discussed that removal of the zero pads may lead to incompatibilities in the ground motion intensity measures, especially in the spectral accelerations at long periods (periods longer than 10 seconds). An exercise is performed to see the effect of zero pad cut-off on the orientation-independent horizontal spectral accelerations (GMRotI50 as used in the NGA-W1 models) by adding zeros to the shorter horizontal component (denoted by zero added in Figure 3.6) and cutting the zero-pad in the longer horizontal component (denoted by pad-stripped in Figure 3.6) to align two components and calculating the horizontal response spectra for each case. The difference in the horizontal spectra calculated by these two procedures is negligible as shown in Figure 3.6 for the scope of this project

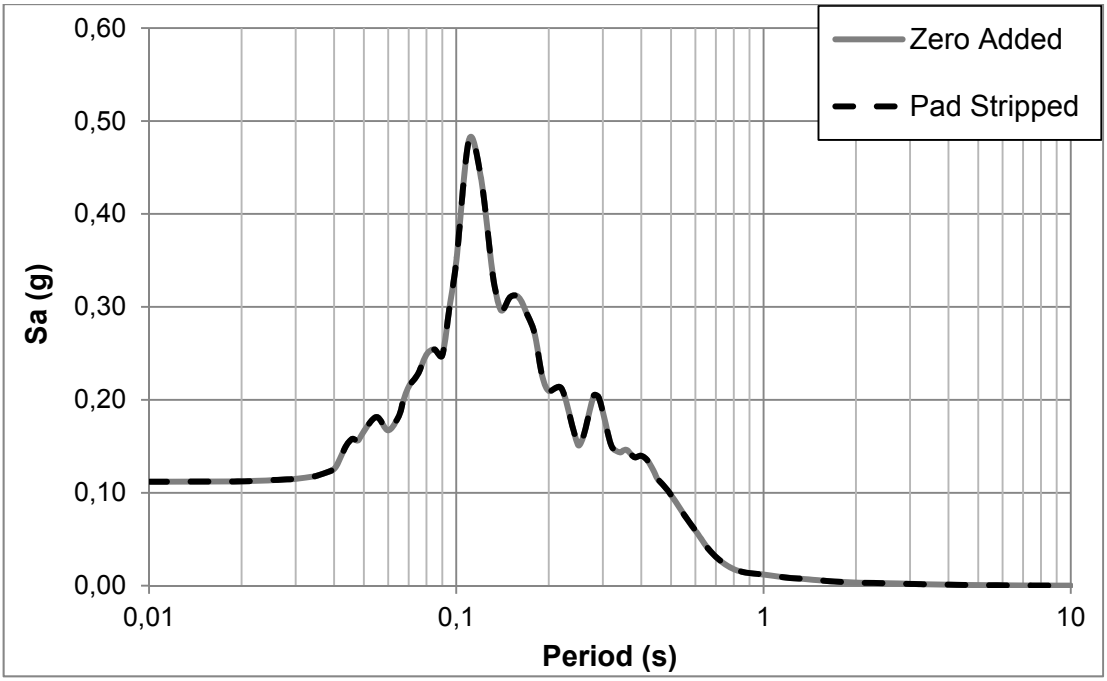

Figure 3.6 GMRotI50 horizontal spectra for the same recording with zero pads cut-off (denoted by pad-stripped) from the long component and zero added to the short component for alignment (denoted by zero-added) (Record name: 19991107165434_9906)

A systematic screening procedure was performed on the waveforms in the comparison dataset and the short horizontal component was shifted by adding zero pads to align it with the longer horizontal component in each recording with a time lag. The shifted waveform for the time-lagged recording in Figure 3.5 is presented in Figure 3.7.

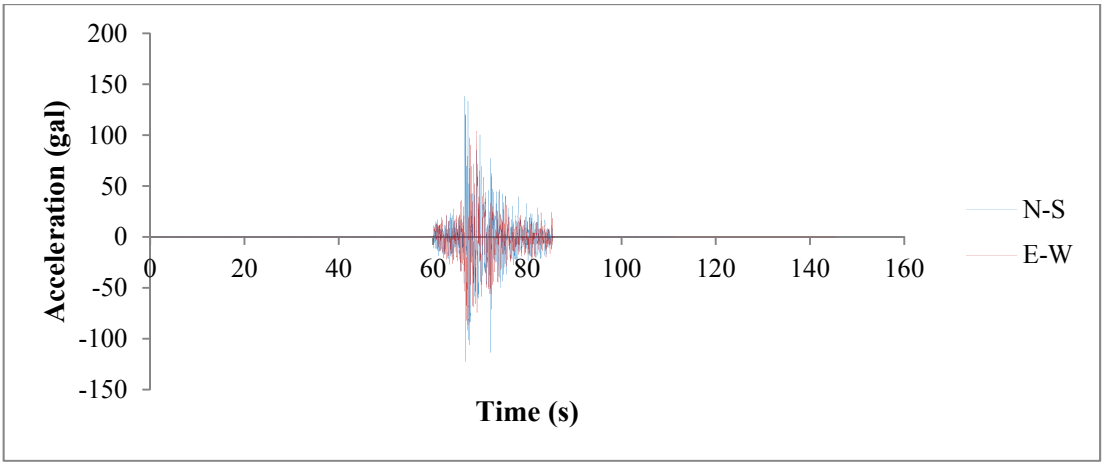

Figure 3.7 Waveform of the same recording after shifting to align the start times (Record name: 19990817000139_1404)

Example time histories of acceleration, velocity and displacement for the original and zero-added record are presented in Figure 3.8. Fourier spectra for the original and zero-added version of the same recording are plotted in Figure 3.9. As Figures 3.8 and 3.9 imply, the zero-adding procedure does not create any distortion in velocity and displacement time histories and any incompatibilities in the frequency content. However, it is remarkable that adding zero pads to the time histories to align the horizontal components creates very long recordings which would increase the computational time significantly for other engineering applications.

3.2.3 Orientation Independent Ground Motion Intensity Measures

Response spectrum is a widely used frequency content measure in earthquake engineering practice (Kramer, 1996). Earth scientists usually incorporate the geometric mean response spectra in their analysis (Baker and Cornell 2006), which is calculated by taking the geometric mean of estimated response spectra of each orthogonal horizontal component of strong motion.

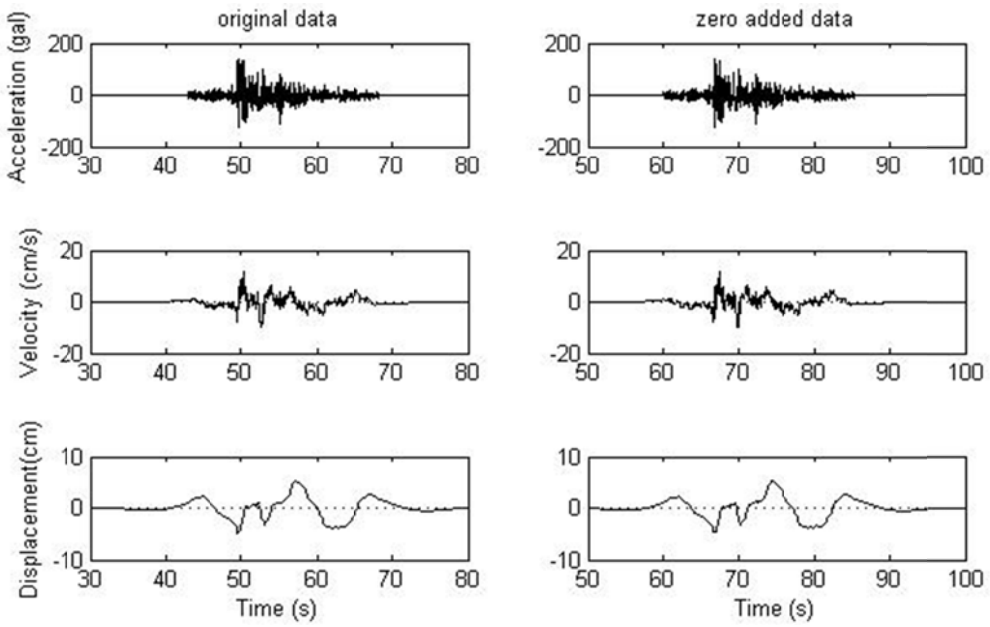

Figure 3.8 Acceleration, velocity and displacement time histories of North-South component of original (a) and shifted 19990817000139_1404 recording (b).

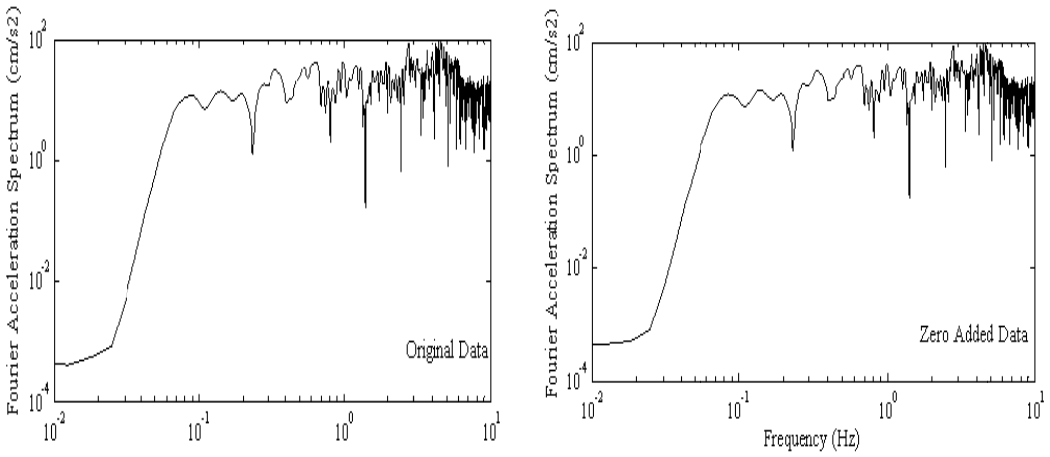

(a) (b)

Figure 3.9 Fourier spectra of North-South component of (a) original recording and (b) shifted recording (Record Name: 19990817000139_1404).

Geometric mean of response spectra is proven to be a good measure as it includes less aleatory uncertainty compared to other measures. Although geometric mean of response spectra is a relatively good measure, it has one important disadvantage; it is dependent on orientation of the orthogonal components of accelerograph (Boore et al. 2006).

Boore et al. (2006) defined two orientation-independent measures for ground motion intensity; GMRotDpp and GMRotIpp, where GM stands for geometric mean, Rot means rotations are used over all non-redundant angles, D states that period dependent rotations are used whereas I states that the rotations are period independent, and pp stands for percentile value of the measure. These measures are calculated through rotated response spectra of as-recorded motions as summarized below:

a. Calculation of GMRotIpp requires the use of GMRotDpp so the latter one is calculated first. Initially, response spectra for each individual component are calculated for rotation angle, θ, being equal to 0. Then these response spectral values are rotated by an increment Δθ and the geometric means are calculated from these rotated response spectra for the new angle using Equation 3.4 and 3.5:

$$R_{s,1}(t,\theta) = R_{s,1}(t,0) * \cos(\theta) + R_{s,2}(t,0) * \sin(\theta) \quad (3.4)$$

$$R_{s,2}(t,\theta) = -R_{s,1}(t,0) * \sin(\theta) + R_{s,2}(t,0) * \cos(\theta) \quad (3.5)$$

where $R_{s,1}(t,\theta)$ and $R_{s,2}(t,\theta)$ defined as the response spectra of the component North-South and East-West, respectively. Response spectra $R_{s,1}(t,\theta)$ and $R_{s,2}(t,\theta)$ are defined for a given oscillator damping and usable period range. This geometric mean response spectrum is assigned to the specific angle θ. This process is then repeated for the angle θ = θ + Δθ until θ angle equals to 90 degrees.

b. After obtaining geometric mean response spectra for all angle increments, spectral values for each period are ranked by the

ascending order. GMRotDpp is obtained for the ppth percentile of ranked values. For example; GMRotD50 corresponds to the median of the ranked values for a given period.

c. All GMRotDpp values are normalized by GMRotDpp for a defined pp value that will be used in GMRotIpp calculation. After that, a penalty function is calculated using the formula given below:

$$penalty(\theta) = \frac{1}{N_{per}} \sum_{i=1}^{h} [\frac{GM(\theta,T_i)}{GMRotDpp(T_i)} - 1]^2 \quad (3.6)$$

where T_i refers to usable spectra period and $GM(\theta,T_i)$ refers to geometric mean of response spectra for period T_i at angle θ. This penalty function is calculated for all θ values and the rotation angle that gives the minimum penalty value is determined.

d. Using the selected rotation angle, as-recorded motions are rotated and response spectra are calculated from each rotated component motion. Then the geometric mean of these response spectra is calculated and this spectrum is defined as GMRotIpp.

Median value of GMRotIpp (GMRotI50) was adopted as the ground motion intensity measure in NGA-W1 GMPE models. Therefore, GMRotI50 values are calculated for each recording in the comparison dataset for 23 spectral periods (0.01, 0.02, 0.03, 0.04, 0.05, 0.075, 0.10, 0.15, 0.20, 0.25, 0.30, 0.40, 0.50, 0.75, 1.0, 1.5, 2.0, 3.0, 4.0, 5.0, 7.5, 10.0 seconds). Calculated GMRotI50 values are consistent with the values in NGA-W1 database as shown in Figure 3.10 and Figure 3.11 for two well-recorded earthquakes (1999 Kocaeli and Düzce Earthquakes).

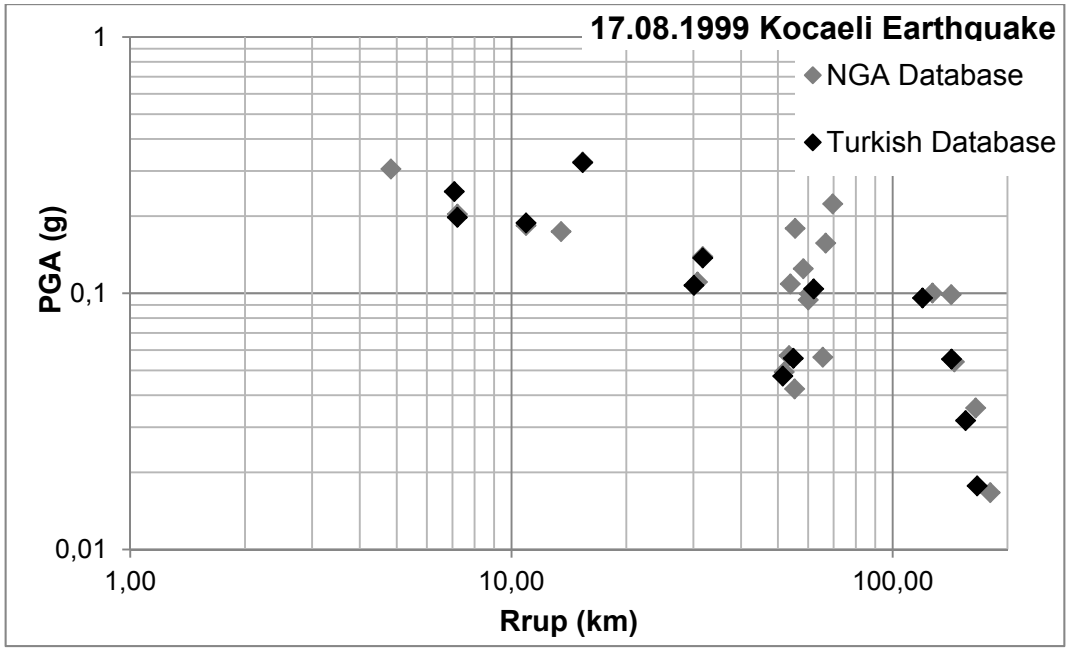

Figure 3.10 GMRotI50 values for 1999 Kocaeli Earthquake in the NGA Database and in the comparison dataset

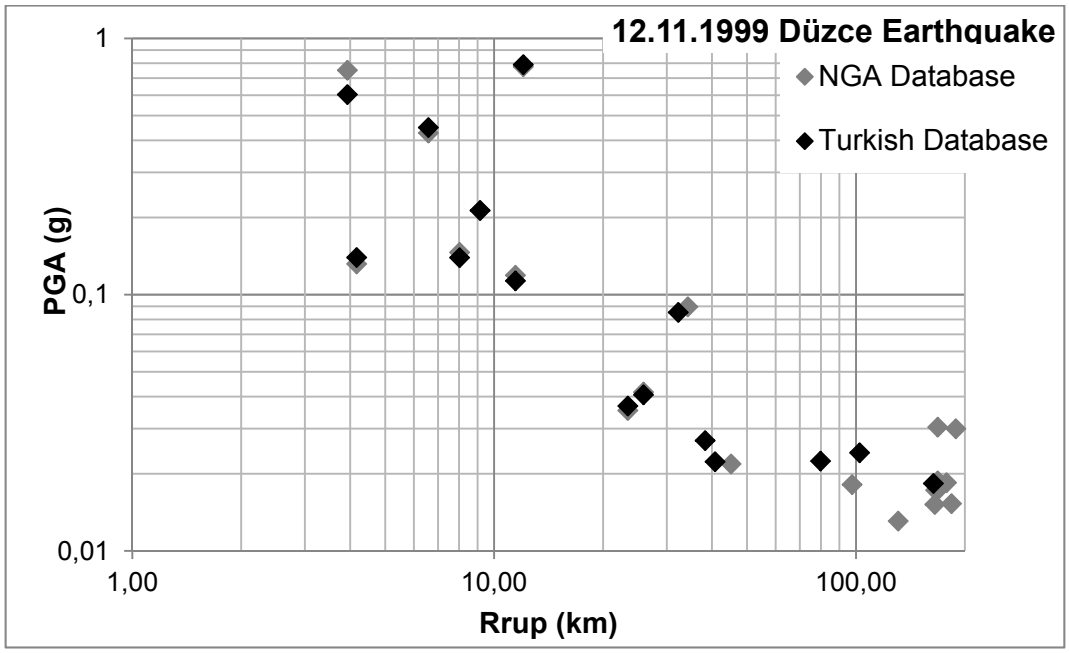

Figure 3.11 GMRotI50 values for 1999 Düzce Earthquake in the NGA Database and in the comparison dataset

3.2.4 Final Comparison Dataset Flatfile

Final flatfile used in the comparison includes 1142 recordings from 288 events with the earthquake metadata (moment magnitude, style of faulting, rake and dip angles, etc.), source-to-site distance metrics for the recordings (R_{Rup} and R_{JB}), V_{s30} values for the recording stations, and horizontal component spectral values in terms of GMRotI50 for 23 spectral periods (0.01, 0.02, 0.03, 0.04, 0.05, 0.075, 0.10, 0.15, 0.20, 0.25, 0.30, 0.40, 0.50, 0.75, 1.0, 1.5, 2.0, 3.0, 4.0, 5.0, 7.5, 10.0 seconds). Statistics of the comparison dataset is provided through Figures 3.11-3.15 to discuss the limitations and reliability of the dataset for assessment of NGA-W1 predictive models. Figure 3.12 shows the distribution of the recordings in the magnitude-distance space and Figure 3.13 presents the number of processed and unprocessed recordings in each magnitude bin. As Figure 3.12 implies, the recordings obtained from events with magnitudes between 6.0 and 7.0 (Zone 1), and recordings from the moderate-to-large magnitude events within 30 kilometer from the rupture (Zone 2) are rather sparse. This feature of the dataset is not the outcome of the excluded data points as discussed in Section 3.2.1, same phenomenon was also observed by Akkar et al. (2010) for the TSMD database.

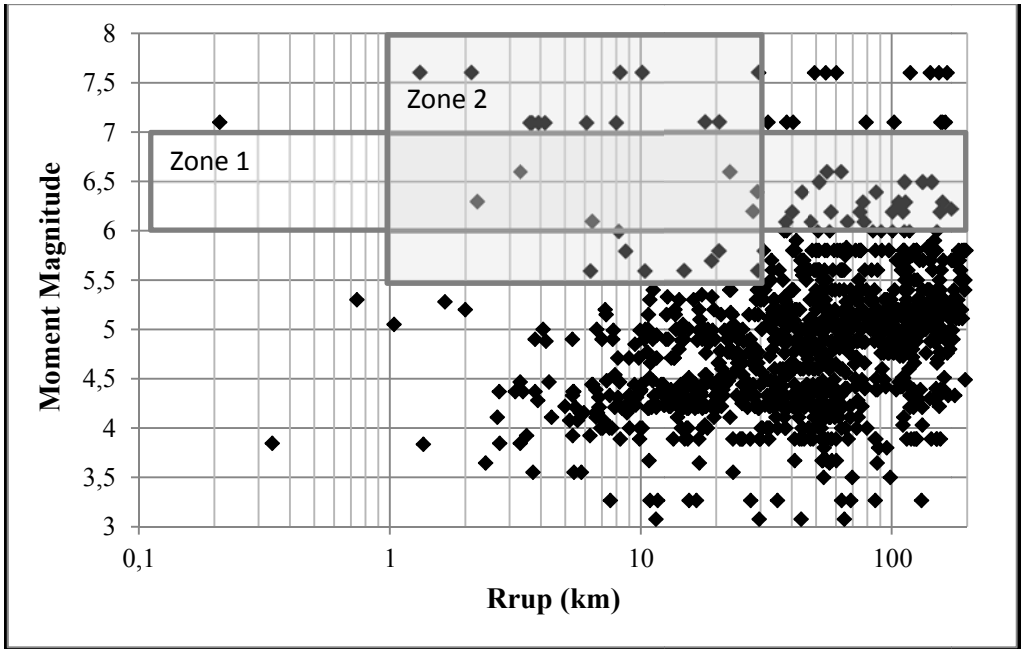

Figure 3.12 Magnitude-distance distribution of records in comparison dataset

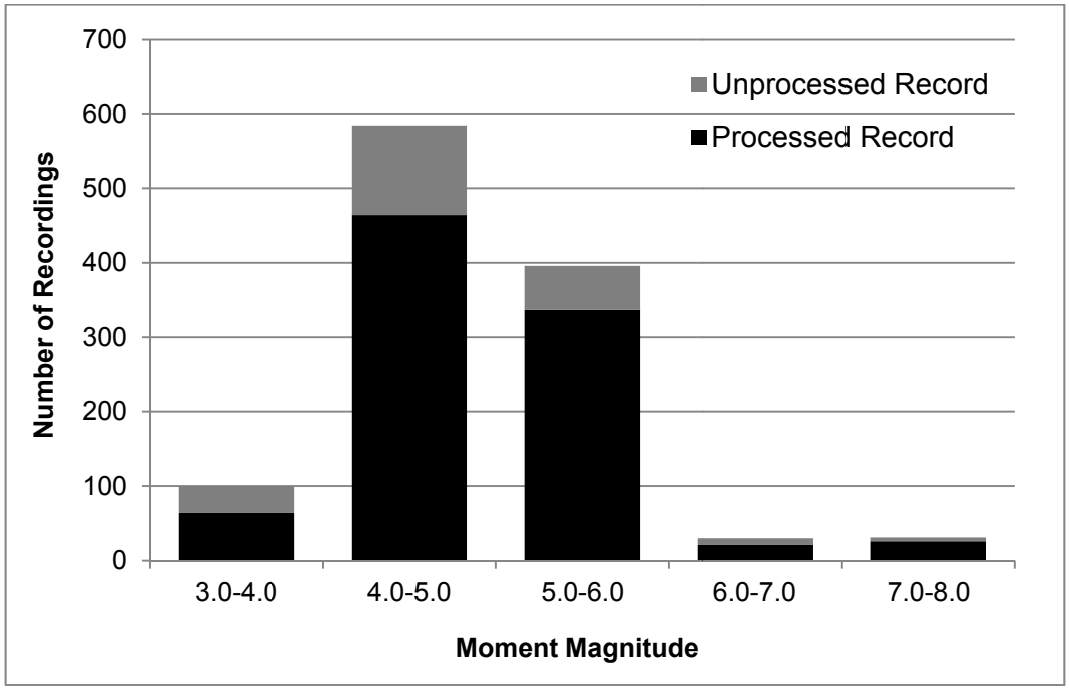

Figure 3.13 Distribution of processed (Processed by Akkar et al., 2010) and unprocessed data with respect to magnitude bins.

Figure 3.13 shows that the majority of the earthquakes with magnitude larger than 6 was processed by Akkar et al. (2010), however the ratio of unprocessed to processed recordings increases as the magnitude decreases. For each recording, there is a minimum useable frequency provided in the NGA-W1 database and the response spectral values for the recordings in the dataset are only used in the regression analysis if the spectral frequencies are greater than 1.25 times the high-pass corner frequency (Chiou et al., 2008). Same limitation was applied to the comparison dataset, therefore size of the dataset used in the comparison analysis decreases as the spectral period increases. The useable frequency range for the unprocessed recordings is assumed as 0.3-3 Hz. The resulting period dependence of the number of recordings is shown in Figure 3.14. The significant drop in the number of recordings at 2.6 seconds indicates that the long-period results of this study are not well constrained by the empirical data.

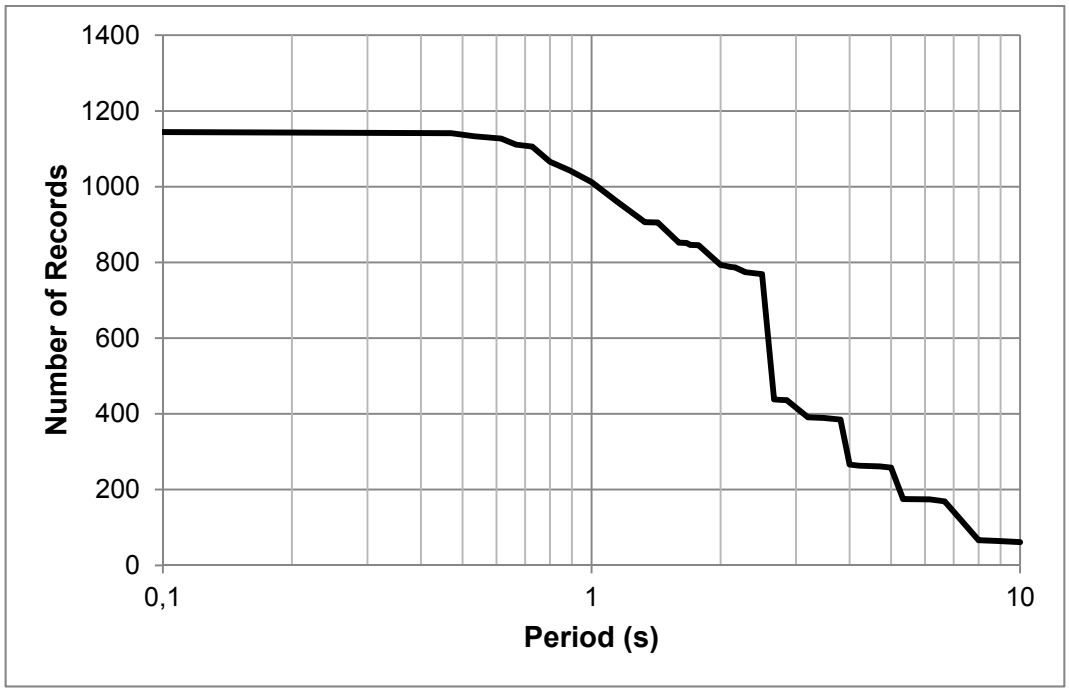

Figure 3.14 Period dependence of number of earthquakes used in comparison

Throughout the dataset compilation, the parameters in TSMD database were used when available; however a handful of parameters had to be estimated in order to keep sample size as high as possible. In Figure 3.15, number of recordings with estimated and measured (taken from TSMD database) V_{S30} in various V_{S30} bins is presented. The number of recordings from stations with estimated V_{S30} is quite small (10%) within the whole set. Similarly in Figure 3.16, number of recordings with estimated and measured distance metrics is plotted with respect to R_{jb}. Majority of the estimated distance values is within the near source range (0-30 km) as shown in Figure 3.16. The presented statistics in this section suggests that the comparison dataset adequately represent the Turkish strong ground motion database.

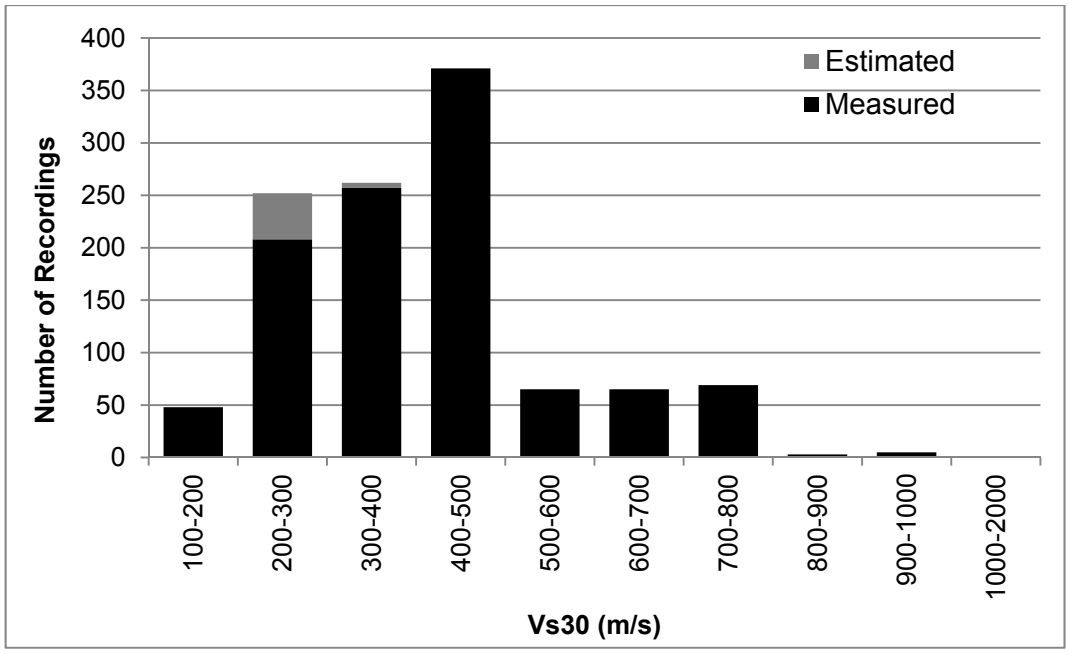

Figure 3.15 Distribution of estimated and TSMD database records according to V_{S30}

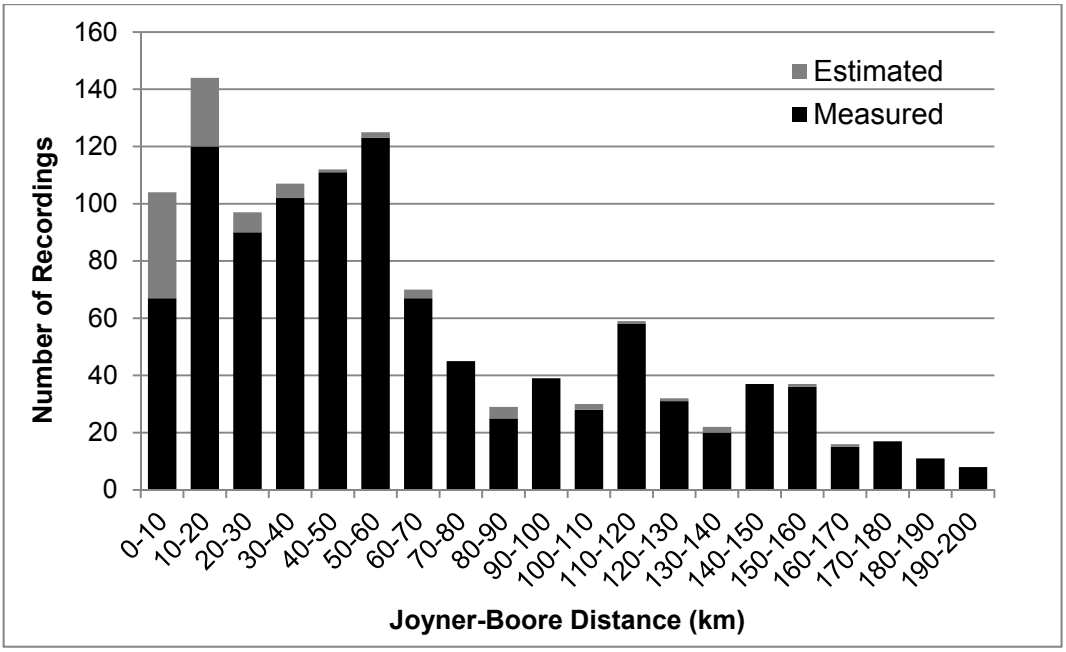

Figure 3.16 Distribution of estimated records and TSMD database records according Joyner-Boore Distance (R_{jb})

CHAPTER 4

COMPATIBILITY OF THE NGA-W1 GROUND MOTION PREDICTION MODELS WITH TURKISH STRONG MOTION DATABASE

The NGA-W1 ground motion prediction models were developed for shallow crustal earthquakes in active tectonic regions and even though the target area was Western US (California), they are intended to use for all of such regions around the world. Slowly, these models are introduced in seismic hazard assessment studies in various regions by further carrying the discussions of their applicability in these regions. A closer look at the NGA-W1 database would show that the Turkish ground motion records are not very well presented. Table 4.1 shows the number of events and number of recordings from the events occurred in Turkey that was included in the NGA developers' datasets. According to Table 4.1, only seven events and at most 52 recordings were included in the developers' datasets, therefore Turkish strong motion data may show a divergence from the NGA-W1 model predictions.

This chapter presents the applied methodology for checking the compatibility of magnitude scaling, distance scaling and site effects scaling of NGA-W1 models with that of Turkish strong motion comparison dataset. Initially, the proposed methodology for comparing any global GMPEs with regional dataset is briefly summarized. Results of the comparison and adjustments on

each NGA-W1 model are broadly explained in Section 4.2. Final forms of the Turkey-Adjusted NGA-W1 models will be presented in Chapter 5.

Table 4.1 Number of events and number of recordings from Turkey that are included in the NGA developers' datasets

Event Name	Event ID in NGA-W1 Database	Year	Mw	AS08	BA08	CB08	CY08	ID08
Izmir	44	1977	5.30	0	0	0	1	0
Dursunbey	47	1979	5.34	1	0	0	1	1
Erzincan	121	1992	6.69	1	0	1	1	0
Dinar	134	1995	6.4	2	4	2	2	0
Kocaeli	136	1999	7.51	17	26	22	17	6
Duzce	138	1999	7.14	13	22	14	12	7
Caldiran	141	1976	7.21	1	0	1	1	0
Total				**35**	**52**	**40**	**36**	**14**

4.1 Comparison Methodology

The preferred methodology for evaluating the differences between the model predictions and actual data is the analysis of model residuals. Following procedure is applied:

1. The orientation-independent ground motion intensity measures (GMRotI50 as adopted by the NGA-W1 models) are calculated for each recording at 23 spectral periods. These periods are 0.01, 0.02, 0.03, 0.04, 0.05, 0.075, 0.10, 0.15, 0.20, 0.25, 0.30, 0.40, 0.50, 0.75, 1.0, 1.5, 2.0, 3.0, 4.0, 5.0, 7.5, 10.0 seconds since the model coefficients only for these periods were published by NGA-W1

developers. The GMRotI50 for each recording (i) at each period (j) is denoted by *actual(i,j)*.

2. Median predictions of each NGA-W1 model (k) at each period (j) for each recording (i) are calculated and denoted by *predicted(i,j,k)*.

3. Total residuals are calculated by:

$$R(i,j,k) = \ln(actual(i,j)) - \ln(predictions(i,j,k)) \quad (4.1)$$

4. Total residuals are separated into three components; the mean offset representing the average bias of the actual data relative to the model predictions (c_k), the event terms (or inter-event residuals, φ) and the intra-event residuals (τ) using the random effects regression:

$$R_{i,j,k} = c_k + \varphi + \tau \quad (4.2)$$

5. The event terms (φ) are plotted against moment magnitude to test the ability of the GMPE to capture the magnitude scaling of the actual data.

6. If a trend is observed, and adjustment function is fitted to the event terms to modify the original GMPE at each period. To define the adjustment function, the functional forms and cut-off or hinge coefficients of the original models are taken into consideration.

7. Step 4 is repeated using the modified forms of the original model.

8. The intra-event residuals (τ) are plotted against the distance and V_{s30} to test the ability of the GMPE to capture the distance and site effects scaling of the actual data.

9. If a trend is observed, and adjustment function is fitted to the intra-event residuals to modify the original GMPE at each period. To define the adjustment function, the functional forms and cut-off or hinge coefficients of the original models are taken into consideration.

10. Step 4 is repeated using the modified forms of the original model. The remaining mean-offset after the modifications is neglected if small, or added to the constant term of the modified GMPE.

4.2 Evaluating the Compatibility of the NGA-W1 Models

Results of the comparison and adjustments on each NGA-W1 model are presented individually in each sub-section below.

4.2.1 Abrahamson and Silva 2008 (AS08) Model

The basic form of the AS08 model for strike-slip earthquakes recorded on rock sites was modeled with a break in the magnitude scaling at M=6.75 allowing for saturation of the short period ground motion at short distances as shown in Equation 4.3:

$$f_1(M, R_{rup}) = \begin{cases} a_1 + [a_2 + a_3(M - c_1)]\ln(R) \\ + \begin{cases} a_4(M - c_1) + a_8(8.5 - M)^2 \rightarrow for(M \le c_1) \\ a_5(M - c_1) + a_8(8.5 - M)^2 \rightarrow for(M > c_1) \end{cases} \end{cases} \quad (4.3)$$

where a_1-a_8 are the model coefficients, M is the moment magnitude and R is distance defined by Equation 4.4 using rupture distance and the fictitious depth term (c_4). A full saturation with the magnitude limit was imposed to the regression using Equation 4.5 (Abrahamson and Silva, 2007):

$$R = \sqrt{R_{rup}{}^2 + c_4{}^2} \quad (4.4)$$

$$a_5 = -a_3 \ln(c_4) \quad (4.5)$$

As a part of the process for developing a smooth model as a function of the spectral period, the magnitude dependent slope (a_3) and bi-linear coefficients (a_4 and a_5) were estimated for the PGA and then constrained to be independent of the period. The period dependence of the magnitude scaling was accommodated only through the a_8*(8.5-M)^2 term.

As the first step towards checking the compatibility of AS08 model with the comparison dataset, total inter-event residuals are plotted with respect to moment magnitude for PGA as shown in Figure 4.1 (total inter-event residuals presented by grey dots). According to the figure, the ground motions in the dataset are overestimated by the AS08 model significantly, especially for small-to-moderate magnitude earthquakes. The trend is persistent for all spectral periods, residual plots for 0.2, 0.5 and, 1 second spectral periods are provided in Figure 4.3.

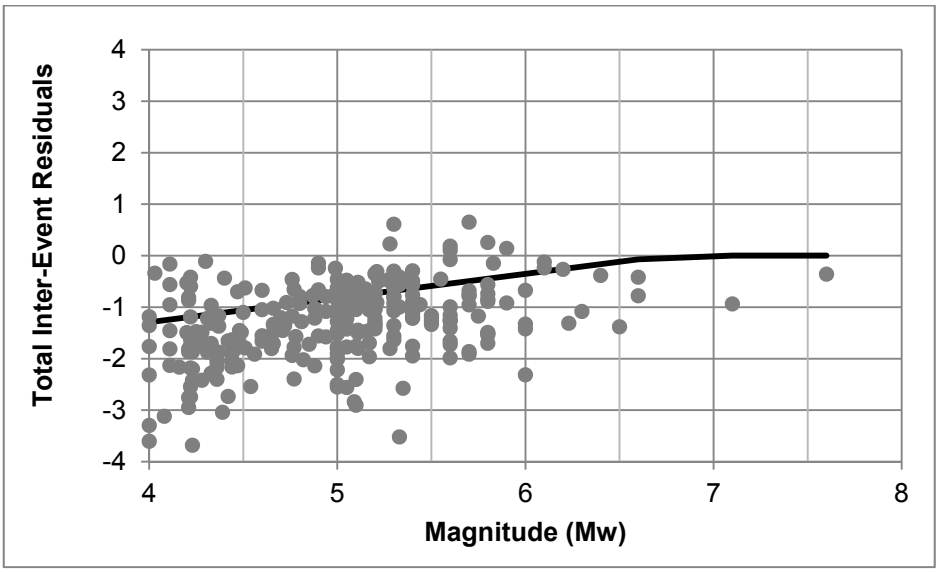

Figure 4.1 Residuals vs. M_w at a) T = 0.01 secs, b) T =0.20 secs and c) T = 1.00 secs for original Abrahamson and Silva (2008)

Figures 4.1 and 4.3 suggest that the magnitude scaling of the comparison dataset is drastically different that the AS08 model and this feature needs to be fixed to consider the model applicable in Turkey. On the other hand, preserving the well-constrained pieces of the model is critical, since the large magnitude earthquakes are poorly represented in the comparison dataset (see Figure 3.11) and any changes on large magnitude parameters will have

a major impact on the hazard calculations. Considering these aspects, the misfit between the actual and predicted data is modeled by Equation 4.6:

$$f_{1\_TA}(M) = \begin{cases} \Delta a_4 (M - 6.75) \rightarrow for (M \leq 6.75) \\ 0 \rightarrow for (M > 6.75) \end{cases} \quad (4.6)$$

where Δa_4 is the adjustment coefficient determined by regression. The model fit to the residuals by Equation 4.6 is presented in Figure 4.1 by the black line. Please note that the selected adjustment function has a cut-off value at M=6.75. This cut-off value is selected to be consistent with the AS08 basic model (Equation 4.3) and to preserve the well-constrained large magnitude parameters of the AS08 model.

Mean values and standard deviations of Δa_4 coefficients across the spectral periods are shown in Figure 4.2. To develop a smooth model as a function of the spectral period, Δa_4 values are smoothed (smoothed values represented by the red line in Figure 4.2). The smoothed Δa_4 values are added to original a_4 values in Equation 4.3 in the Turkey-Adjusted AS08 model. List of the adjusted a_4 values (denoted by a_4*) is provided in Table 4.2 at the end of this chapter.

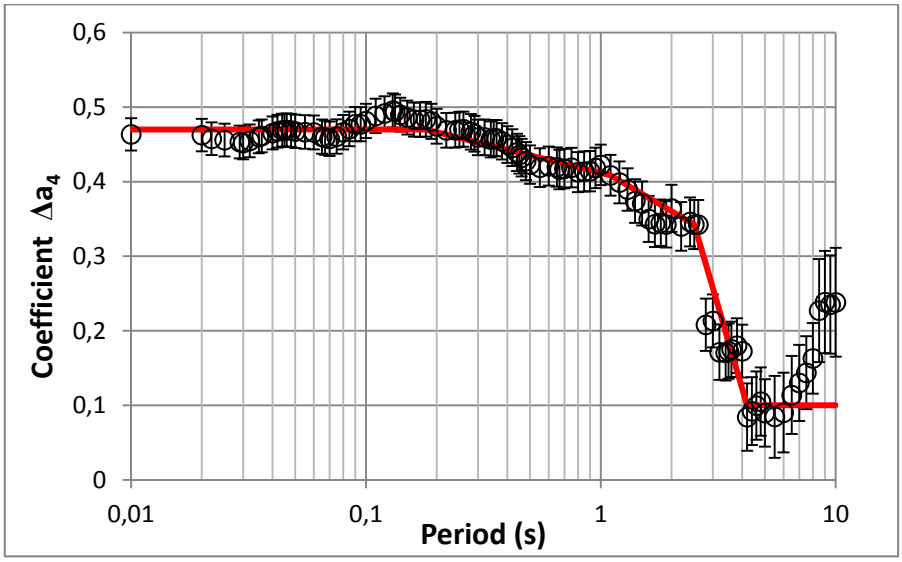

Figure 4.2 Adjustment coefficient Δa_4 for Abrahamson and Silva (2008)

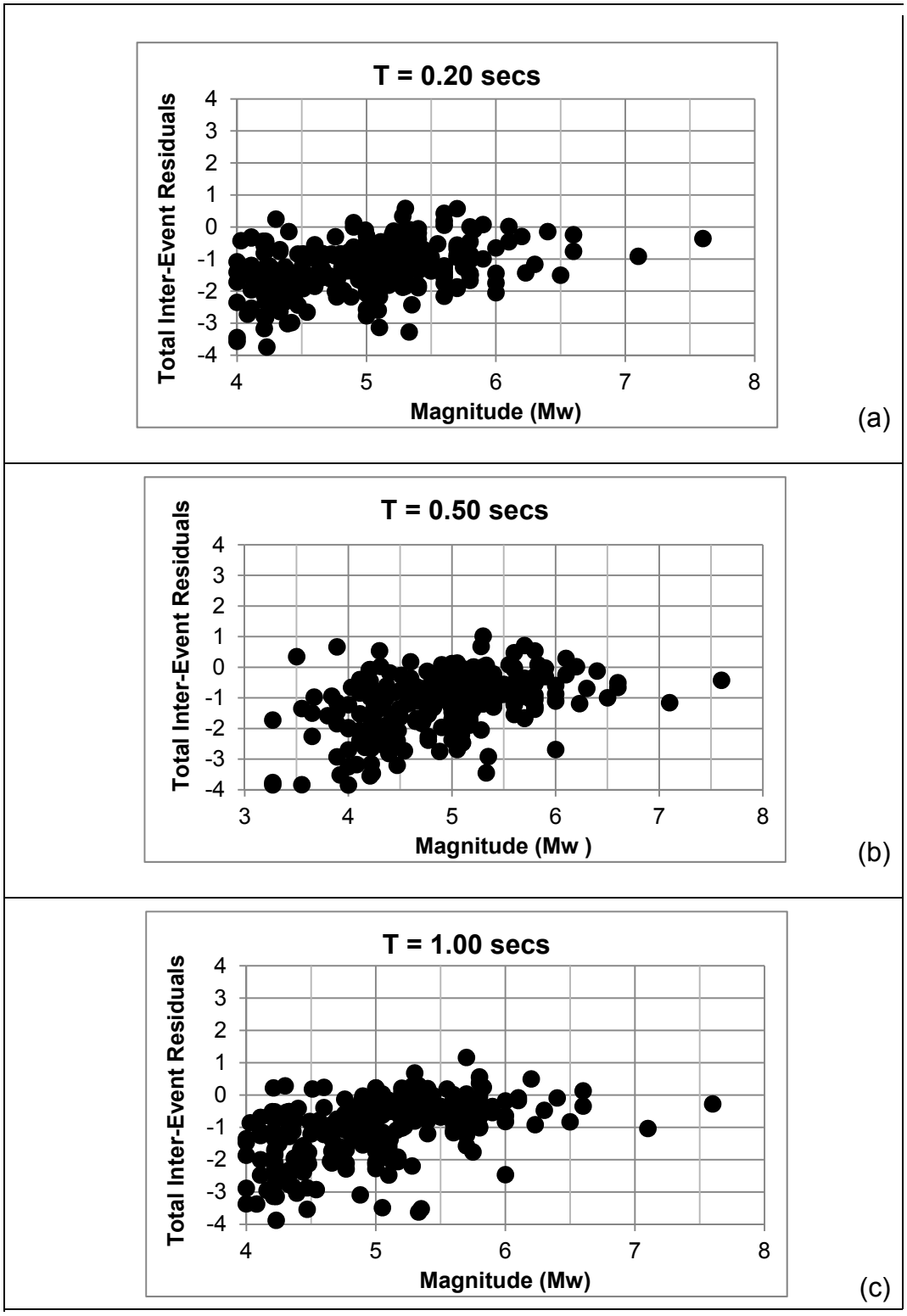

Figure 4.3 Residuals vs. M_w at a) T = 0.2 secs, b) T =0.5 secs and c) T = 1.00 secs for original Abrahamson and Silva (2008)

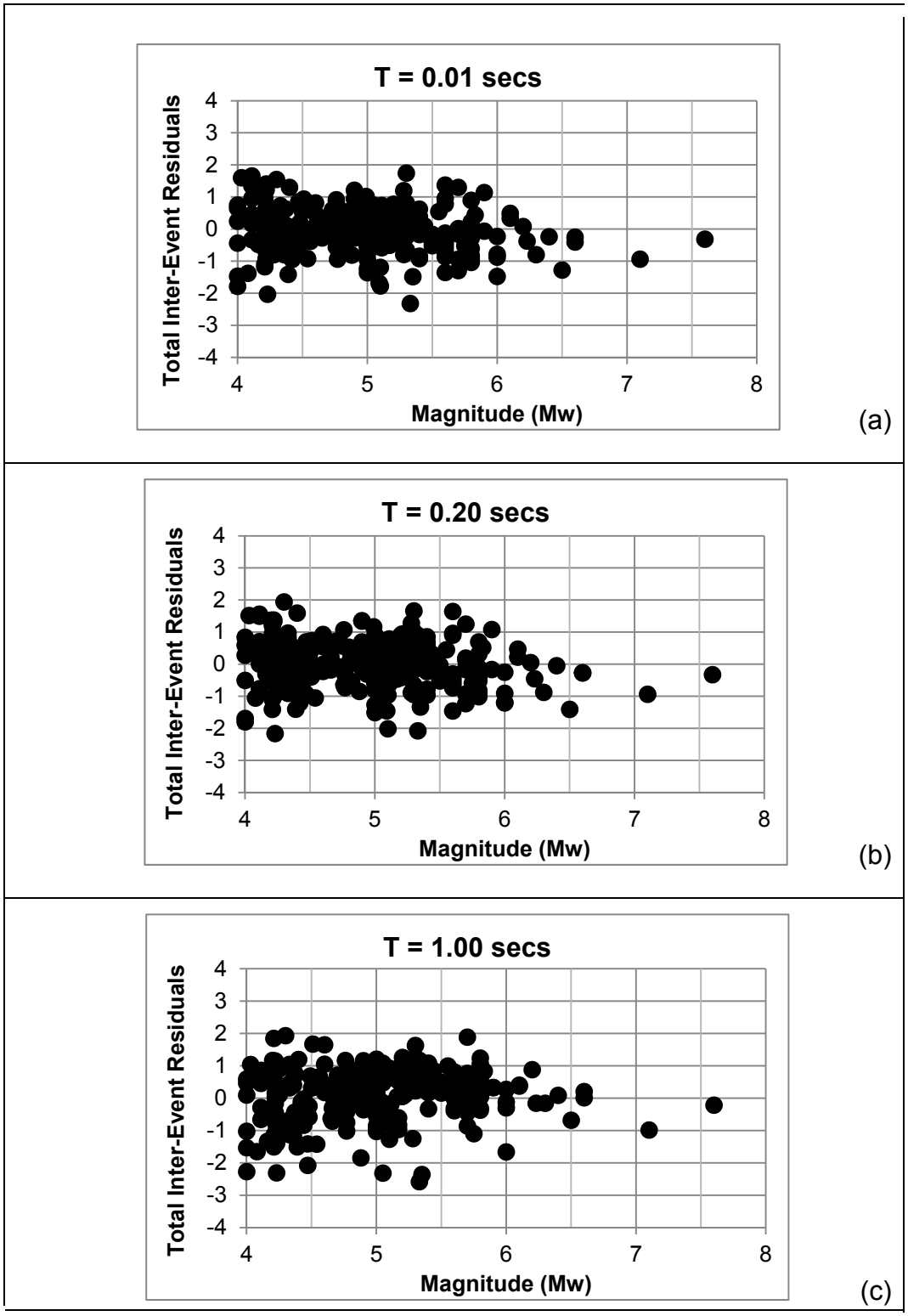

Figure 4.4 Residuals vs. M_w at a) T = 0.01 secs, b) T =0.20 secs and c) T = 1.00 secs for modified Abrahamson and Silva (2008)

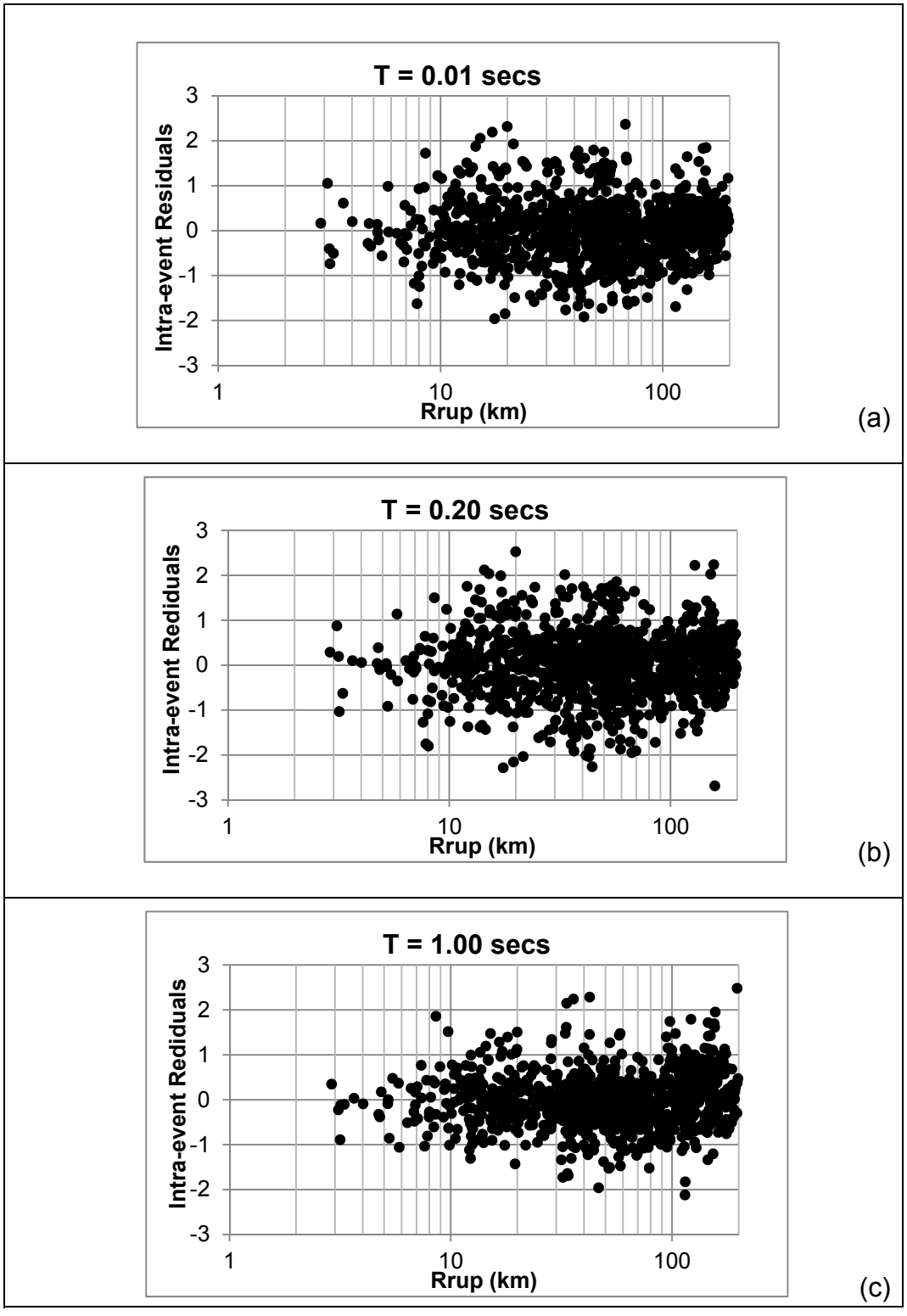

Figure 4.5 Residuals vs. R_{rup} at a) T = 0.01 secs, b) T =0.20 secs and c) T = 1.00 secs for original Abrahamson and Silva (2008)

After the magnitude adjustment, the model residuals are re-calculated using the modified form of AS08 model. The total inter-event residuals after the magnitude adjustment are plotted by moment magnitude in Figure 4.4 for 0.01, 0.2 and, 1 second spectral periods showing that the total inter-event residuals of the adjusted model are evenly distributed along the zero line. Intra-event residuals are plotted with respect to rupture distance in Figure 4.5 for PGA, T=0.2, and T=1 second spectral periods, suggesting no trend within the applicability range of the NGA-W1 models for tectonic regions other than Western US (100 kilometers, Power et al., 2008). However, AS08 model slightly underestimates the ground motions in Turkish comparison dataset for rupture distances within 100-200 km range. The large distance scaling (denoted as the gamma-term) piece of the AS08 model is shown in Equation 4.7:

$$\gamma = \begin{cases} 0 \rightarrow for(R_{rup} < 100) \\ a_{18}(R_{rup} - 100)T_6(M) \rightarrow for(R_{rup} \geq 100) \end{cases} \quad (4.7)$$

where a_{18} is the regressed coefficient and $T_6(M)$ is the magnitude taper defined in Abrahamson and Silva (2008) as:

$$T_6(M) = \begin{cases} 1 \rightarrow for(M < 5.5) \\ 0.5(6.5 - M) + 0.5 \rightarrow for(5.5 \leq M \leq 6.5) \\ 0.5 \rightarrow for(M > 6.5) \end{cases} \quad (4.8)$$

The gamma term of AS08 model is adjusted for the comparison dataset by modifying the a_{18} coefficient as:

$$a_{18}{}^{*} = \Delta a_{18} + a_{18} \quad (4.9)$$

where Δa_{18} values across the periods are determined by regressing the residuals using the functional form presented in Equation 4.7. Mean values and standard deviations of Δa_{18} coefficient across the spectral periods are presented in Figure 4.6. To develop a smooth model as a function of the spectral period, Δa_{18} values are smoothed (shown by the red line in Figure 4.6). The smoothed Δa_{18} values are added to original a_{18} values as given in

Equation 4.9 in the Turkey-Adjusted AS08 model and list of the adjusted a_{18} values is provided in Table 4.2.

After the distance adjustment, the intra-event residuals are re-calculated using the modified form of AS08 model. Intra-event residuals of the modified model are plotted with respect to rupture distance in Figure 4.7 for PGA, T=0.2, and T=1 second spectral periods, indicating that the modified large distance scaling of the model is compatible with the comparison dataset.

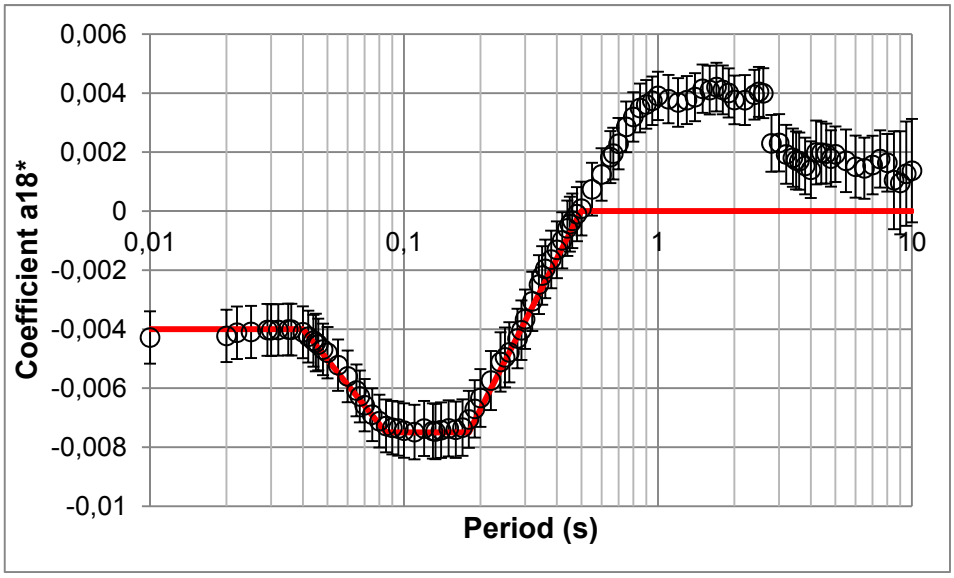

Figure 4.6 Adjustment coefficient $a_{18}{}^{*}$ for Abrahamson and Silva (2008)

Next step is to evaluate the site effects scaling of the AS08 model by plotting the re-calculated intra-event residuals using the modified form of AS08 model, a sample residual plot for PGA is provided in Figure 4.11. It is observed that the AS08 model slightly under-predicts the ground motions in the Turkey comparison dataset at stiff soil/engineering rock sites but this effect diminishes as Vs30 decreases.

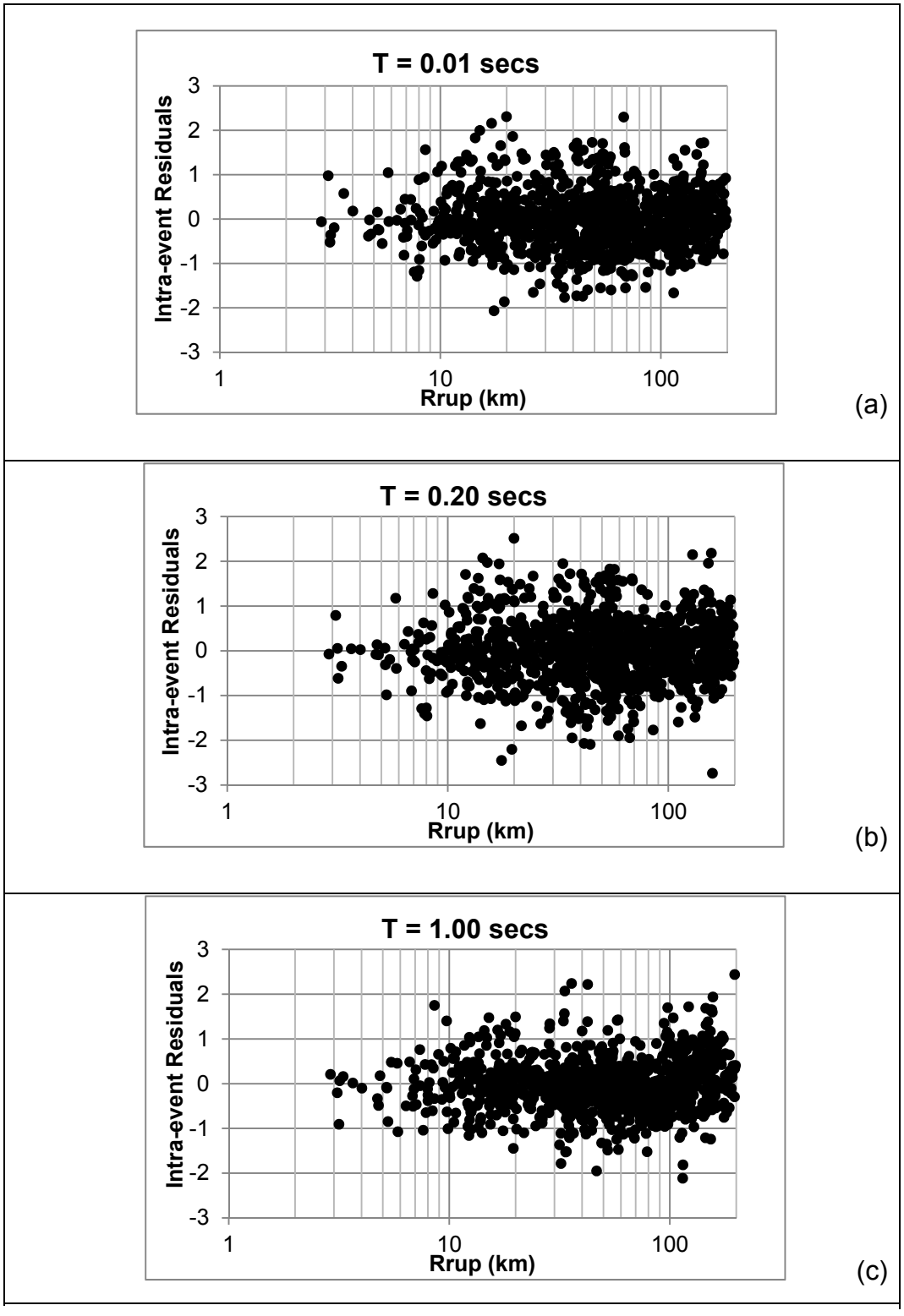

Figure 4.7 Residuals vs. R_{rup} at a) T = 0.01 secs, b) T =0.20 secs and c) T = 1.00 secs for modified Abrahamson and Silva (2008)

This observation may be expected since approximately 40% of the AS08 model dataset consist of data from Taiwan (1999 Chi-Chi Earthquake) and deeper shear wave velocity profiles of the recording stations in Taiwan and Western US were found to be different by Lin et al. (2007). Same trend is also observed in other spectral periods, residual plots for 0.2, 0.5 and, 1 second spectral periods are provided in Figure 4.12. Therefore, the adjustment term for the site effects is chosen as:

$$f_{5\_TA} \begin{cases} 0 \rightarrow for(V_{S30}{}^{*} < V_{S30,hinge}(T)) \\ a_9 * ln(V_{S30}{}^{*}/V_{S30,hinge}(T) \rightarrow for(V_{S30}{}^{*} \geq V_{S30,hinge}(T))) \end{cases} \quad (4.10)$$

where $V_{S30,hinge}(T)$ is the cut-off shear wave velocity value for a particular period T, below which no trend is observed in the residuals, $V_{S30}{}^{*}$ is the shear wave velocity value used in AS08 model and a_9 is the regression coefficient. For each period, the $V_{S30,Hinge}(T)$ is determined statistically as the beginning point of the curvature for the 3rd degree polynomial fit to the residuals (shown in Figure 4.8).

$V_{S30,hinge}(T)$ values across the periods are presented in Figure 4.9, along with the $V_{S30,LIN}(T)$ values which represent the end of non-linear site effects in AS08 model. It is significant that for periods longer than 0.6 seconds, these two values are very close to each other. Mean values and standard deviations of a_9 coefficient across the spectral periods are shown in Figure 4.10 along with the smoothed values (the red line in Figure 4.9). The adjustment function provided in Equation 4.10 is added to the Turkey-Adjusted AS08 model and the intra event residuals were re-plotted to observe that the intra-event residuals for the Turkey-Adjusted AS08 model are evenly distributed along the zero line (Figure 4.13). List of the a_9 and $V_{S30,hinge}$ coefficients is provided in Table 4.2.

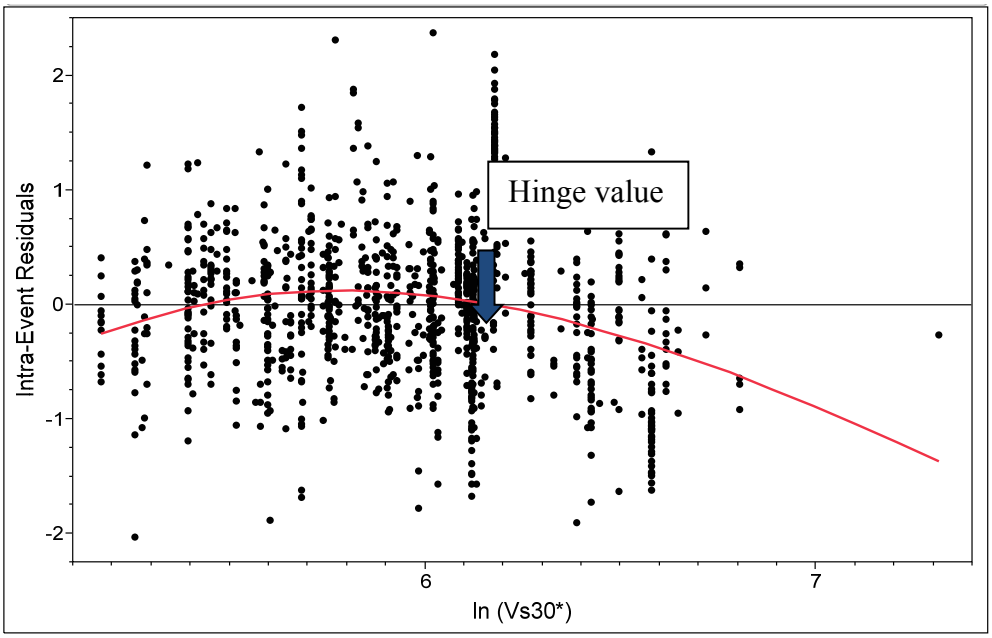

Figure 4.8 Intra-Event Residuals vs. ln(V_{S30}) for Abrahamson and Silva (2008)

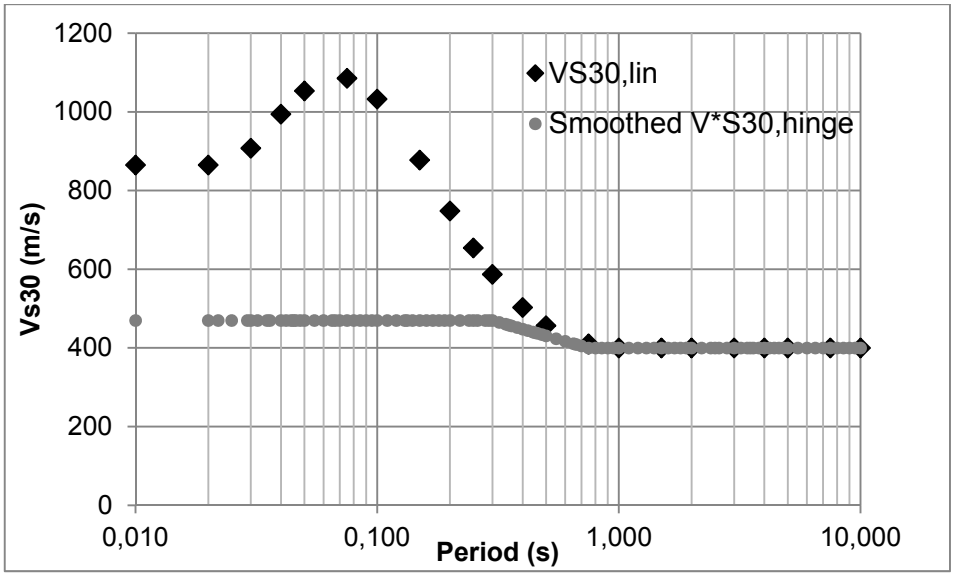

Figure 4.9 $V_{S30,lin}$ and $V^{*}_{S30,hinge}$ vs. period graph for Abrahamson and Silva (2008)

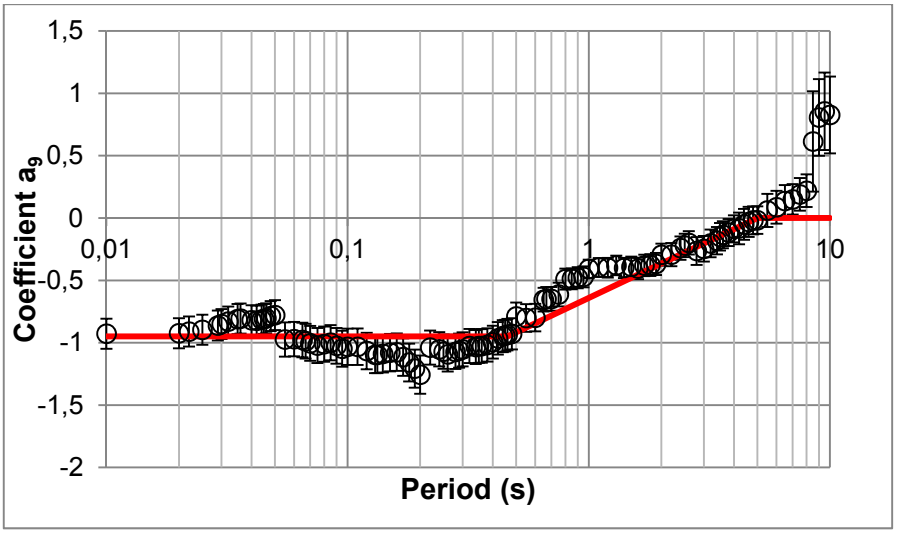

Figure 4.10 Adjustment coefficient a_9 for Abrahamson and Silva (2008)

Finally, the mean-offset values before and after the adjustments are presented in Figure 4.11. Remaining mean offset values are insignificant when compared to the original AS08 model up to 2 seconds spectral period, therefore the constant term in the model is not modified to reflect the remaining main offset.

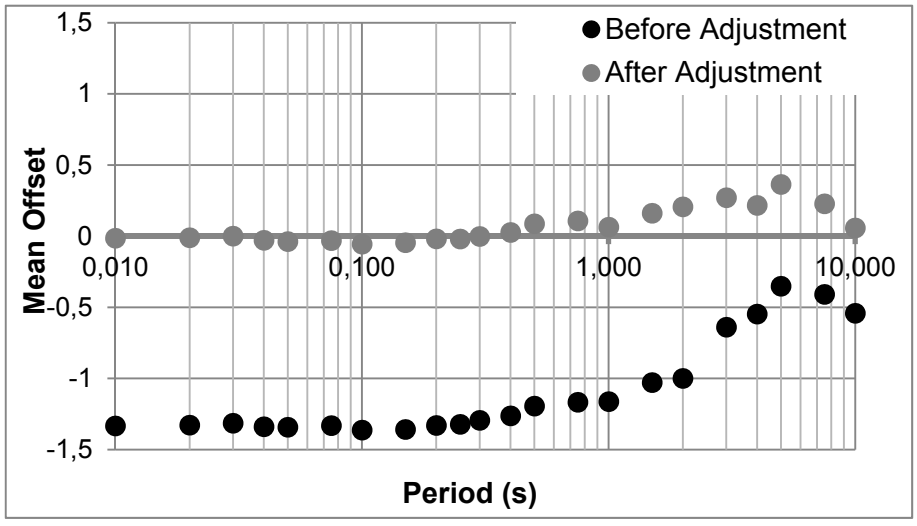

Figure 4.11 Mean offset vs. period for modified Abrahamson and Silva (2008) model

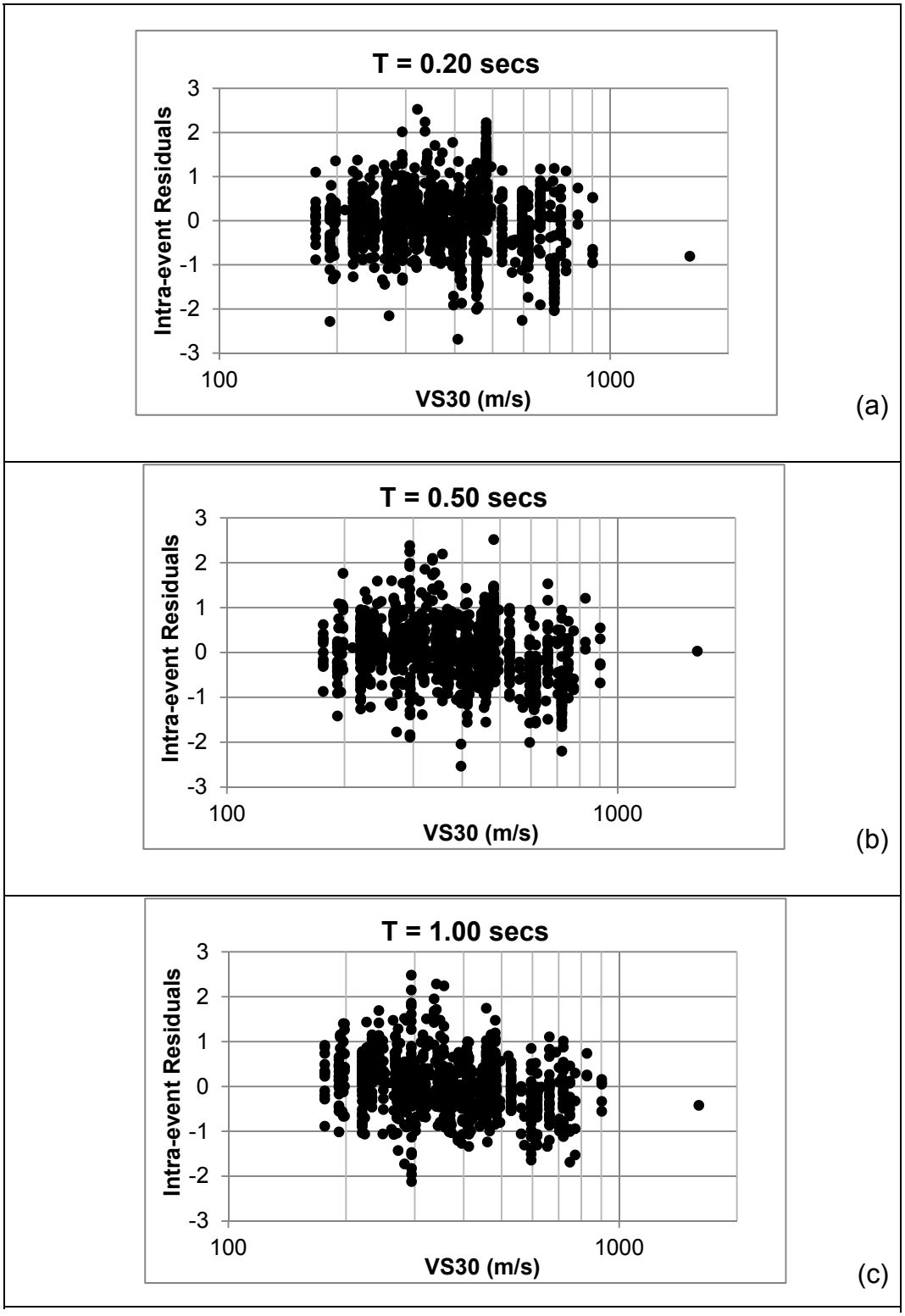

Figure 4.12 Residuals vs Vs30 at a) T = 0.20 secs, b) T =0.50 secs and c) T = 1.00 secs for original Abrahamson and Silva (2008)

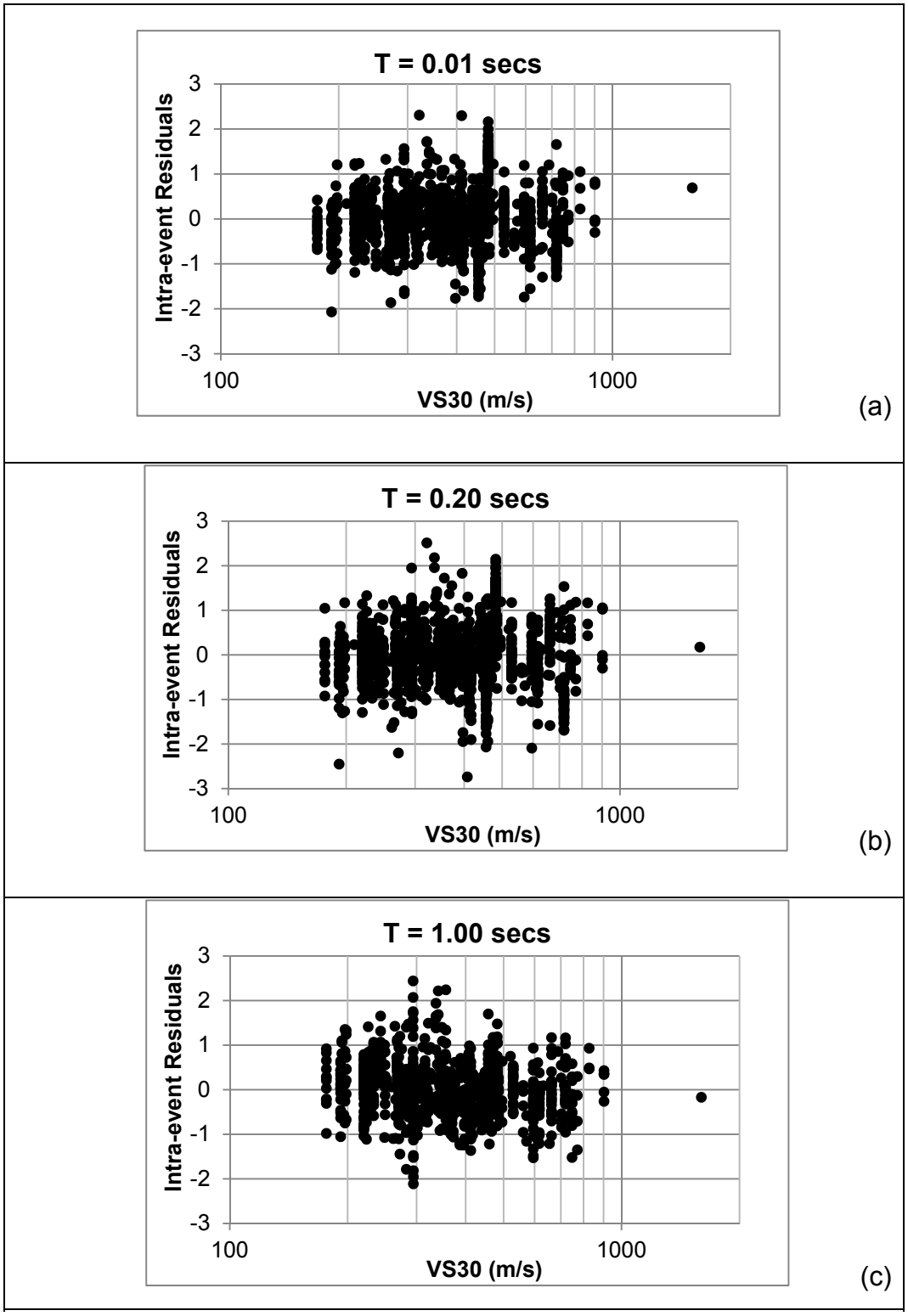

Figure 4.13 Residuals vs Vs30 at a) T = 0.01 secs, b) T =0.20 secs and c) T = 1.00 secs for modified Abrahamson and Silva (2008)

4.2.2 Boore and Atkinson 2008 (BA08) Model

Boore and Atkinson (2008) aimed a simple functional form with minimum required predictor variables for their GMPE. Magnitude scaling term of their function is modeled with a break in the magnitude scaling with period dependent regression coefficient M_h (hinge magnitude):

a) $M \leq M_h$

$$F_M(M) = e_1 U + e_2 SS + e_3 NS + e_4 RS + e_5 (M - M_h) + e_6 (M - M_h)^2 \quad (4.11a)$$

b) $M > M_h$

$$F_M(M) = e_1 U + e_2 SS + e_3 NS + e_4 RS + e_7 (M - M_h) \quad (4.11b)$$

where e_1-e_7 are the model coefficients, M is the moment magnitude, M_h is hinge magnitude, U, SS, NS and RS are dummy variables used for denoting unspecified, strike-slip, normal-slip, and reverse-slip fault type, respectively.

Initially, the total inter-event residuals are plotted with respect to moment magnitude for PGA as shown in Figure 4.14 (total inter-event residuals presented by grey dots).

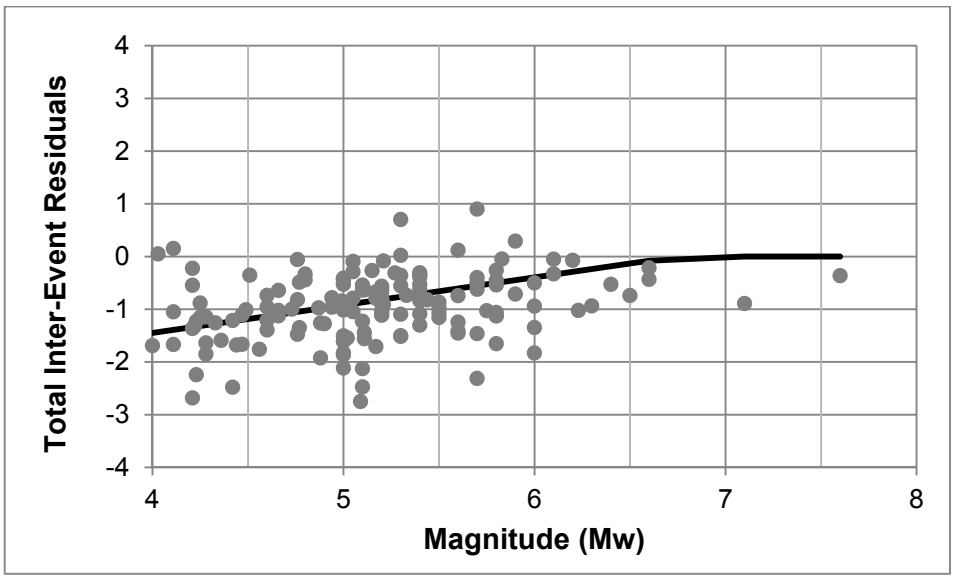

Figure 4.14 Residuals vs. M_w at PGA for original Boore and Atkinson (2008)

Again, it is observed that ground motions in the dataset are overestimated, especially for small-to-moderate magnitude earthquakes by this model. This trend is persistent for all spectral periods, as can be seen from the provided residual plots for 0.2, 0.5 and, 1 second spectral periods given in Figure 4.16. Figures 4.14 and 4.16 suggest that the magnitude scaling of the comparison dataset is drastically different that the BA08 model and this feature needs to be fixed to consider the model applicable in Turkey. As previously mentioned, preserving the well-constrained pieces of the model is critical, since the large magnitude earthquakes are poorly represented in the comparison dataset (see Figure 3.11) and any changes on large magnitude parameters will have a major impact on the hazard calculations. Considering these aspects, the misfit between the actual and predicted data is modeled by Equation 4.12:

$$F_{M\_TA}(M) = \begin{cases} \Delta e_5 * (M_w - 6.75) \rightarrow for (M_w \leq 6.75) \\ 0 \rightarrow for (M_w > 6.75) \end{cases} \quad (4.12)$$

where M_w is moment magnitude and Δe_5 is the adjustment coefficient determined by regression. The model fit to the residuals by Equation 4.12 is presented in Figure 4.14 by the black line. It should be noted that the selected adjustment function has a cut-off value at M=6.75. In BA08 model hinge magnitude (M_h) for magnitude scaling function is given as 6.75 for periods up to 5 seconds and as 8.00 for the rest of the periods. The cut-off value at M=6.75 is selected as to be consistent with the BA08 basic model (Equation 4.11) and to preserve the well-constrained large magnitude parameters of the BA08 model. Mean values and standard deviations of Δe_5 coefficients across the spectral periods are shown in Figure 4.15. Δe_5 values are smoothed (smoothed values represented by the red line in Figure 4.16) to develop a smooth model as a function of the spectral period. The smoothed Δe_5 values are added to original e_5 values in Equation 4.11 in the Turkey-Adjusted BA08 model. List of the adjusted e_5 values (denoted by $e_5 *$) is provided in Table 4.2.

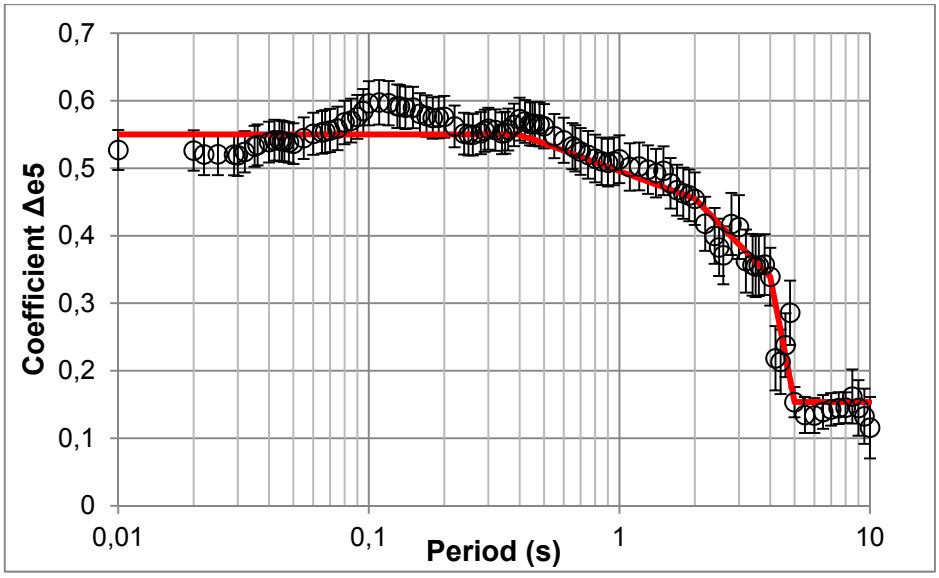

Figure 4.15 Adjustment coefficient Δe_5 for Boore and Atkinson (2008)

After the magnitude adjustment, the model residuals are re-calculated using the modified form of BA08 model. The total inter-event residuals after the magnitude adjustment are plotted by moment magnitude in Figure 4.17 for 0.01, 0.2 and, 1 second spectral periods. From inspecting these plots, it is observed that the total inter-event residuals of the adjusted model are evenly distributed along the zero line. Intra-event residuals are plotted with respect to rupture distance in Figure 4.18 and with respect to V_{S30} in Figure 4.19 for PGA, T=0.2, and T=1 second spectral periods. Unlike AS08 model, BA08 model does not include any trend in site effects scaling term as this model does not include aftershock events mainly from Taiwan in its database. For distance scaling, a trend is observed at large distance similar to AS08 model. But, since the BA08 model does not include any large distance term in their function, this trend is not corrected. Therefore no adjustment is made for distance scaling and site effects scaling terms of BA08 model.

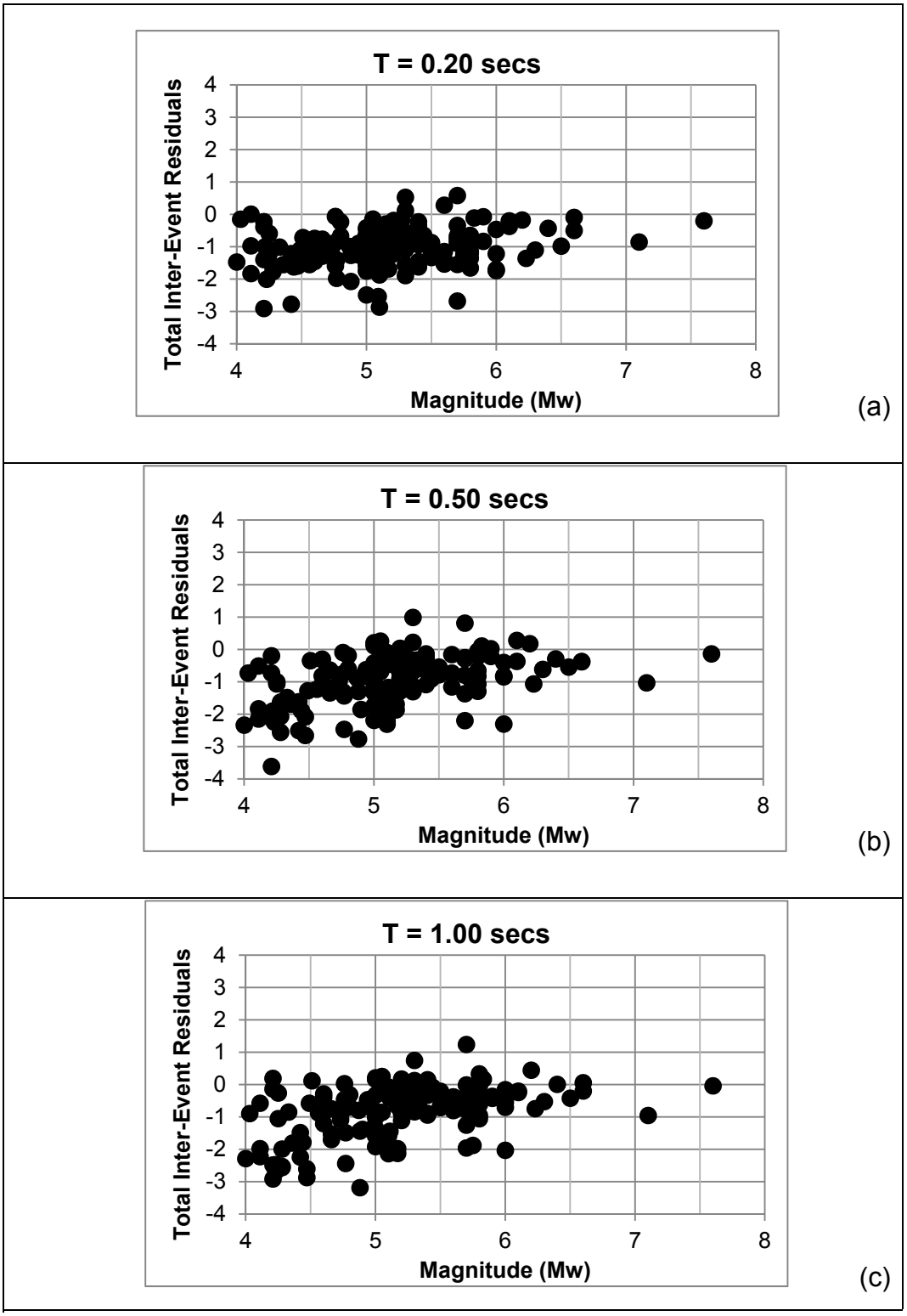

Figure 4.16 Residuals vs. M_w at a) T = 0.20 secs, b) T =0.50 secs and c) T = 1.00 secs for original Boore and Atkinson (2008)

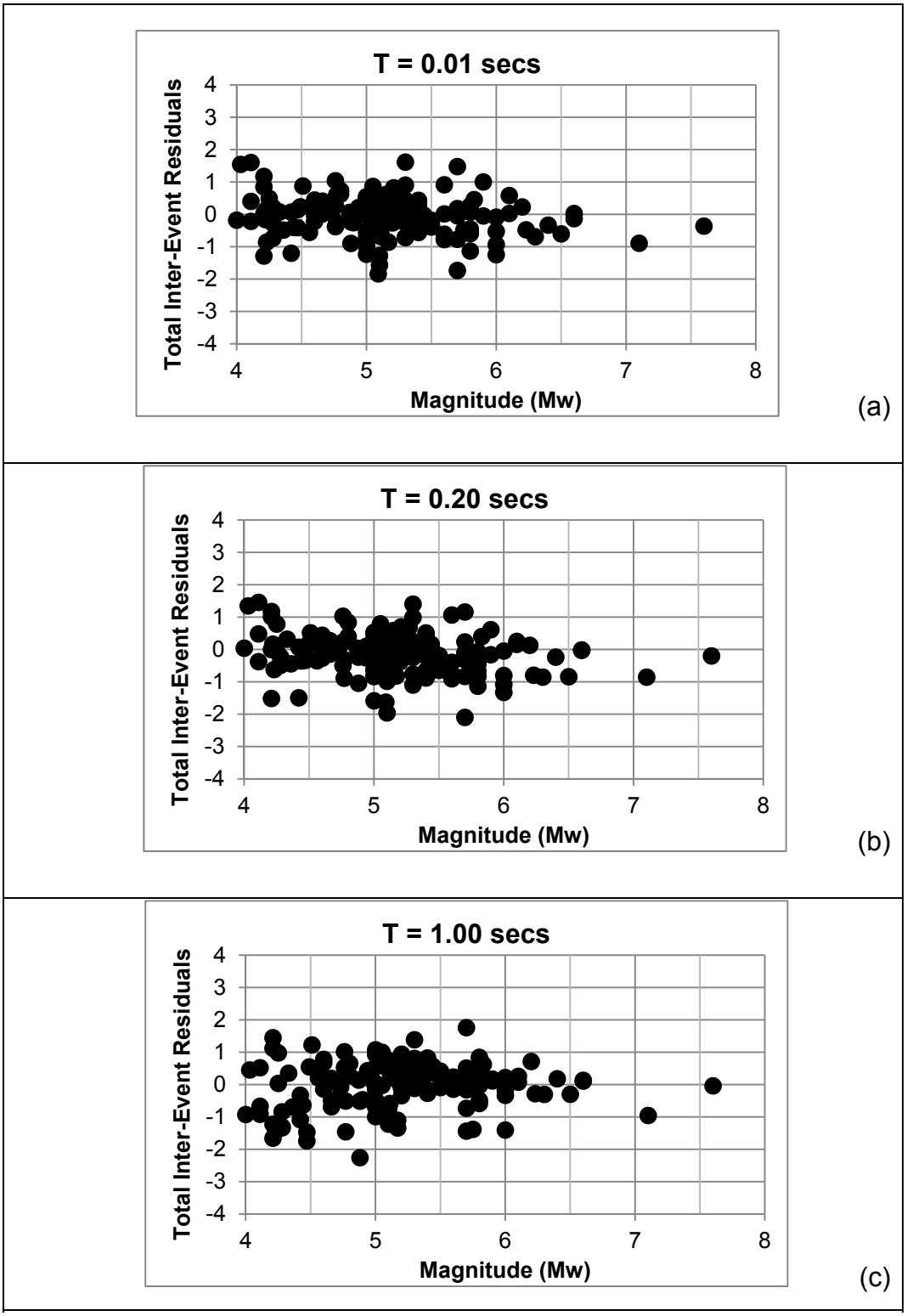

Figure 4.17 Residuals vs. M_w at a) T = 0.01 secs, b) T =0.20 secs and c) T = 1.00 secs for modified Boore and Atkinson (2008)

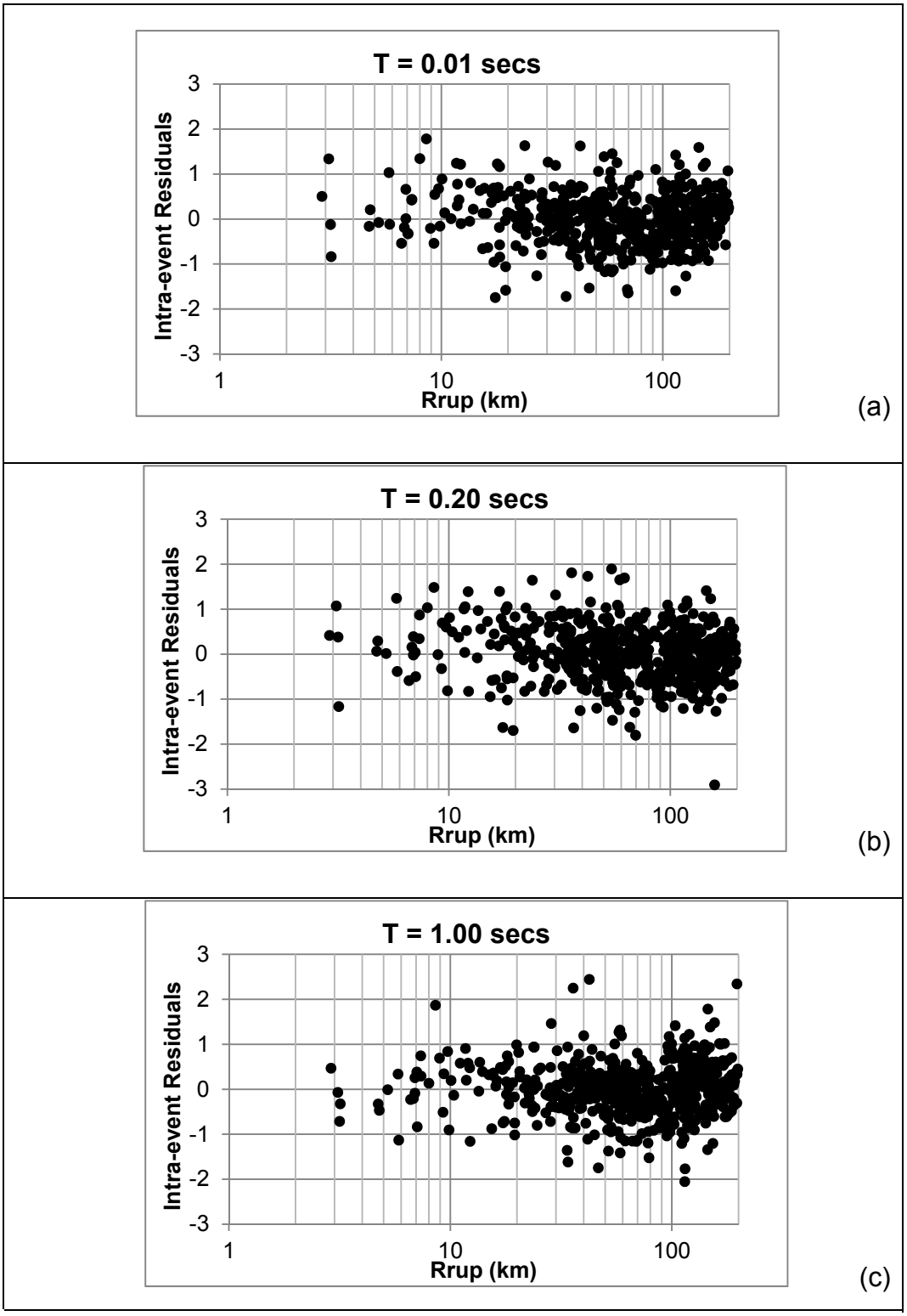

Figure 4.18 Residuals vs. R_{rup} at a) T = 0.01 secs, b) T =0.20 secs and c) T = 1.00 secs for original Boore and Atkinson (2008)

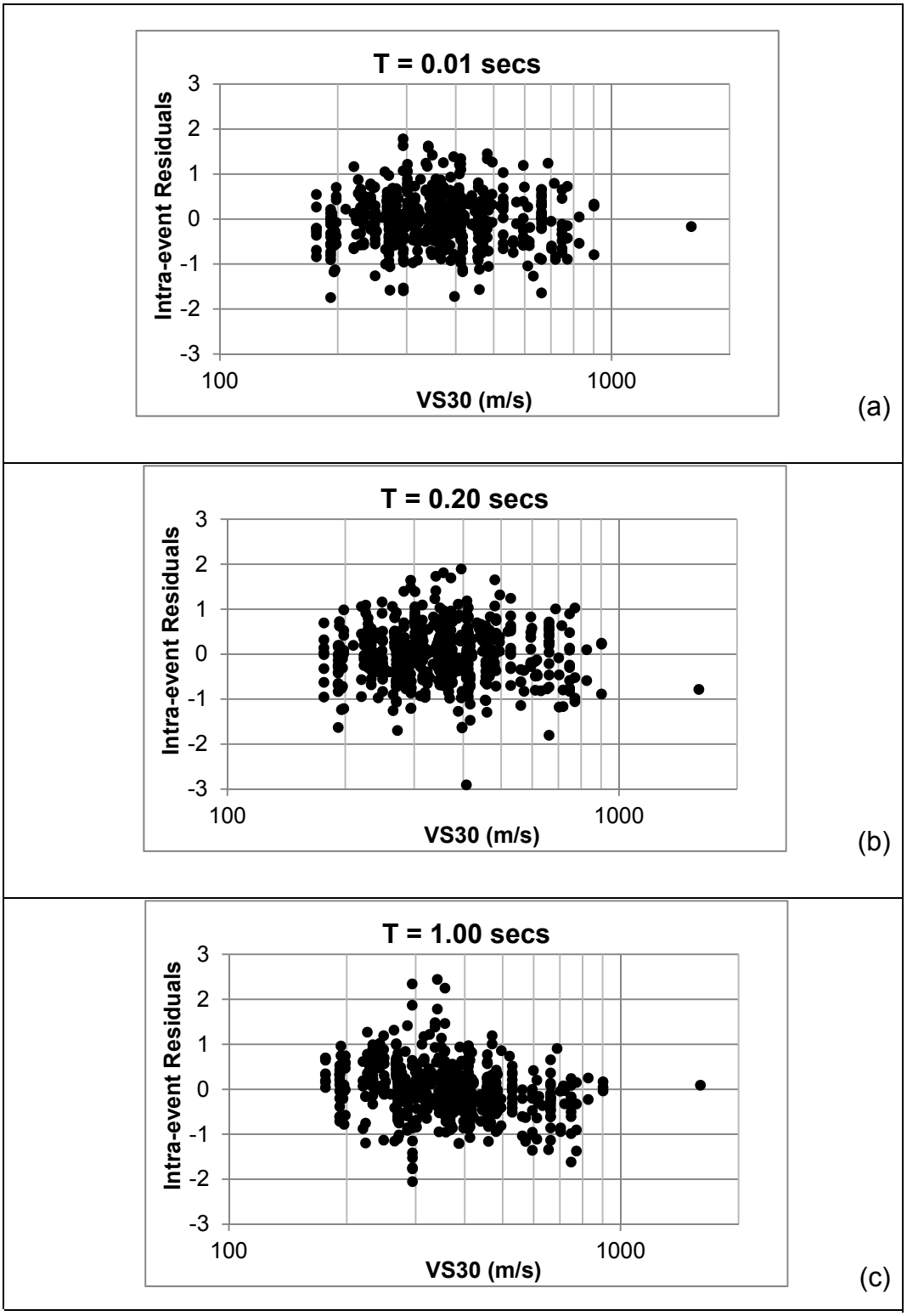

Figure 4.19 Residuals vs Vs30 at a) T = 0.01 secs, b) T =0.20 secs and c) T = 1.00 secs for original Boore and Atkinson (2008)

Finally, the mean-offset values for before and after the adjustments are presented in Figure 4.20. Remaining mean offset values are insignificant when compared to the original BA08 model, therefore the constant term in the model is not modified.

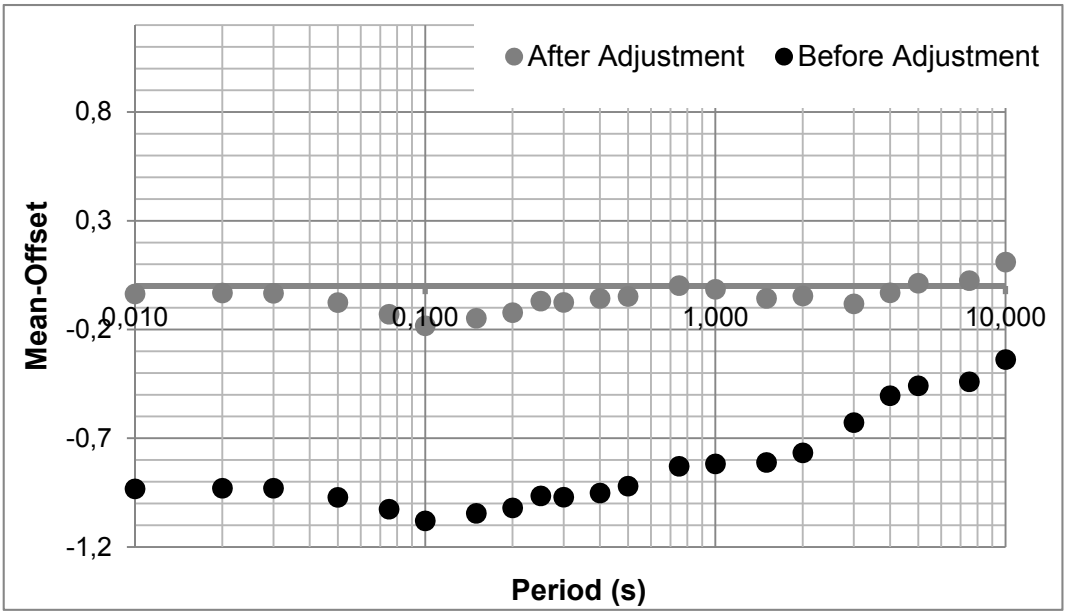

Figure 4.20 Mean offset vs. period for modified Boore and Atkinson (2008) model

4.2.3 Campbell and Bozorgnia 2008 (CB08) Model

The basic form of the CB08 model for strike-slip earthquakes recorded on rock sites was modeled using piecewise linear relationship as shown in Equation 4.13:

$$f_{mag} = \begin{cases} c_0 + c_1 M & M \leq 5.5 \\ c_0 + c_1 M + c_2(M - 5.5) & 5.5 < M \leq 6.5 \\ c_0 + c_1 M + c_2(M - 5.5) + c_3(M - 6.5) & M > 6.5 \end{cases} \quad (4.13)$$

where c_0-c_3 are the model coefficients and M is the moment magnitude.

Initially, total inter-event residuals are plotted with respect to moment magnitude for PGA as shown in Figure 4.21 (total inter-event residuals presented by grey dots). Similar with AS08 and BA08 models, ground motions in the dataset are overestimated by the CB08 model significantly, especially for small-to-moderate magnitude earthquakes. The trend is persistent for all spectral periods, residual plots for 0.2, 0.5 and, 1 second spectral periods are provided in Figure 4.23. Figures 4.21 and 4.23 suggest that the magnitude scaling of the comparison dataset is drastically different than the CB08 model and this feature needs to be fixed to consider the model applicable in Turkey.

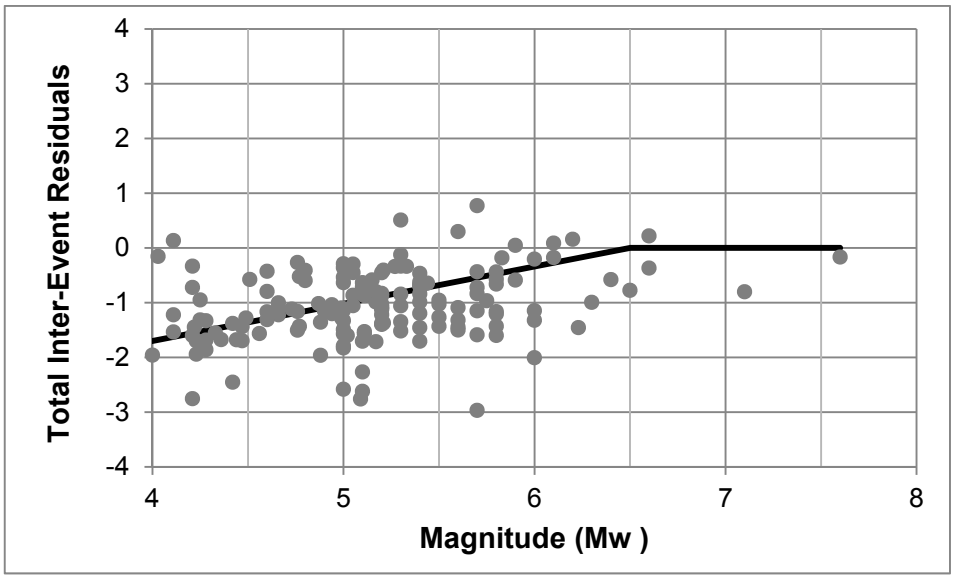

Figure 4.21 Residuals vs. M_w at PGA for original CB08 model

The misfit between the actual and predicted data is modeled by Equation 4.14:

$$f_{mag\_TA} = \begin{cases} c_{13} * (M - 6.50) \rightarrow for(M \leq 6.50) \\ 0 \rightarrow for(M > 6.50) \end{cases} \quad (4.14)$$

Where M is moment magnitude and c_{13} is the new defined coefficient determined by regression. The model fit to the residuals by Equation 4.14 is

presented in Figure 4.21 by the black line. Please note that the selected adjustment function has a cut-off value at M=6.50 which is different value from AS08 and BA08 models. This cut-off value is selected to be consistent with the functional form of CB08 basic model (Equation 4.13) and to preserve the well-constrained large magnitude parameters of the model. Rather than modifying the given coefficients, a new coefficient is introduced into the model. The main reason behind this decision is not to change the large magnitude piece of the model while modifying c_0 for the trend. In order to avoid any correction at large magnitudes, this new function with hinge magnitude given in Equation 4.14 is added to the model.

Mean values and standard deviations of c_{13} coefficients across the spectral periods are shown in Figure 4.22. To develop a smooth model as a function of the spectral period, c_{13} values are smoothed (smoothed values represented by the red line in Figure 4.22). The smoothed c_{13} values are used in the Turkey-Adjusted CB08 model in terms of adding Equation 4.14 to the original CB08 model. List of the adjusted c_{13} values is provided in Table 4.2.

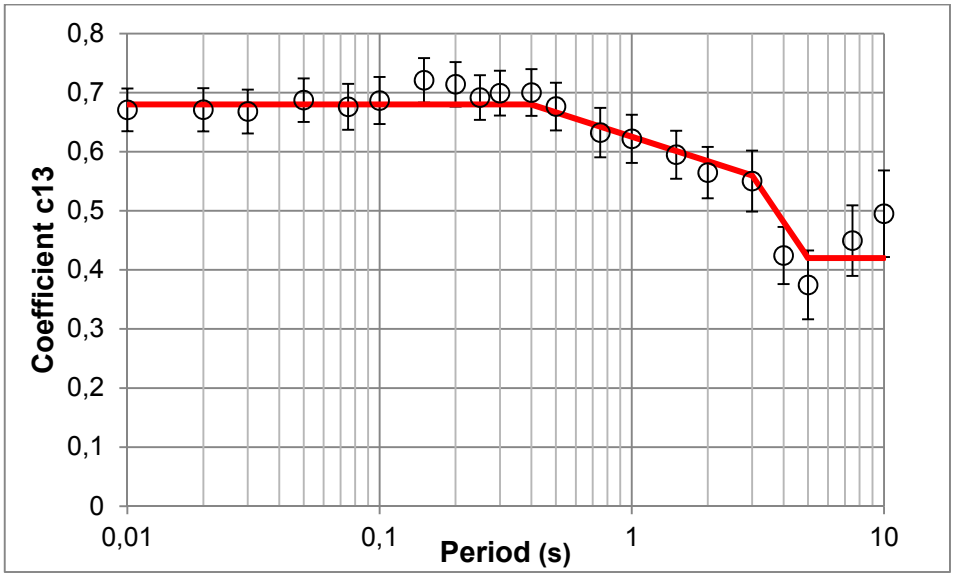

Figure 4.22 Adjustment coefficient c_{13} for Campbell and Bozorgnia (2008)

After the magnitude adjustment, the model residuals are re-calculated using the modified form of CB08 model. The total inter-event residuals after the magnitude adjustment are plotted by moment magnitude in Figure 4.25 for 0.01, 0.2 and, 1 second spectral periods. These plots show that the total inter-event residuals of the adjusted model are evenly distributed along the zero line which signifies the success of magnitude scaling adjustment.

Intra-event residuals are plotted with respect to rupture distance in Figure 4.26 and with respect to V_{S30} in Figure 4.27 for PGA, T=0.2, and T=1 second spectral periods. Only trend is observed in distance scaling at large distances. Since the CB08 model does not have a large distance term (gamma term) this trend cannot be corrected. Similar to BA08 model, CB08 model does not include any trend within site effects scaling, as this model does not include aftershock events in its database. Thus no adjustment is made for distance scaling and site effects scaling terms of CB08 model. The mean-offset values for before and after the adjustments are presented in Figure 4.23. Remaining mean offset values are scattered around -0.20 – 0.20 values therefore the constant term in the model is not modified.

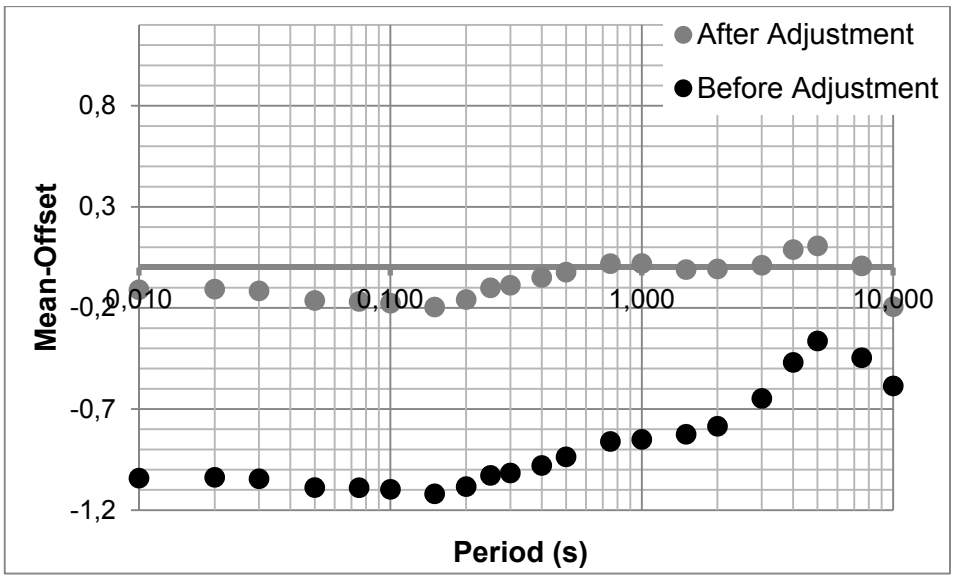

Figure 4.23 Mean offset vs. period for modified Campbell and Bozorgnia (2008) model

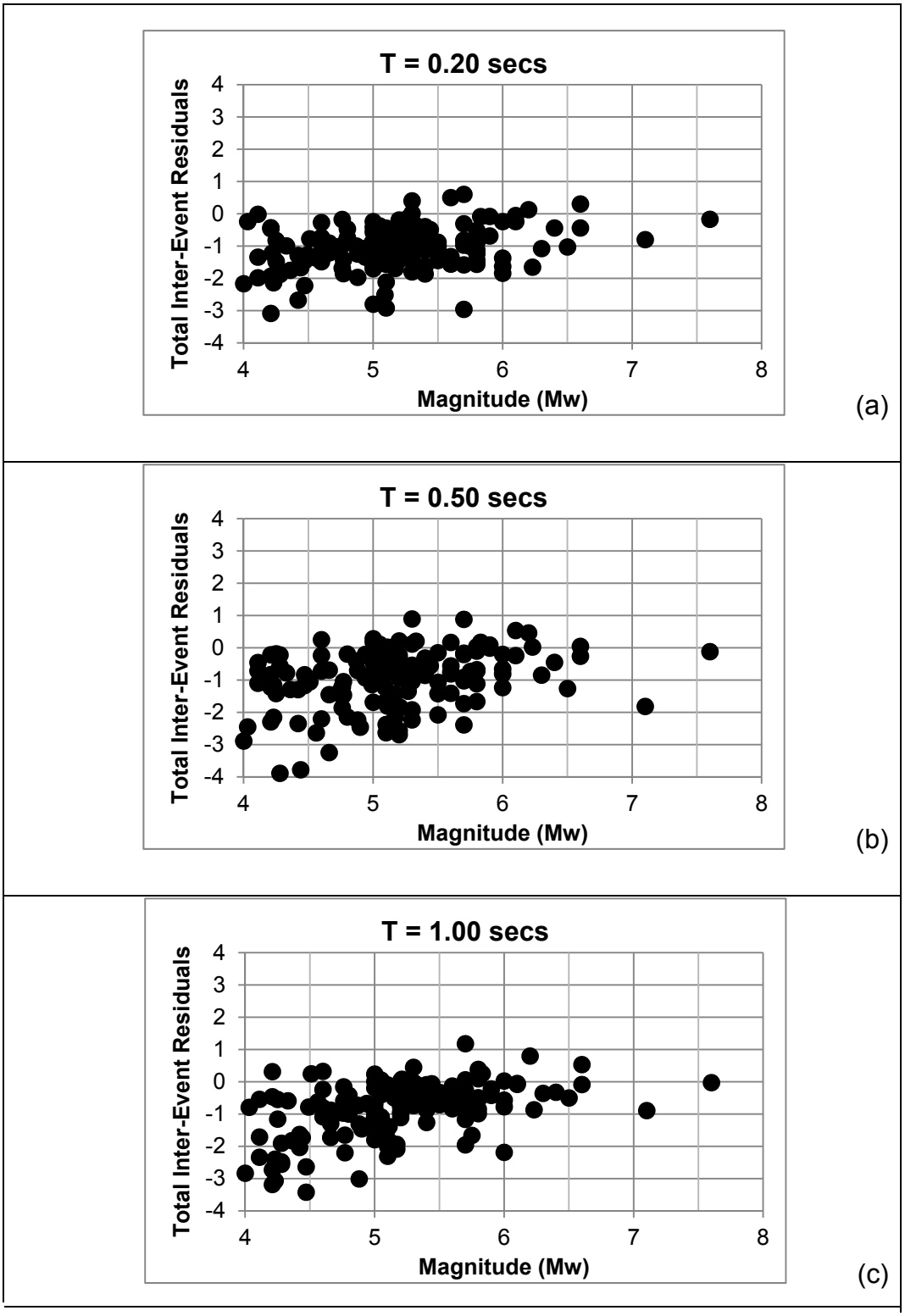

Figure 4.24 Residuals vs. M_w at a) T = 0.20 secs, b) T =0.50 secs and c) T = 1.00 secs for original Campbell and Bozorgnia (2008)

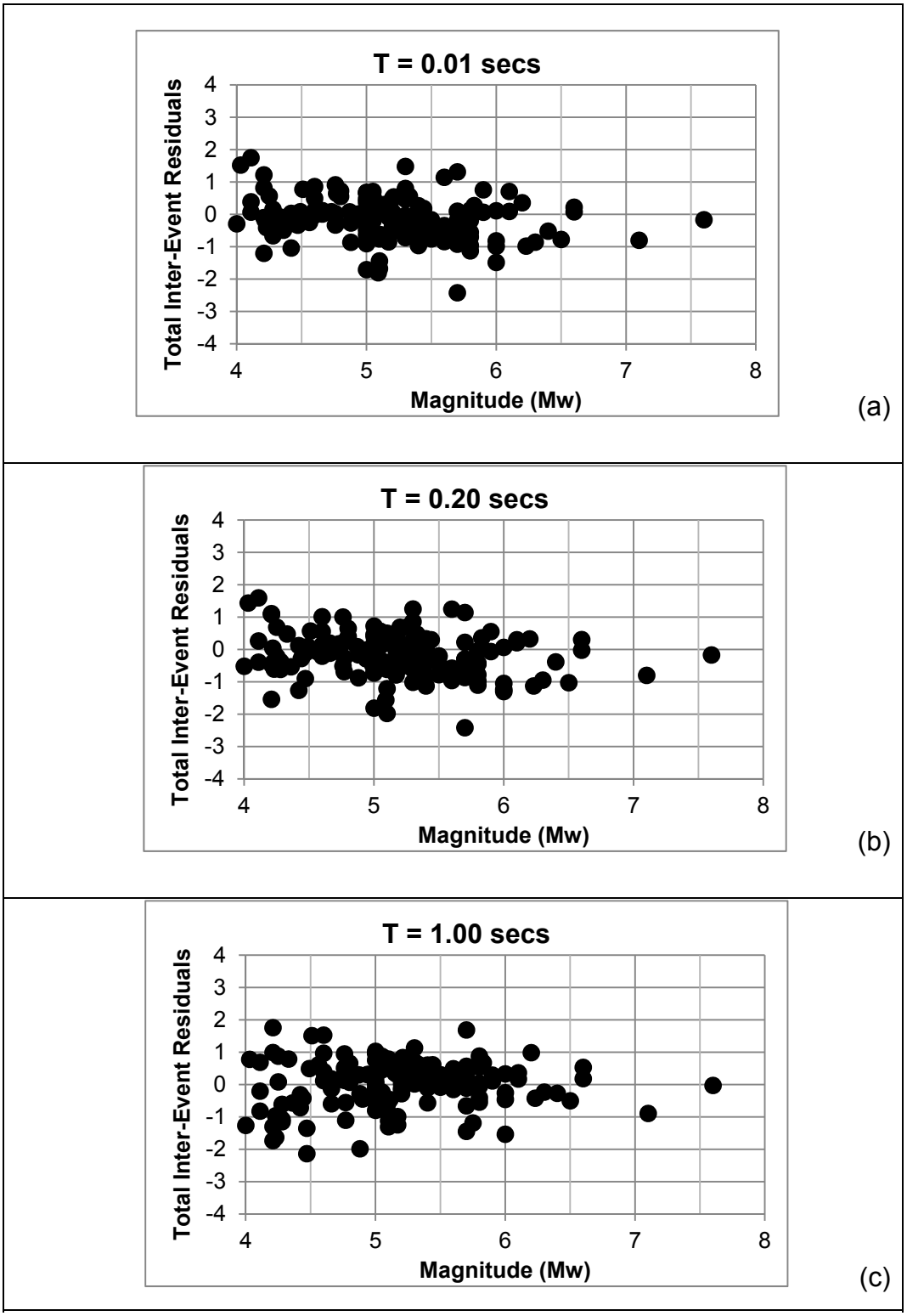

Figure 4.25 Residuals vs. M_w at a) T = 0.01 secs, b) T =0.20 secs and c) T = 1.00 secs for modified Campbell and Bozorgnia (2008)

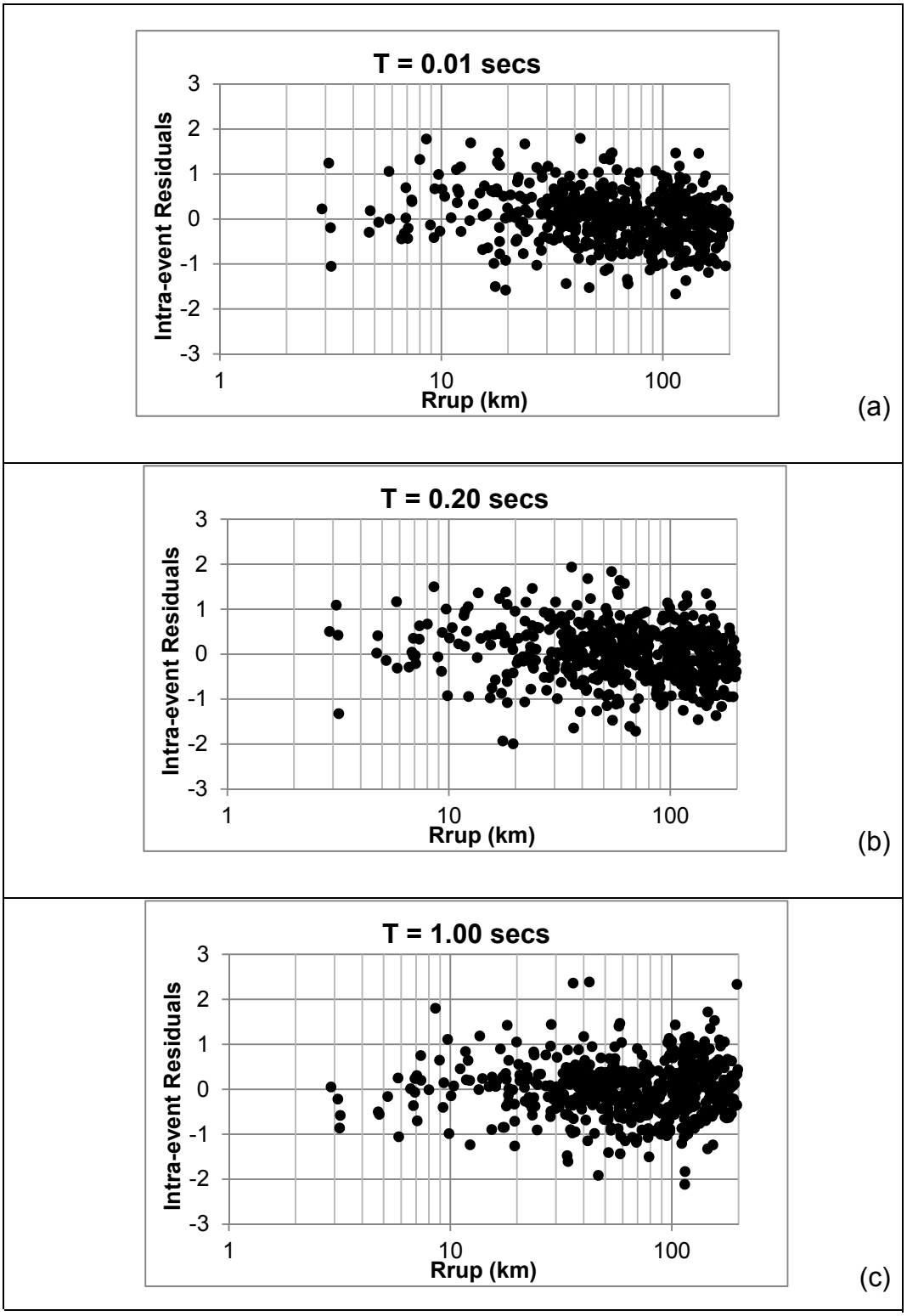

Figure 4.26 Residuals vs. R_{rup} at a) T = 0.01 secs, b) T =0.20 secs and c) T = 1.00 secs for original Campbell and Bozorgnia (2008)

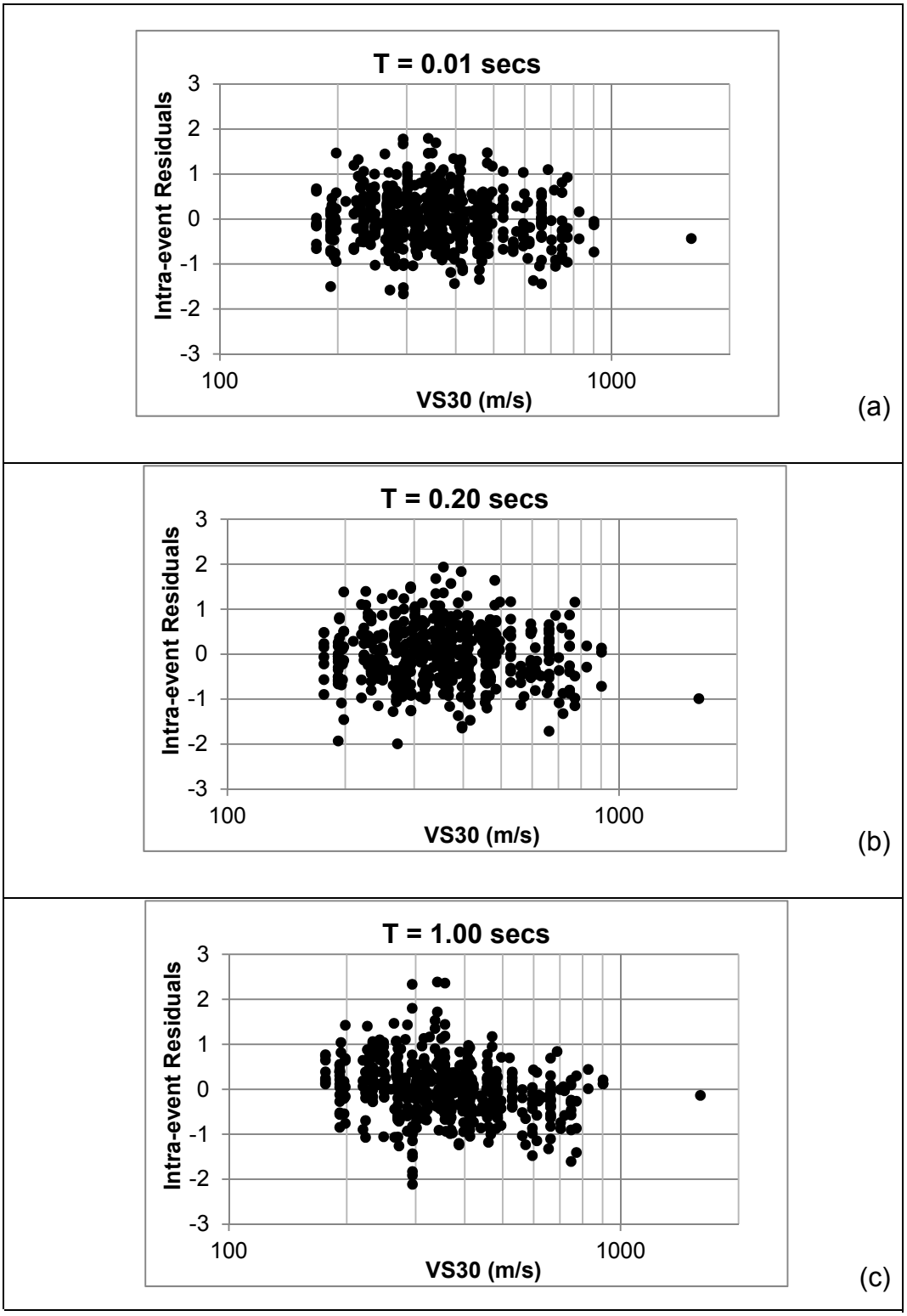

Figure 4.27 Residuals vs Vs30 at a) T = 0.01 secs, b) T =0.20 secs and c) T = 1.00 secs for original Campbell and Bozorgnia (2008)

4.2.4 Chiou and Youngs 2008 (CY08) Model

CY08 model shows similar aspect with AS08 model thus similar modifications are done for this model. The magnitude scaling function of CY08 model for strike-slip earthquakes recorded on rock sites was modeled with a functional form shown in Equation 4.15:

$$\ln(y) \propto c_2 M + \frac{(c_2 - c_3)}{c_n} * \ln(1 - \exp(c_n(c_m - M))) \quad (4.15)$$

where c_2 and c_3 are slope terms for magnitude scaling relationship, c_n is the controlling coefficient which governs the magnitude range over which transition from c_2 scaling to c_3 scaling occurs, c_m is the coefficient for defining magnitude value in the middle of this range and M is the moment magnitude.

Initially, total inter-event residuals are plotted with respect to moment magnitude for PGA as shown in Figure 4.28 (total inter-event residuals presented by grey dots). The ground motions in the dataset are overestimated by the CY08 model significantly, especially for small-to-moderate magnitude earthquakes similar to previously modified models. The trend is persistent for all spectral periods, which can be seen at residual plots for 0.2, 0.5 and, 1 second spectral periods provided in Figure 4.29. Figures 4.28 and 4.29 suggest that the magnitude scaling of the comparison dataset is drastically different that the CY08 model and this feature needs to be fixed to consider the model applicable in Turkey. The misfit between the actual and predicted data is modeled by Equation 4.16:

$$\Delta f_{mag\_TA}(M) = \begin{cases} c_{ta}(M - 6.75) \rightarrow for(M \leq 6.75) \\ 0 \rightarrow for(M > 6.75) \end{cases} \quad (4.16)$$

where $\Delta f_{mag\_TA}(M)$ is the magnitude term to be added to CY08 model and c_{ta} is the new defined adjustment coefficient to be determined by regression. The model fit to the residuals by Equation 4.16 is presented in Figure 4.28 by the black line.

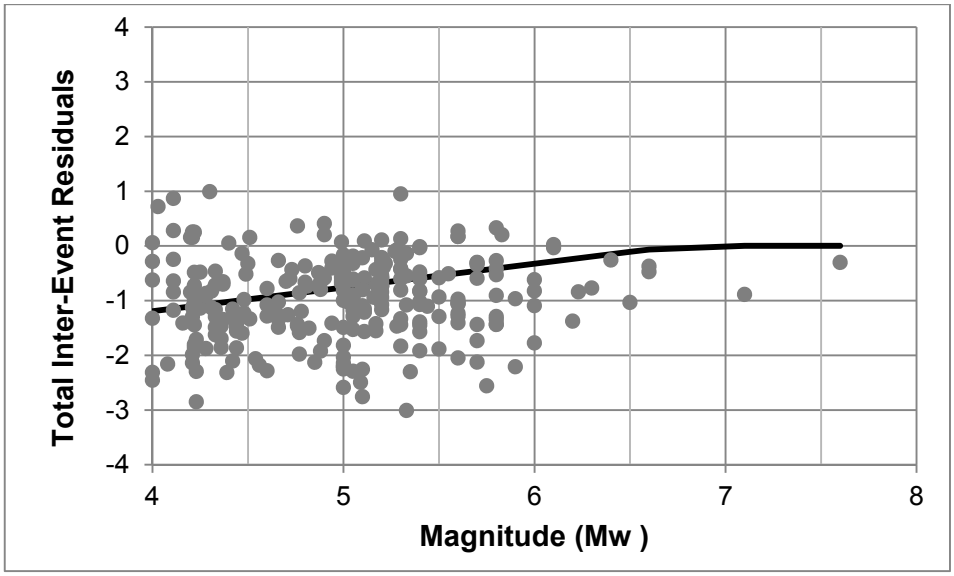

Figure 4.28 Residuals vs. M_w at PGA for original Chiou and Youngs (2008)

Selected adjustment function has a cut-off value at M=6.75 similar to AS08 and BA08 models. This cut-off value is selected due to preserving the well-constrained large magnitude parameters of the CY08 model. Similar to magnitude correction of CB08 model, rather than modifying the given coefficients, a new coefficient is introduced into the model. Reason behind this decision is that coefficients are dependent with each other and single modification of a coefficient is not possible. So, this new function with hinge magnitude given in Equation 4.16 is added to the model.

Mean values and standard deviations of c_{ta} coefficients across the spectral periods are shown in Figure 4.30. To develop a smooth model as a function of the spectral period, c_{ta} values are smoothed (smoothed values represented by the red line in Figure 4.30). The smoothed c_{ta} values are used in the Turkey-Adjusted CY08 model where the Equation 4.15 is added to the magnitude scaling term of the original CY08 model. List of the adjusted c_{ta} values (denoted by $c_{ta}*$) is provided in Table 4.2.

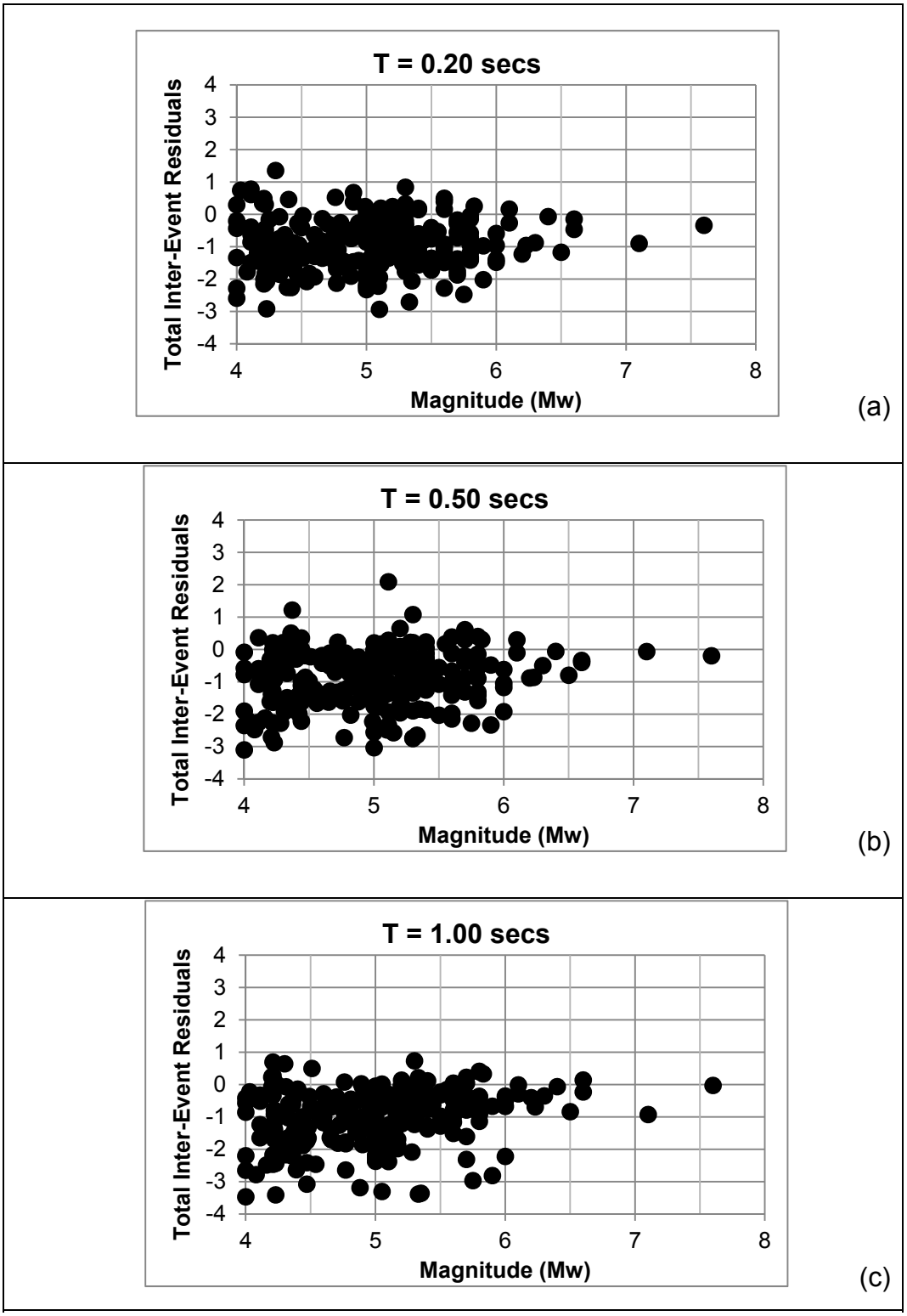

Figure 4.29 Residuals vs. M_w at a) T = 0.20 secs, b) T =0.50 secs and c) T = 1.00 secs for original Chiou and Youngs (2008)

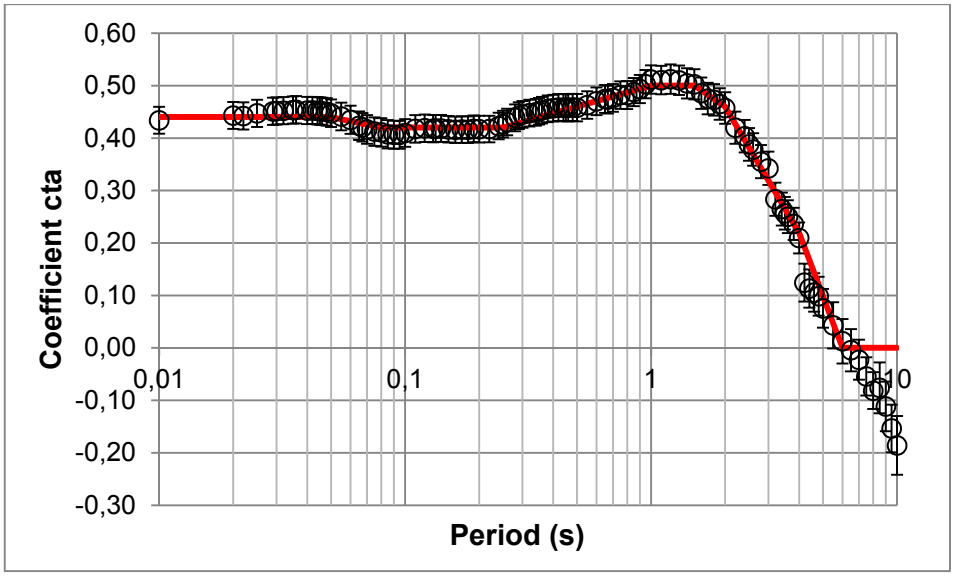

Figure 4.30 Adjustment coefficient c_{ta} for Chiou and Youngs (2008)

After the magnitude adjustment, the model residuals are re-calculated using the modified form of CY08 model. The total inter-event residuals after the magnitude adjustment are plotted by moment magnitude in Figure 4.32 for 0.01, 0.2 and, 1 second spectral periods showing that the total inter-event residuals of the adjusted model are evenly distributed along the zero line. Intra-event residuals are plotted with respect to rupture distance in Figure 4.33 for PGA, T=0.2, and T=1 second spectral periods, suggesting no trend within the applicability range of the NGA-W1 models for tectonic regions other than Western US. However, similar to AS08 model, CY08 model slightly underestimates the ground motions in Turkish comparison dataset for rupture distances within 100-200 km range. The gamma term of CY08 model is adjusted for the comparison dataset by introducing a new coefficient named $c_{\gamma 4}$ which is obtained from regressing the residuals using the functional form defined as:

$$\Delta\gamma = \begin{cases} 0 \rightarrow for(R_{rup} < 100) \\ c_{\gamma 4} * \left(R_{rup} - 100\right) \rightarrow for(R_{rup} \geq 100) \end{cases} \quad (4.17)$$

where $\Delta\gamma$ is the large-distance term to be added to CY08 model and R_{rup} is the rupture distance. Mean values and standard deviations of $c_{\gamma 4}$ coefficient across the spectral periods are presented in Figure 4.31. $c_{\gamma 4}$ values are smoothed (shown by the red line in Figure 4.31) to develop a smooth model as a function of the spectral period,. The smoothed $c_{\gamma 4}$ values are used in the Turkey-Adjusted CY08 model where the Equation 4.17 is added to the distance scaling term of the original CY08 model. List of the adjusted $c_{\gamma 4}$ values is provided in Table 4.2.

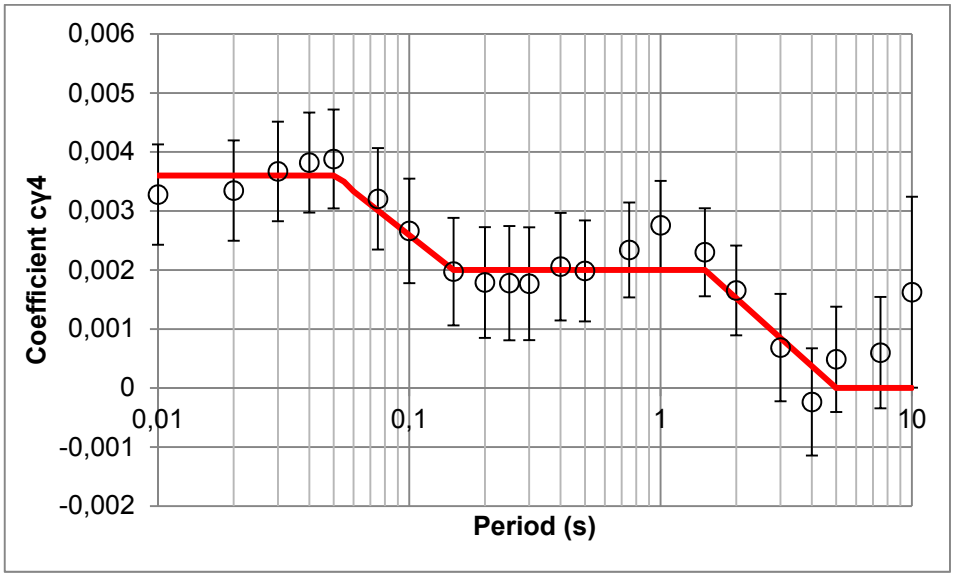

Figure 4.31 Coefficient $c_{\gamma 4}$ for Chiou and Youngs (2008) model

After the distance adjustment, the intra-event residuals are re-calculated using the modified form of CY08 model. Intra-event residuals of the modified model are plotted with respect to rupture distance in Figure 4.34 for PGA, T=0.2, and T=1 second spectral periods, indicating that the modified large distance scaling of the model is compatible with the comparison dataset.

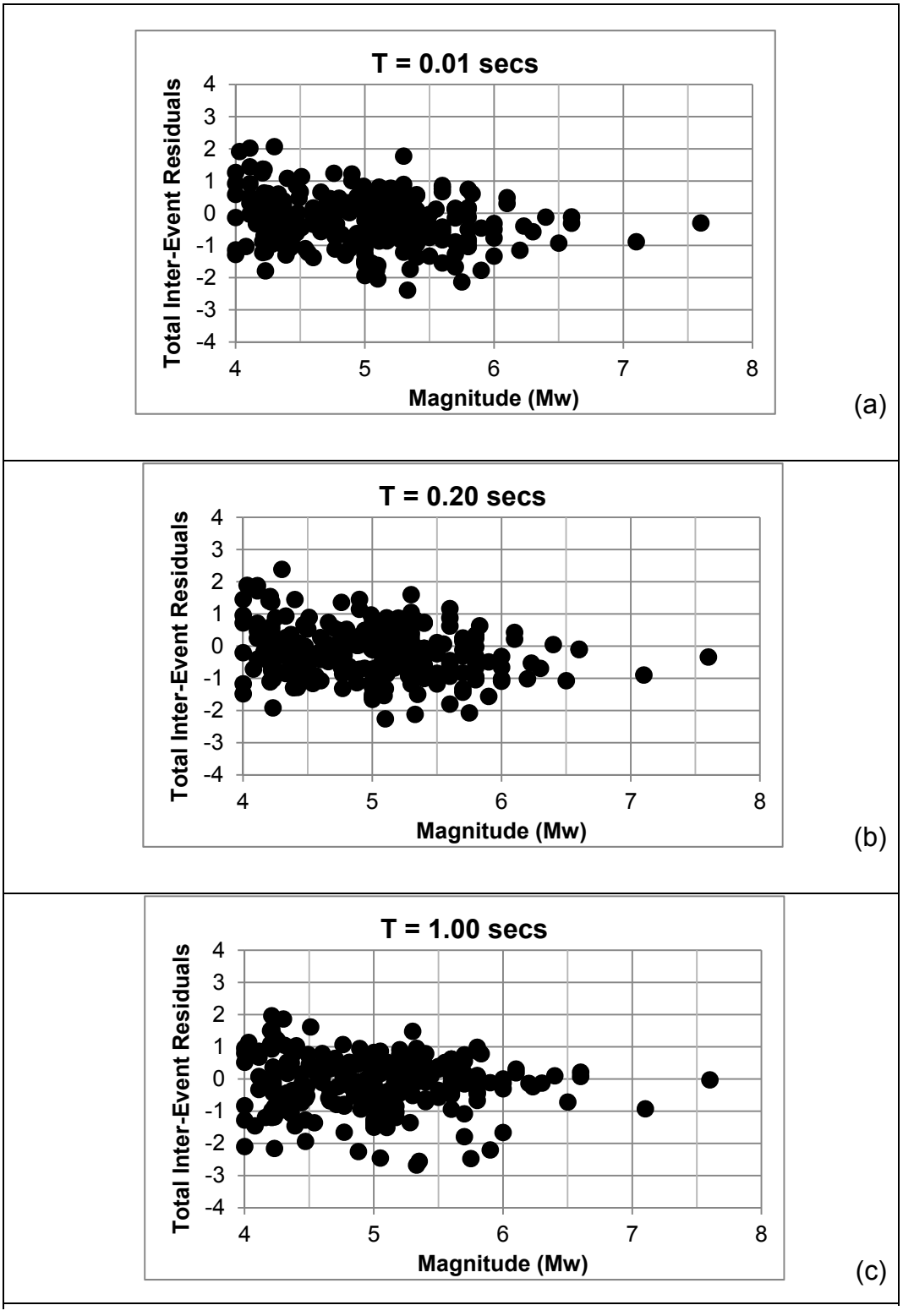

Figure 4.32 Residuals vs. M_w at a) T = 0.01 secs, b) T =0.20 secs and c) T = 1.00 secs for modified Chiou and Youngs (2008)

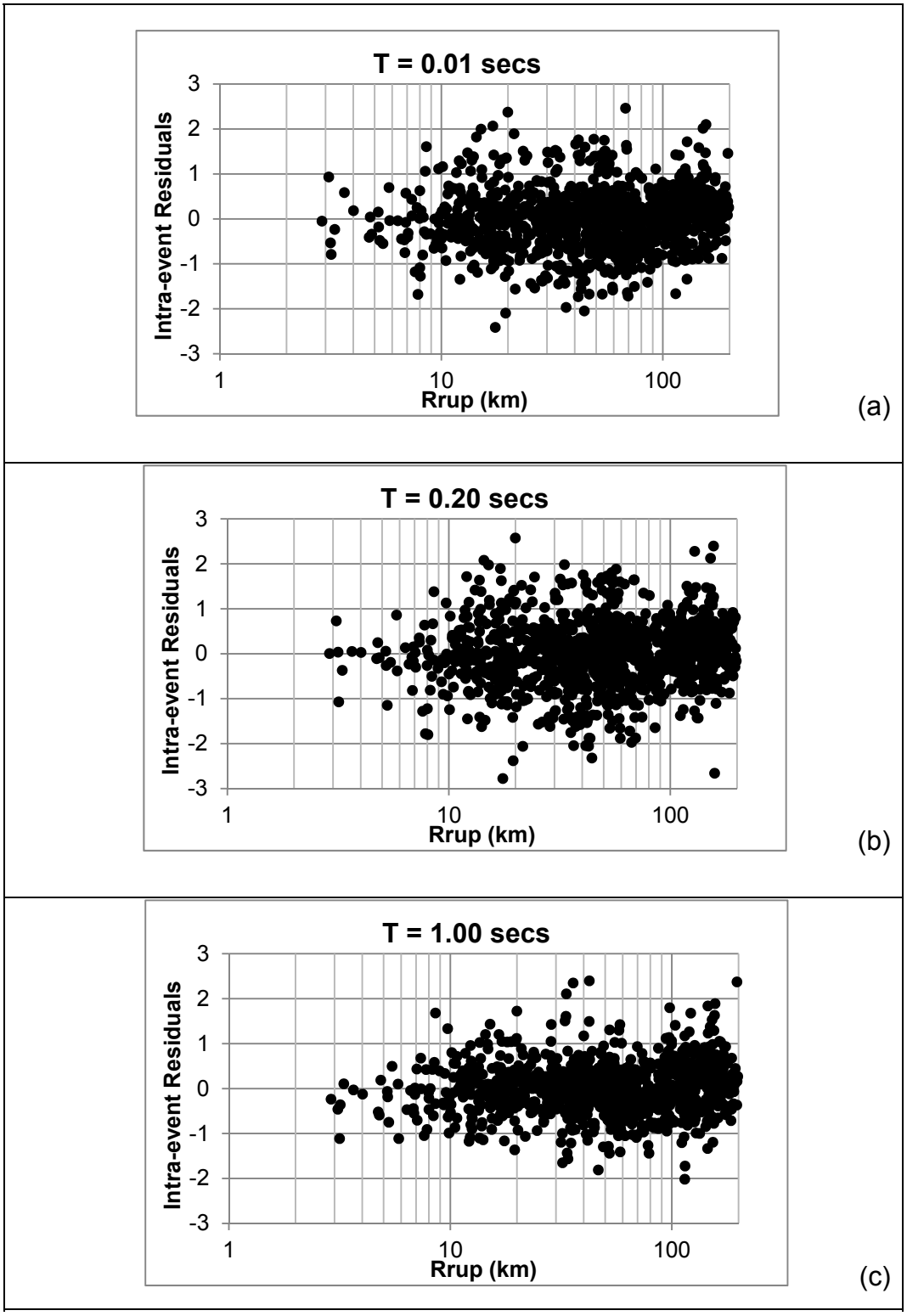

Figure 4.33 Residuals vs. R_{rup} at a) T = 0.01 secs, b) T =0.20 secs and c) T = 1.00 secs for original Chiou and Youngs (2008)

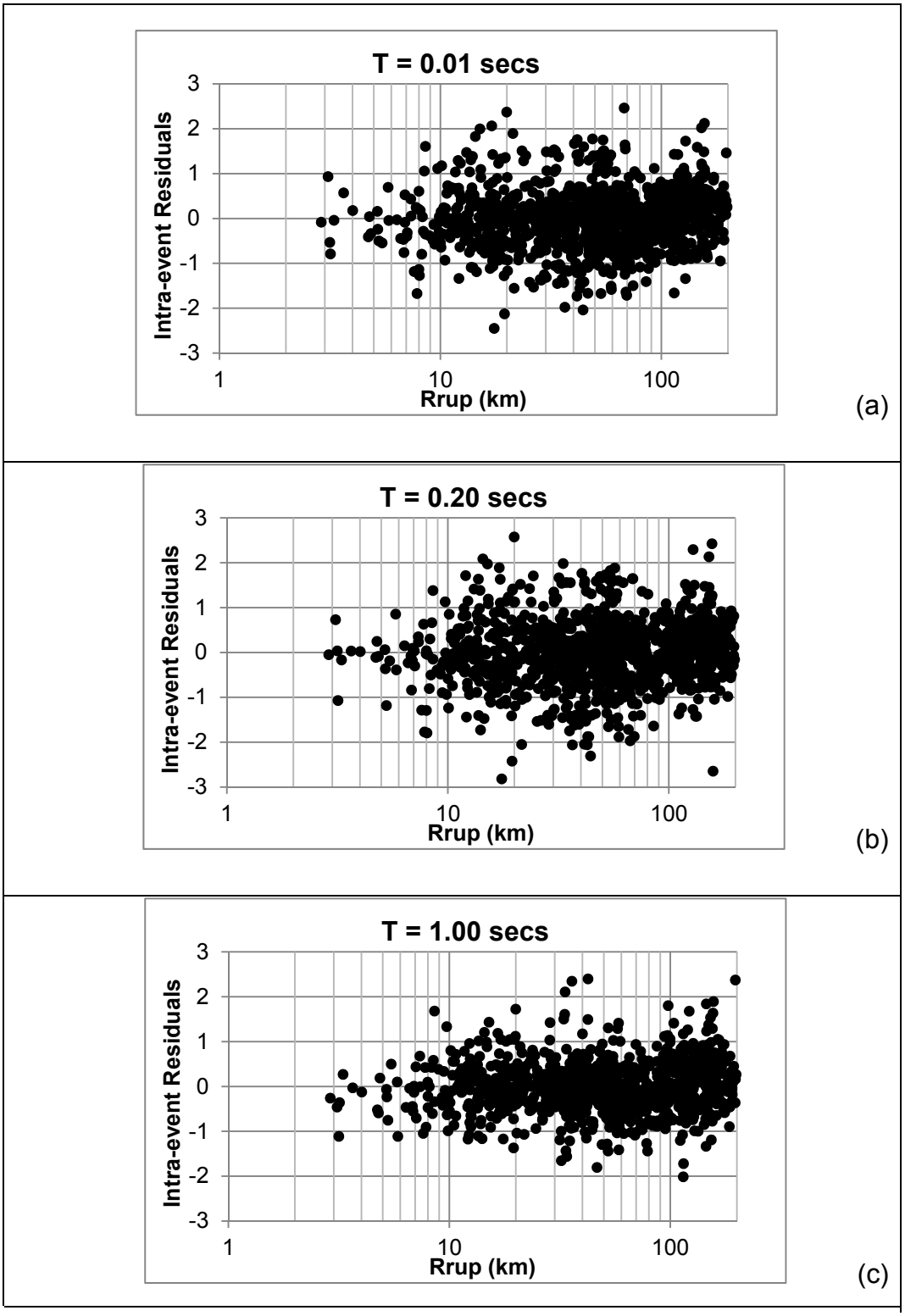

Figure 4.34 Residuals vs. R_{rup} at a) T = 0.01 secs, b) T =0.20 secs and c) T = 1.00 secs for modified Chiou and Youngs (2008)

Next step is to evaluate the site effects scaling of the CY08 model by plotting the re-calculated intra-event residuals using the modified form of CY08 model. A sample residual plot for PGA is provided in Figure 4.35. It is observed that the CY08 model slightly under-predicts the ground motions in the Turkey comparison dataset at stiff soil/engineering rock sites but this effect diminishes as V_{S30} decreases, similar to AS08 model. This observation may be expected since a major portion of CY08 model dataset consist of data from Taiwan (1999 Chi-Chi Earthquake) and deeper shear wave velocity profiles of the recording stations in Taiwan and Western US were found to be different by Lin et al. (2007). Same trend is also observed in other spectral periods up to 3 seconds. Residual plots for 0.2, 0.5 and, 1 second spectral periods are provided in Figure 4.39.

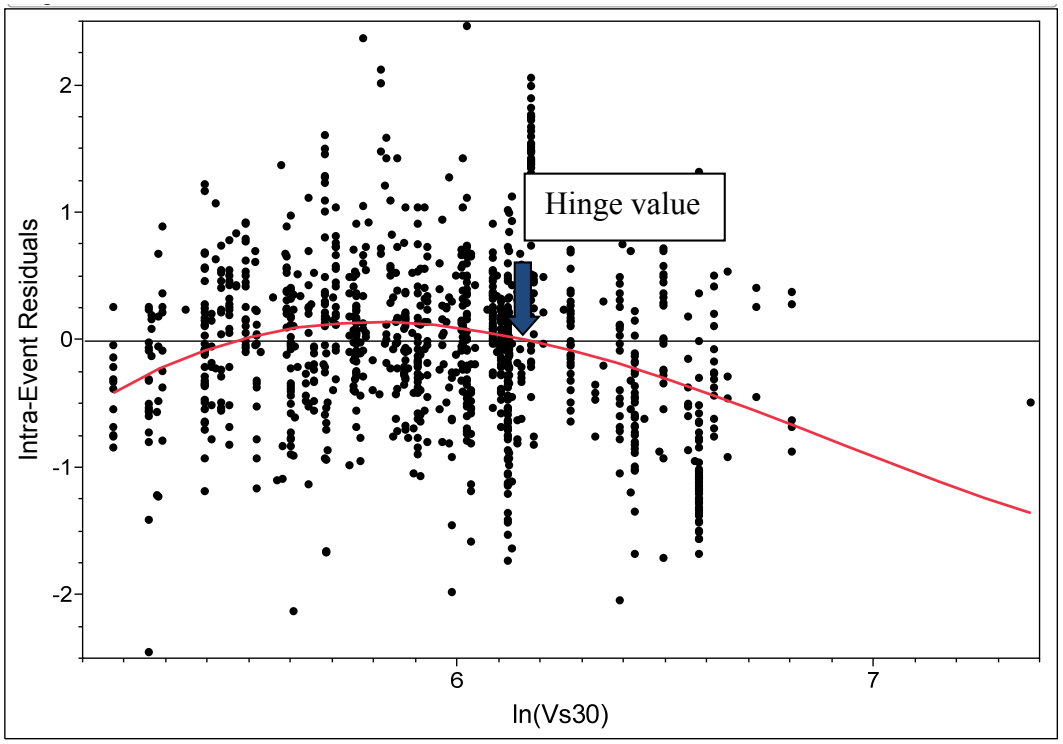

Figure 4.35 Intra-Event Residuals vs. ln(V_{S30}) for Chiou and Youngs (2008)

Therefore, the adjustment term for the site effects is chosen as:

$$\Delta f_{site\_TA} = \begin{cases} 0 \rightarrow for(V_{S30} < V_{S30,hinge}(T)) \\ \phi_9 * ln(V_{S30}/V_{S30,hinge}(T)) \rightarrow for(V_{S30} \geq V_{S30,hinge}(T)) \end{cases} \quad (4.18)$$

where $V_{S30,hinge}(T)$ is the cut-off shear wave velocity value for a particular period T, below which no trend is observed in the residuals, V_{S30} is the shear wave velocity value and ϕ_9 is the regression coefficient. For each period, the $V_{S30,Hinge}(T)$ is determined statistically as the beginning point of the curvature for the 3rd degree polynomial fit to the residuals (shown in Figure 4.35). $V_{S30,hinge}(T)$ values are smoothed across the periods and presented in Figure 4.36 with red line representing the smoothed values. Mean values and standard deviations of ϕ_9 coefficient across the spectral periods are shown in Figure 4.37 along with the smoothed values (the red line in Figure 4.37). Note that the ϕ_9 values beyond period 3 second are set to 0 since no trend is observed at these periods.

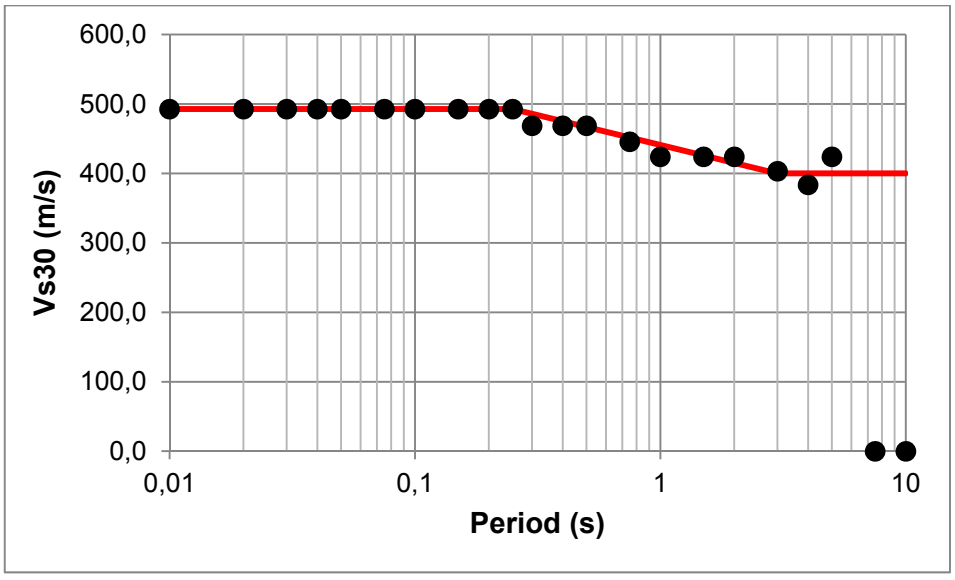

Figure 4.36 $V_{S30,hinge}$ coefficient for Chiou and Youngs (2008)

The adjustment function provided in Equation 4.18 is added to the Turkey-Adjusted CY08 model and the intra event residuals were re-plotted to observe that the intra-event residuals for the adjusted model are evenly distributed along the zero line (Figure 4.40). The mean-offset values before and after the adjustments are presented in Figure 4.38. Remaining mean offset values are insignificant, therefore the constant term is not modified.

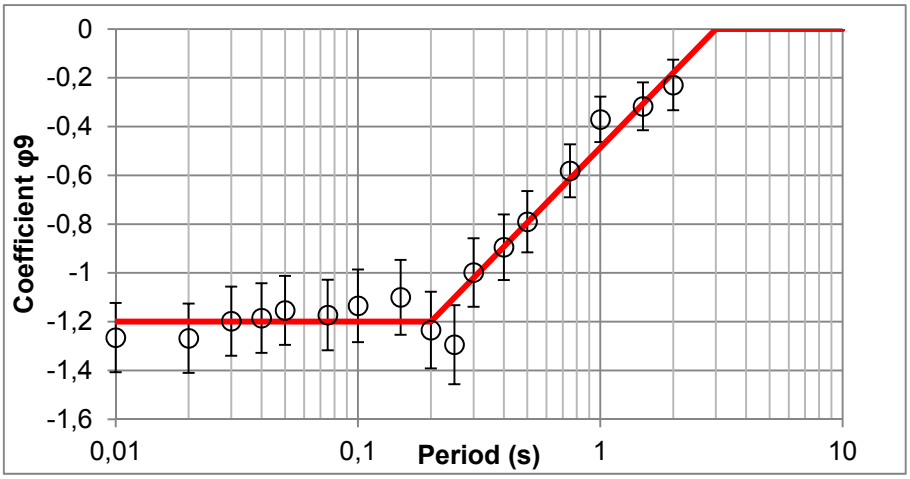

Figure 4.37 ϕ_9 coefficient for Chiou and Youngs (2008)

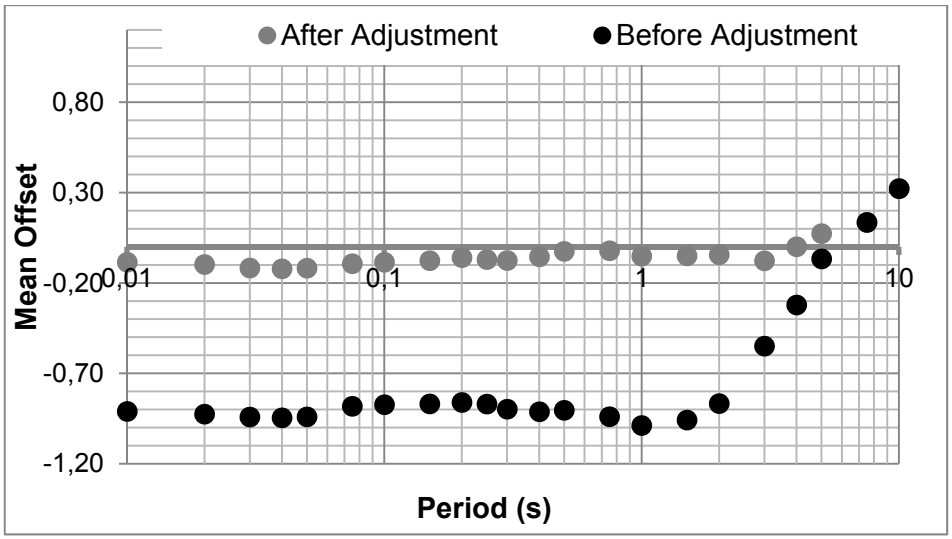

Figure 4.38 Mean offset vs. period for modified Chiou and Youngs (2008) model

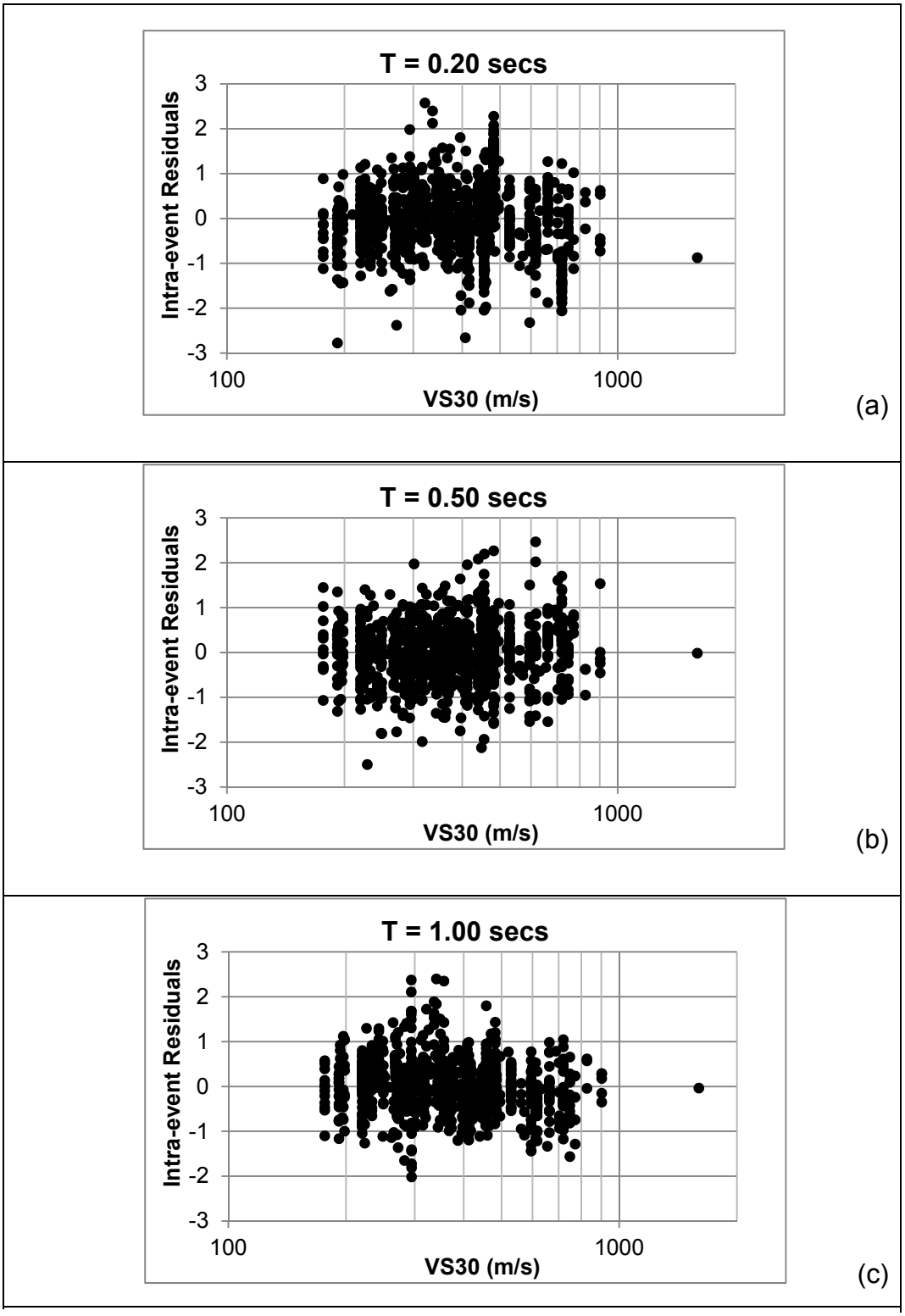

Figure 4.39 Residuals vs Vs30 at a) T = 0.20 secs, b) T =0.50 secs and c) T = 1.00 secs for original Chiou and Youngs (2008)

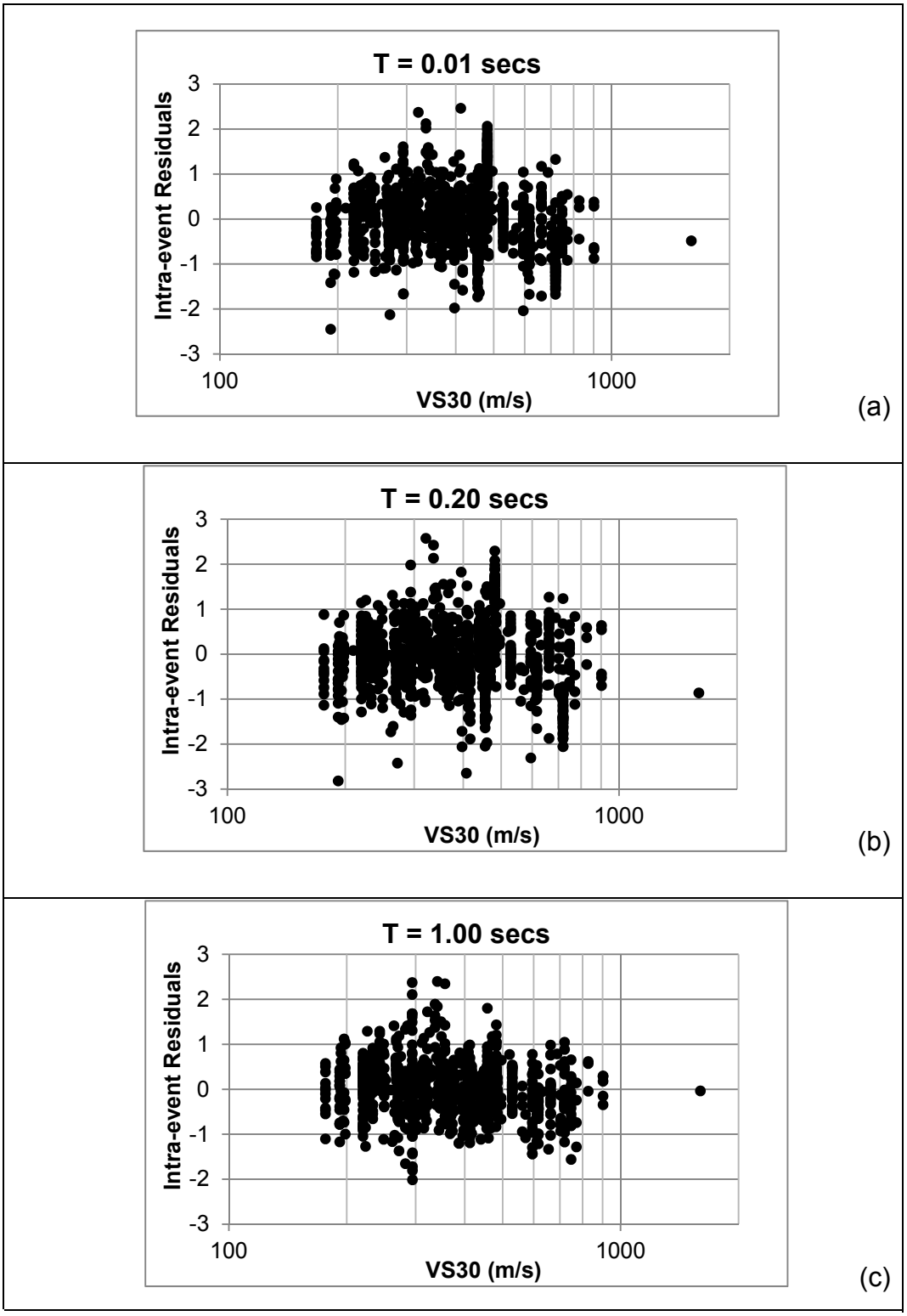

Figure 4.40 Residuals vs. Vs30 at a) T = 0.01 secs, b) T =0.20 secs and c) T = 1.00 secs for modified Chiou and Youngs (2008)

4.2.5 Idriss 2008 (ID08) Model

Idriss (2008) defined a simple functional form for strike-slip earthquakes recorded on rock sites as shown in Equation 4.19:

$$\ln\big(PSA(T)\big) = \alpha_1(T) + \alpha_2(T)M - (\beta_1(T) + \beta_2(T)M)\ln\big(R_{rup} + 10\big) + \gamma(T)R_{rup} + \varphi(T)F \quad (4.19)$$

where $\alpha_1, \alpha_2, \beta_1, \beta_2, \gamma, \varphi$ are the model coefficients, M is the moment magnitude, R_{rup} is rupture distance and F is fault mechanism.

Total inter-event residuals of ID08 model are plotted with respect to moment magnitude for PGA as shown in Figure 4.41 (total inter-event residuals presented by grey dots). The ground motions in the dataset are overestimated by the ID08 model significantly, especially for small-to-moderate magnitude earthquakes similar to previously modified NGA models. The trend is persistent for all spectral periods. Residual plots for 0.2, 0.5 and, 1 second spectral periods are provided in Figure 4.44. Figures 4.41 and 4.44 suggest that the magnitude scaling of the comparison dataset is drastically different that the ID08 model and this feature needs to be fixed to consider the model applicable in Turkey. The misfit between the actual and predicted data is modeled by Equation 4.20:

$$\Delta f_{mag\_TA} = \begin{cases} \alpha_3 * (M - 6.75) \rightarrow for(M \leq 6.75) \\ 0 \rightarrow for(M > 6.75) \end{cases} \quad (4.20)$$

Where M is moment magnitude and α_3 is the new defined coefficient determined by regression. The model fit to the residuals by Equation 4.20 is presented in Figure 4.41 by the grey line. Please note that the selected adjustment function has a cut-off value at M=6.75. This cut-off value is selected to be consistent with the ID08 basic model (Equation 4.19) as Idriss (2008) assigned two separate values for model coefficients for the cases M<6.75 and M≥6.75. Mean values and standard deviations of α_3 coefficients across the spectral periods are shown in Figure 4.42. To develop a smooth

model as a function of the spectral period, α_3 values are smoothed (smoothed values represented by the red line in Figure 4.42).

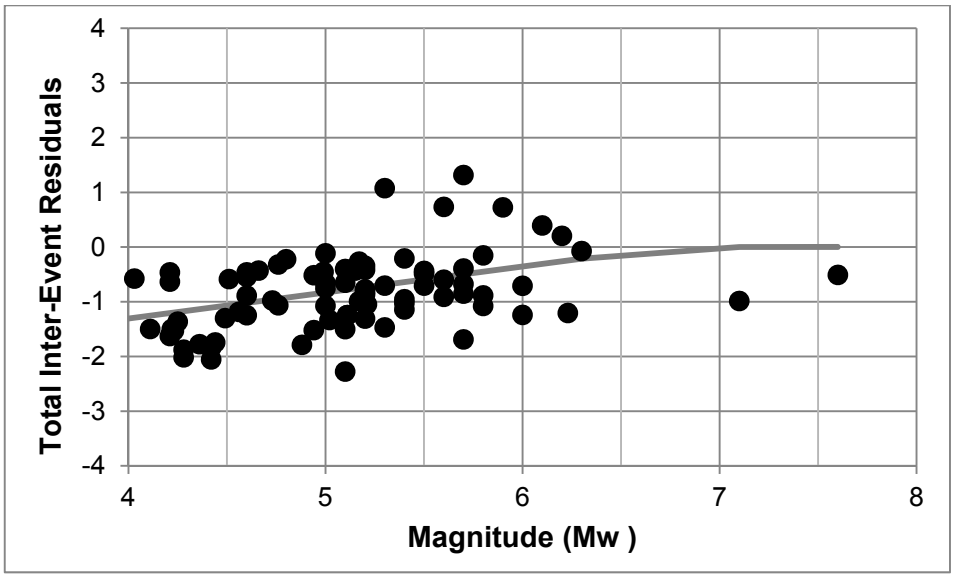

Figure 4.41 Residuals vs. M_w at PGA for original Idriss (2008) model

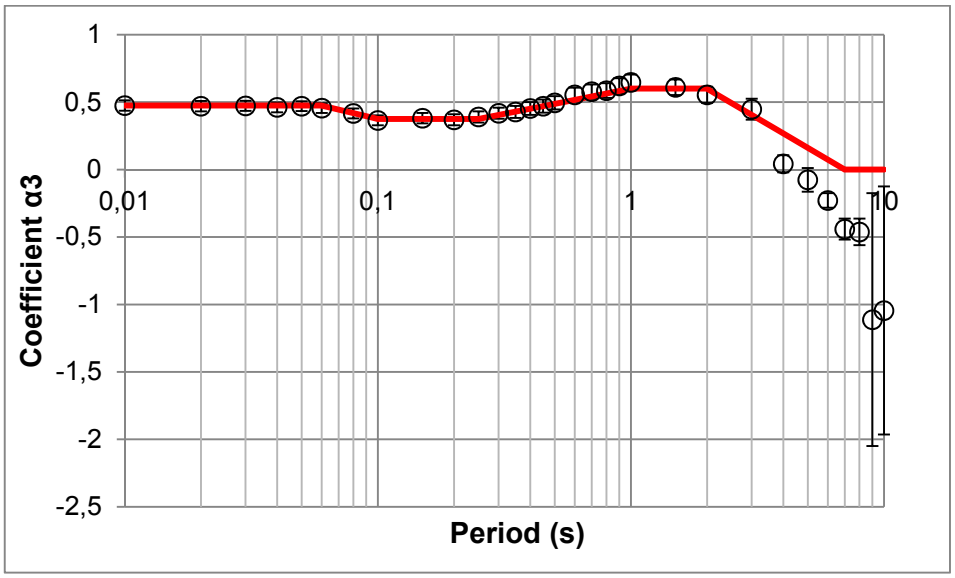

Figure 4.42 Adjustment coefficient α_3 for Idriss (2008)

The smoothed α_3 values are used in the Turkey-Adjusted ID08 model where the Equation 4.19 is added to the magnitude scaling term of the original ID08 model. List of the adjusted α_3 values is provided in Table 4.2. After the magnitude adjustment, the model residuals are re-calculated using the modified form of ID08 model. The total inter-event residuals after the magnitude adjustment are plotted by moment magnitude in Figure 4.45 for 0.01, 0.2 and, 1 second spectral periods showing that the total inter-event residuals of the adjusted model are evenly distributed along the zero line. Intra-event residuals are plotted with respect to rupture distance in Figure 4.46 and with respect to V_{S30} in Figure 4.47 for PGA, T=0.2, and T=1 second spectral periods, suggesting no trend within the intra-event residuals. Thus no adjustment is made for distance scaling and site effects scaling terms of ID08 model.

Finally, the mean-offset values for before and after the adjustments are presented in Figure 4.43.

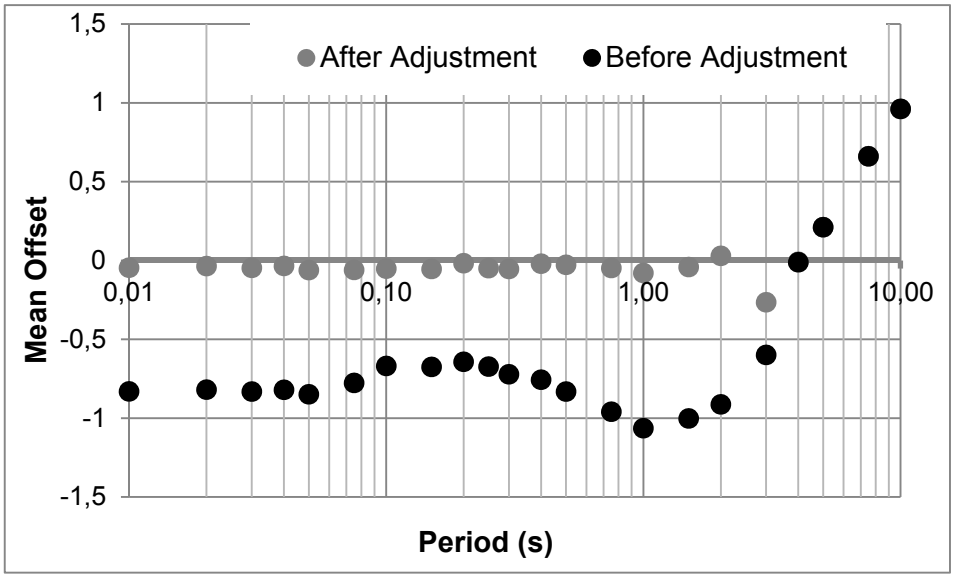

Figure 4.43 Mean offset vs. period for modified Idriss (2008) model

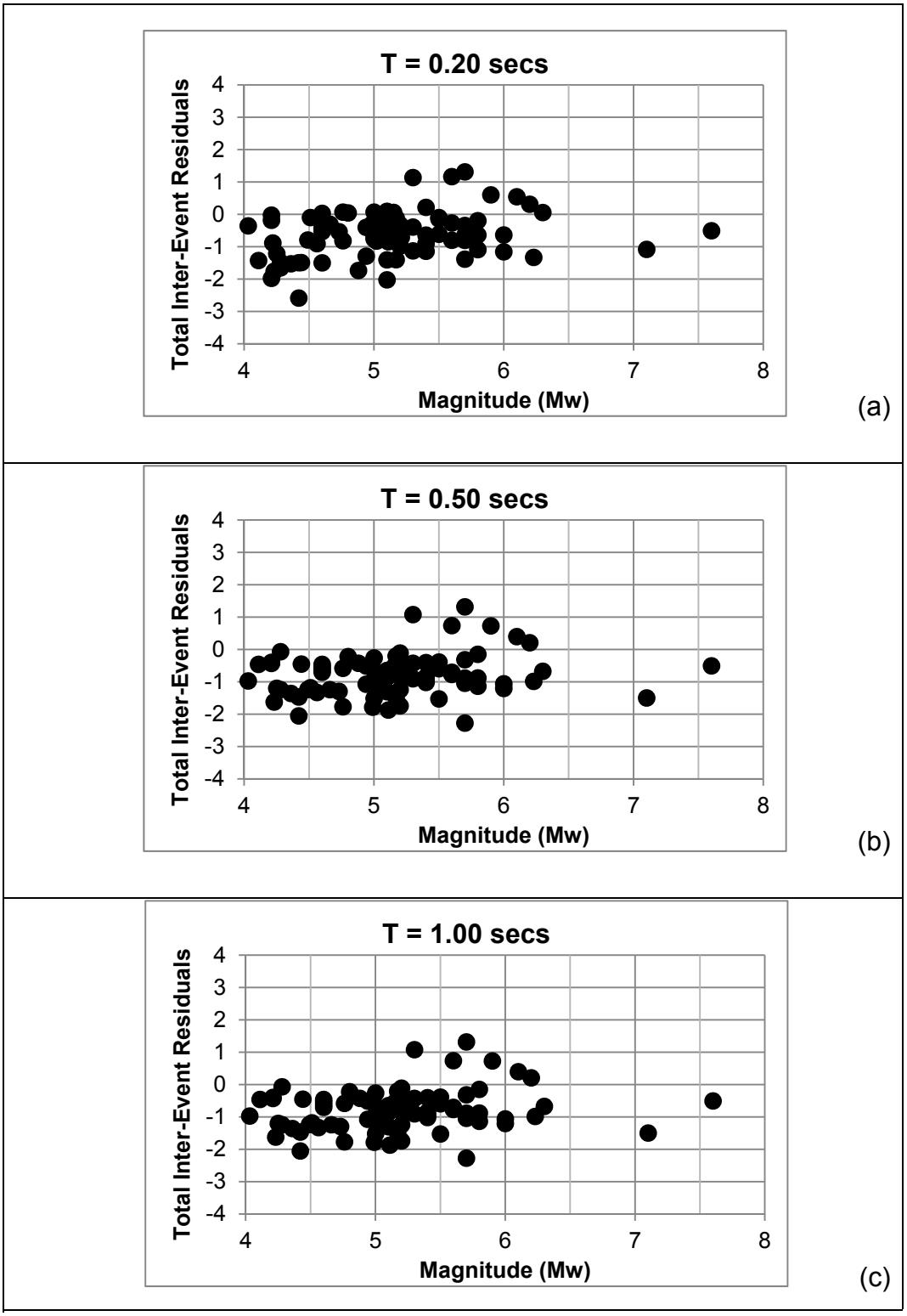

Figure 4.44 Residuals vs. M_w at a) T = 0.20 secs, b) T =0.50 secs and c) T = 1.00 secs for original Idriss (2008)

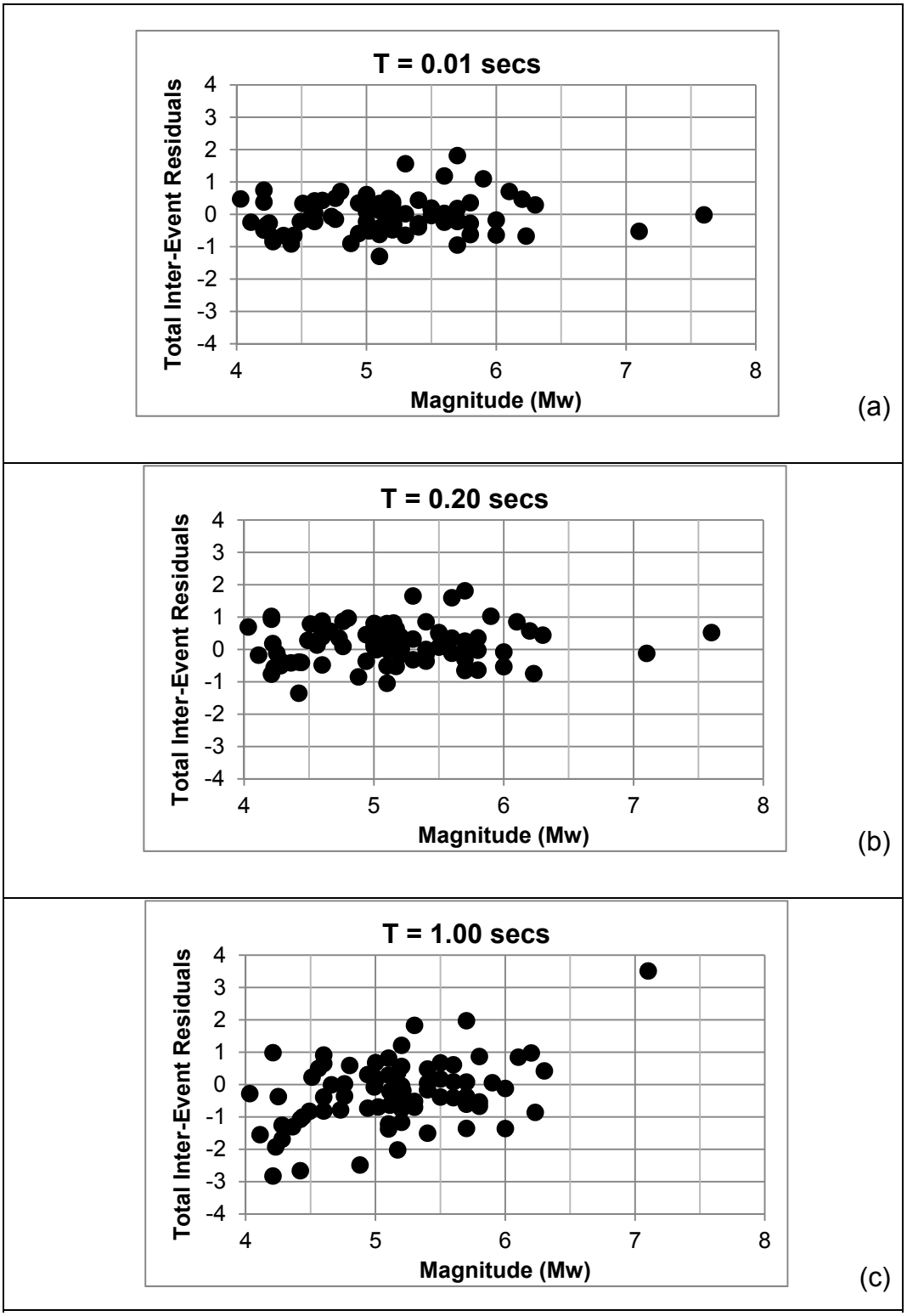

Figure 4.45 Residuals vs. M_w at a) T = 0.01 secs, b) T =0.20 secs and c) T = 1.00 secs for modified Idriss (2008)

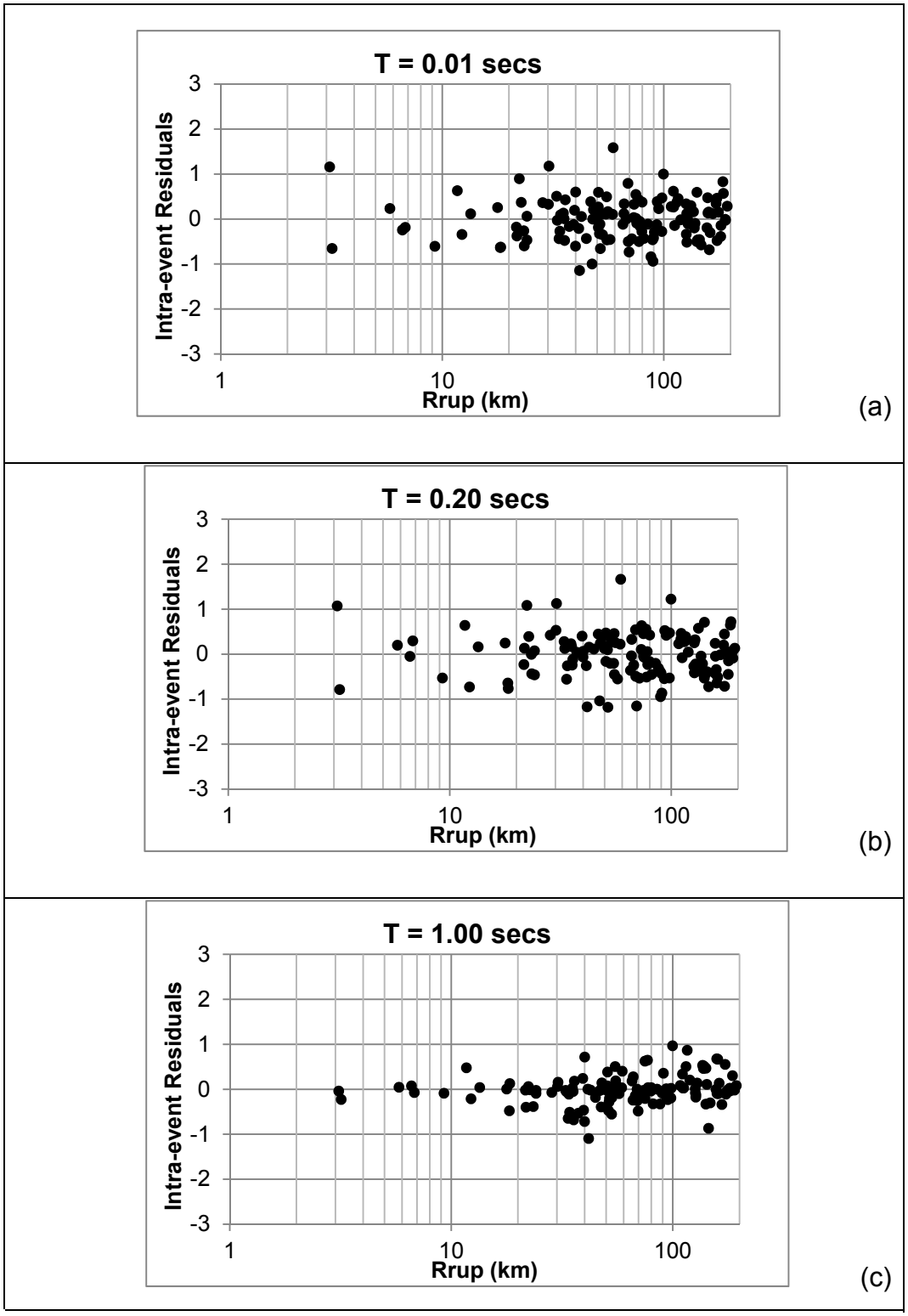

Figure 4.46 Residuals vs. R_{rup} at a) T = 0.01 secs, b) T =0.20 secs and c) T = 1.00 secs for original Idriss (2008)

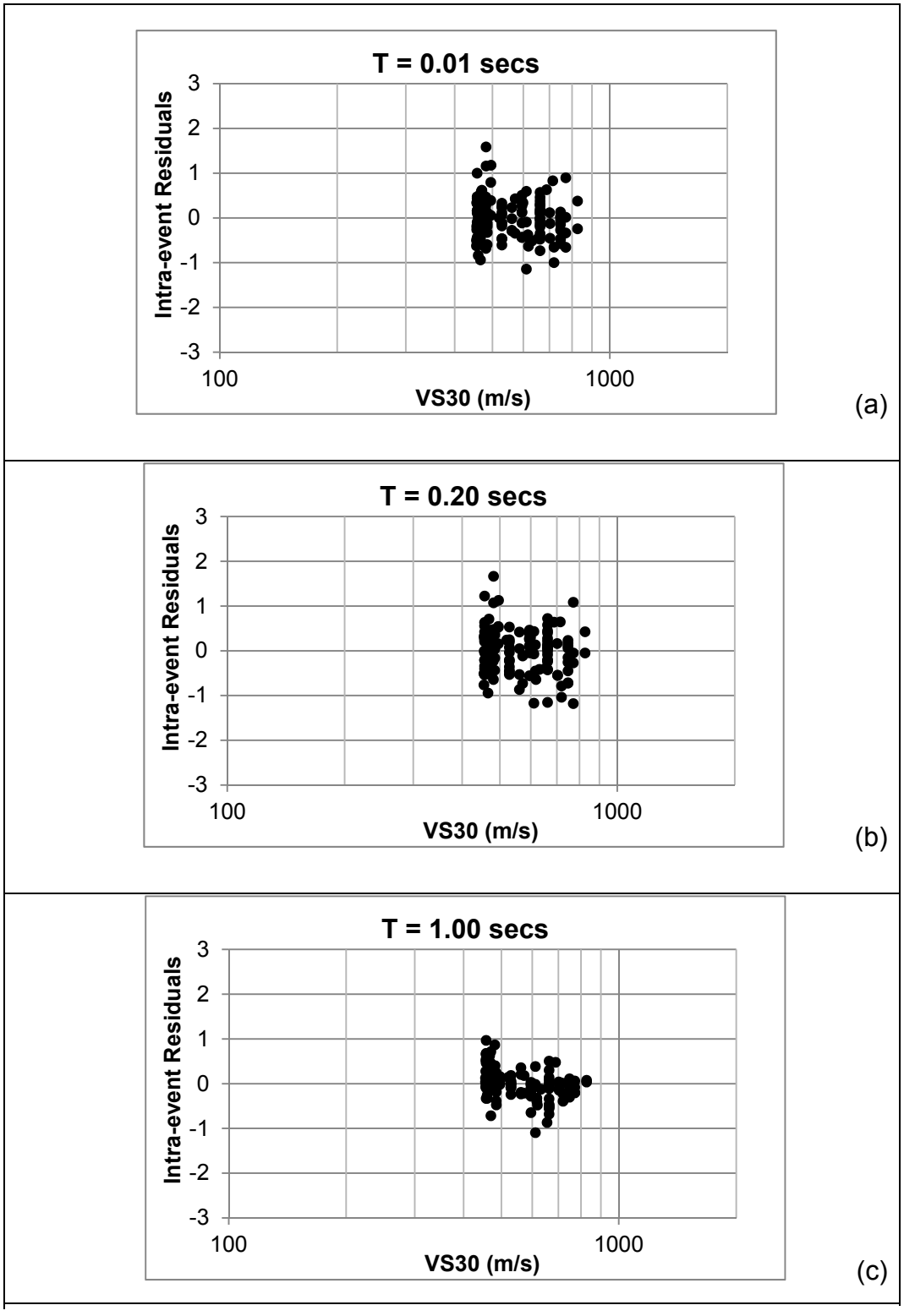

Figure 4.47 Residuals vs Vs30 at a) T = 0.01 secs, b) T =0.20 secs and c) T = 1.00 secs for modified Idriss (2008)

Remaining mean offset values are insignificant up to 2.0 seconds when compared to the original ID08 model, therefore the constant term in the model is not modified to reflect the remaining main offset. Constant term of ID08 model for periods beyond 2.0 seconds is also not corrected since the number of recordings included in the regression is very small at long periods due to frequency cut-off values.

The mean offset values for all 5 Turkey-adjusted NGA-W1 models are presented in Figure 4.48. It is evident from the figure that mean offset values are fairly well scattered around the zero line up to 1 second spectral period for all models. Mean offsets also follow similar distribution up this period, which indicates the uniformity of the modification conducted for all models. But above 1 second spectral period, mean offsets are scattered on the positive side due to the reduced number of recordings used for comparison at those periods.

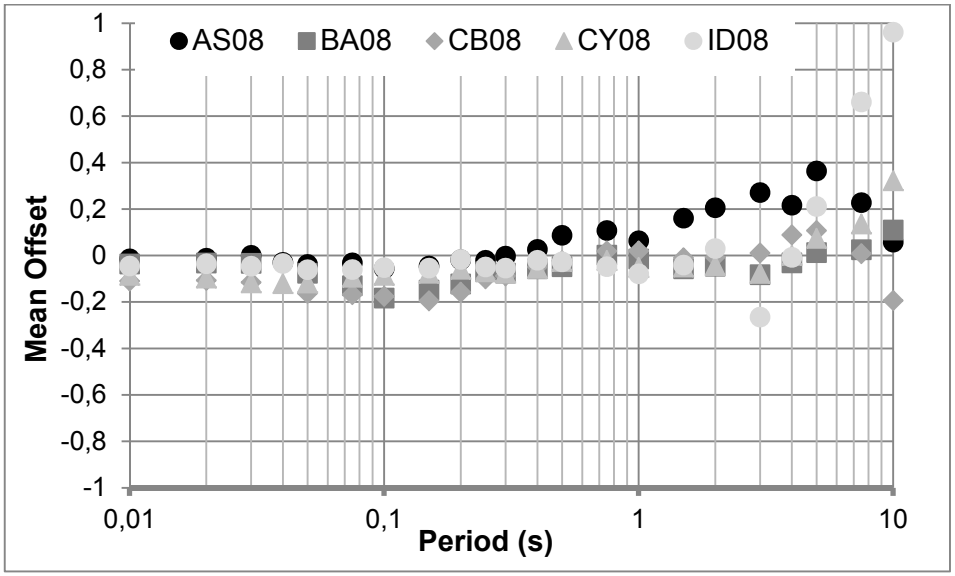

Figure 4.48 Mean offset vs. period for modified NGA models

Table 4.2 Modified coefficients for the Turkey-Adjusted NGA models

	AS08				BA08	CB08	CY08				ID08
T	a_4	a_9	a_{18}	$V_{S30,hinge}$	e_5	c_{13}	c_{ta}	$c_{\gamma 4}$	ϕ_9	$V_{S30,hinge}$	α_3
0.010	0.470	-0.9500	-0.0040	470	0.8390	0.680	0.440	0.0036	-1.2000	493	-0.4750
0.020	0.470	-0.9500	-0.0040	470	0.8014	0.680	0.440	0.0036	-1.2000	493	-0.4750
0.030	0.470	-0.9500	-0.0040	470	0.7298	0.680	0.440	0.0036	-1.2000	493	-0.4750
0.040	0.470	-0.9500	-0.0040	470	N/A	N/A	0.440	0.0036	-1.2000	493	-0.4750
0.050	0.470	-0.9500	-0.0050	470	0.6137	0.680	0.440	0.0036	-1.2000	493	-0.4750
0.075	0.470	-0.9500	-0.0069	470	0.5617	0.680	0.423	0.0030	-1.2000	493	-0.4313
0.10	0.470	-0.9500	-0.0075	470	0.5970	0.680	0.420	0.0026	-1.2000	493	-0.3750
0.15	0.470	-0.9500	-0.0075	470	0.7299	0.680	0.420	0.0020	-1.2000	493	-0.3750
0.20	0.466	-0.9500	-0.0067	470	1.0773	0.680	0.420	0.0020	-1.2000	493	-0.3750
0.25	0.459	-0.9500	-0.0051	470	1.1588	0.680	0.420	0.0020	-1.1011	493	-0.3750
0.30	0.453	-0.9500	-0.0037	470	1.1947	0.680	0.431	0.0020	-1.0203	486	-0.4046
0.40	0.443	-0.9500	-0.0016	448	1.3361	0.680	0.447	0.0020	-0.8929	475	-0.4513
0.50	0.435	-0.9168	0.0000	431	1.3052	0.667	0.460	0.0020	-0.7940	467	-0.4875
0.75	0.422	-0.7554	0.0000	400	1.2646	0.643	0.483	0.0020	-0.6143	452	-0.5533
1.0	0.412	-0.6408	0.0000	400	1.1746	0.625	0.500	0.0020	-0.4868	441	-0.6000
1.5	0.384	-0.4794	0.0000	400	1.1787	0.601	0.500	0.0020	-0.3071	426	-0.6000
2.0	0.360	-0.3648	0.0000	400	1.2347	0.584	0.460	0.0015	-0.1797	415	-0.6000
3.0	0.292	-0.2034	0.0000	400	1.1669	0.560	0.319	0.0008	0.0000	400	-0.4058
4.0	0.212	-0.0888	0.0000	400	1.5890	0.481	0.219	0.0004	0.0000	400	-0.2680
5.0	0.151	0.0000	0.0000	400	0.2962	0.420	0.098	0.0000	0.0000	400	-0.1612
7.5	0.100	0.0000	0.0000	400	0.6776	0.420	0.000	0.0000	0.0000	400	0.0000
10	0.100	0.0000	0.0000	400	0.5574	0.420	0.000	0.0000	0.0000	400	0.0000

CHAPTER 5

SUMMARY AND CONCLUSIONS

The objective of this study is to evaluate the regional differences between the worldwide based NGA-W1 ground motion model predictions and Turkish strong ground motion dataset. Turkish strong ground motion data may show a divergence from the NGA model predictions since the ground motions recorded in the events occurred in Turkey were poorly represented in NGA-W1 database. Differences between the comparison dataset and NGA-W1 model predictions are evaluated in terms of magnitude, distance and site effect terms and these terms are modified when necessary to validate the applicability of the NGA-W1 models in the probabilistic seismic hazard assessment (PSHA) studies conducted in Turkey.

Considering the large number of processed strong motion recordings, completeness and quality of the earthquake metadata and other seismological features, and availability of precious site classification information for the recording stations, TSMD project database was the natural choice as the starting point for the comparison dataset to be used for this study. Tremendous efforts are made to modify the initial TSMD dataset and to estimate the missing parameters required for comparison with the NGA-W1 predictive models. Final flat-file used in the comparison includes 1142 recordings from 288 events with the earthquake metadata (moment magnitude, style of faulting, rake and dip angles, etc.), source-to-site distance metrics for the recordings (R_{rup} and R_{JB}), V_{s30} values for the

recording stations, and horizontal component spectral values in terms of GMRotI50 for 23 spectral periods (0.01, 0.02, 0.03, 0.04, 0.05, 0.075, 0.10, 0.15, 0.20, 0.25, 0.30, 0.40, 0.50, 0.75, 1.0, 1.5, 2.0, 3.0, 4.0, 5.0, 7.5, 10.0 seconds).

To examine the discrepancies between actual strong motion recordings and NGA model predictions, analysis of residuals method is used. Residuals are calculated and separated into three components: mean bias, inter-event residuals and intra-event residuals using random effects regression proposed by Abrahamson and Youngs (1992). Inter-event residuals vs. magnitude plots are examined to observe that the ground motions in the dataset are overestimated by all 5 NGA-W1 models significantly, especially for small-to-moderate magnitude earthquakes. This feature is fixed to consider the model applicable in Turkey without modifying the well-constrained pieces of the model, since the large magnitude earthquakes are poorly represented in the comparison dataset and any changes on large magnitude parameters will have a major impact on the hazard calculations.

In the next step, intra-event residuals vs. distance plots are examined and trends are observed in 5 NGA-W1 models for large distances. Due to absence of large distance formulation in BA08, CB08 and ID08 models, correction is conducted only for AS08 and CY08 models. Then the intra-event residuals vs. V_{S30} plots are examined and trends are observed for AS08 and CY08 models. The existence of trends within site effects term of these two models is attributed to inclusion of aftershock events in these models' databases. Correction of site term is conducted by adding additional term to the site effect functions. After correcting the trends, mean offset values for adjusted models are calculated. By inspecting these mean offset values, it is concluded that they are within reasonable values and no correction is conducted regarding mean bias.

Modifications made on the NGA-W1 models for the Turkish ground motion dataset are summarized in the following section. Plots of Turkey adjusted

NGA-W1 models along with original models for different scenarios are also provided to present the effects of the applied adjustments.

5.1 Final Forms of Turkey Adjusted NGA-W1 Models

Adjustment functions were added to magnitude, distance and site effects terms of AS08 model. Median Turkey-Adjusted AS08 model is formulated as shown in Equation 5.1:

$$\begin{aligned}\ln Sa(g) = {} & f_{1\_TA}(M, R_{rup}) + a_{12}F_{RV} + a_{13}F_{NM} + a_{15}F_{AS} + f_{5\_TA}(P\hat{G}A_{1100}, V_{S30}) \\ & + F_{HW}f_4(R_{jb}, R_{rup,}R_{x,}W, \delta, Z_{TOR}, M) + f_6(Z_{TOR}) + f_{8\_TA}(R_{rup}, M) \\ & + f_{10}(Z_{1.0}, V_{S30}) \end{aligned} \quad (5.1)$$

where $f_{1\_TA}(M, R_{rup})$, $f_{5\_TA}(P\hat{G}A_{1100}, V_{S30})$ and $f_{8\_TA}(R_{rup}, M)$ terms are magnitude scaling, site effects scaling and distance scaling terms of adjusted AS08 model respectively. Magnitude scaling term of adjusted model is defined as:

$$f_{1\_TA}(M, R_{rup}) = \begin{vmatrix} a_1 + [a_2 + a_3(M - c_1)]\ln(R) \\ + \begin{vmatrix} a*_4 (M - c_1) + a_8(8.5 - M)^2 \rightarrow for(M \le c_1) \\ a_5(M - c_1) + a_8(8.5 - M)^2 \rightarrow for(M > c_1) \end{vmatrix} \end{vmatrix} \quad (5.2)$$

where $a*_4$ is the coefficient for adjusted function (Table 4.2). Site effects scaling term of adjusted model is given as:

$$f_{5\_TA}(P\hat{G}A_{1100}, V^*_{S30}) = f_5(P\hat{G}A_{1100}, V^*_{S30}) + \begin{cases} 0 \rightarrow for({V_{S30}}^* < V_{S30,hinge}(T)) \\ a_9 * ln({V_{S30}}^*/V_{S30,hinge}(T) \rightarrow for({V_{S30}}^* \ge V_{S30,hinge}(T))) \end{cases} \quad (5.3)$$

where a_9 and $V_{S30,hinge}(T)$ are defined coefficients for adjusted AS08 model (Table 4.2), $P\hat{G}A_{1100}$ is median peak ground acceleration at rock site, V^*_{S30} is site term defined in original AS08 model and $f_5(P\hat{G}A_{1100}, V^*_{S30})$ is site effects term of original AS08 model. This term is given as:

$$f_5\left(P\hat{G}A_{1100}, V_{S30}^*\right) =$$

$$\begin{cases} a_{10}\ln\left(\frac{V_{S30}^*}{V_{LIN}}\right) - bln\left(P\hat{G}A_{1100} + c\right) + b\ln(P\hat{G}A_{1100} + c\left(\frac{V_{S30}^*}{V_{LIN}}\right)^n) \rightarrow for(V_{S30} < V_{LIN}) \\ (a_{10} + bn)\ln\left(\frac{V_{S30}^*}{V_{LIN}}\right) \rightarrow for(V_{S30} \geq V_{LIN}) \end{cases} \tag{5.4}$$

where a_{10}, b, c, n and V_{LIN} are regression coefficients for site effects term.

Large distance term of the adjusted AS08 model is given as:

$$f_{8\_TA} = \begin{cases} 0 \rightarrow for(R_{rup} < 100) \\ a_{18}^*\left(R_{rup} - 100\right)T_6(M) \rightarrow for(R_{rup} \geq 100) \end{cases} \tag{5.5}$$

where a_{18}^* is coefficient for adjusted AS08 model (Table 4.2).

Turkey-adjusted AS08 model and original AS08 model median curves for magnitude 5 and magnitude 7 earthquakes at the rupture distance of 10 kilometers for V_{s30}=270 m/s and V_{s30}=760 m/s site conditions are presented in Figure 5.1. Turkey adjusted model curves are shown with thick dash lines and original AS08 model is shown with thin solid lines. Figure 5.1 shows that original and Turkey-adjusted curves are quite different in scenarios with magnitude 5. This result is expected since the magnitude adjustment is conducted up to the hinge magnitude of 6.75. Spectral acceleration values of Turkey Adjusted AS08 model are almost the half of the original model for M5 scenarios. For rock sites, original and Turkey-adjusted curves differ from each other for all scenarios due to the site effect term adjustment. Again, there is significant reduction in median spectral acceleration values of adjusted model for all scenarios in rock sites. Figure 5.1 implies that the Turkey-adjusted AS08 model has a similar spectral shape when compared to the original model which proves that the applied modifications did not create any distortion in the spectral shape.

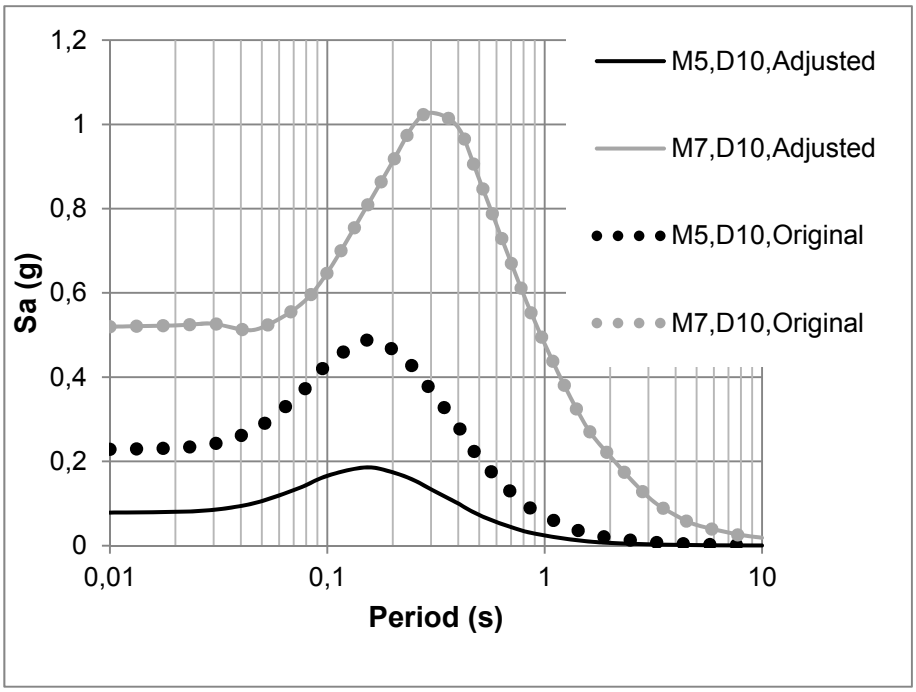

(a)

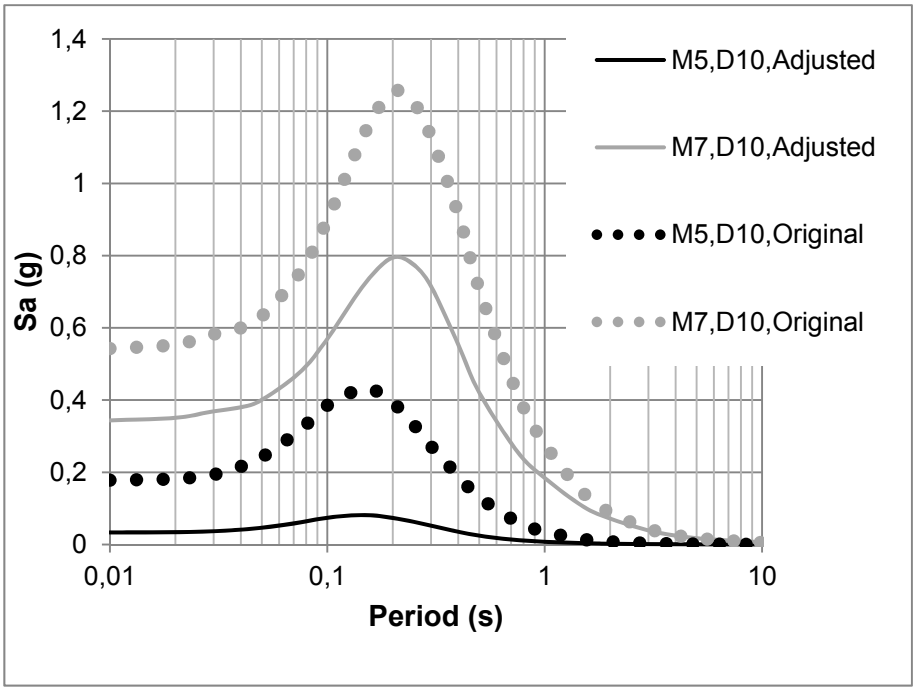

(b)

Figure 5.1 Turkey Adjusted and original AS08 model median predictions vs. Period for sites with a) V_{S30}=270 m/s, b) V_{S30}=760 m/s

Adjustment for BA08 model is conducted only for the magnitude scaling term. Adjusted BA08 model is formulated as shown in Equation 5.6:

$$\ln Y = F_{M\_TA}(M) + F_D(R_{JB}, M) + F_S(V_{S30}, R_{JB}, M) \quad (5.6)$$

where $F_{M\_TA}(M)$ term is the magnitude scaling term of adjusted BA08 model. Magnitude scaling term is obtained by adding adjustment function to the original magnitude scaling term. Magnitude scaling term of adjusted model is defined as:

a) $M \leq M_h$

$$F_M(M) = e_1 U + e_2 SS + e_3 NS + e_4 RS + e_5^*(M - M_h) + e_6(M - M_h)^2 \quad (5.7a)$$

b) $M > M_h$

$$F_M(M) = e_1 U + e_2 SS + e_3 NS + e_4 RS + e_7(M - M_h) \quad (5.7b)$$

where e_5^* is coefficient for adjusted BA08 model (given in Table 4.2).

Turkey adjusted BA08 model and original BA08 model median curves for magnitude 5 and magnitude 7 earthquakes at the rupture distance of 10 kilometers for V_{s30}=270 m/s and V_{s30}=760 m/s site conditions are presented in Figure 5.2. Again, Turkey adjusted model curves are shown with thick dash lines and original BA08 model is shown with thin solid lines. Figure 5.2 shows that the only difference between two models occurs at scenarios with M=5 for soil and rock site conditions since only magnitude correction up to hinge value of 6.75 is applied to BA08 model. Similar to AS08 model, Turkey adjusted BA08 model give almost the half values of median spectral acceleration values of original model. No significant change in attenuation shape is observed in adjusted model.

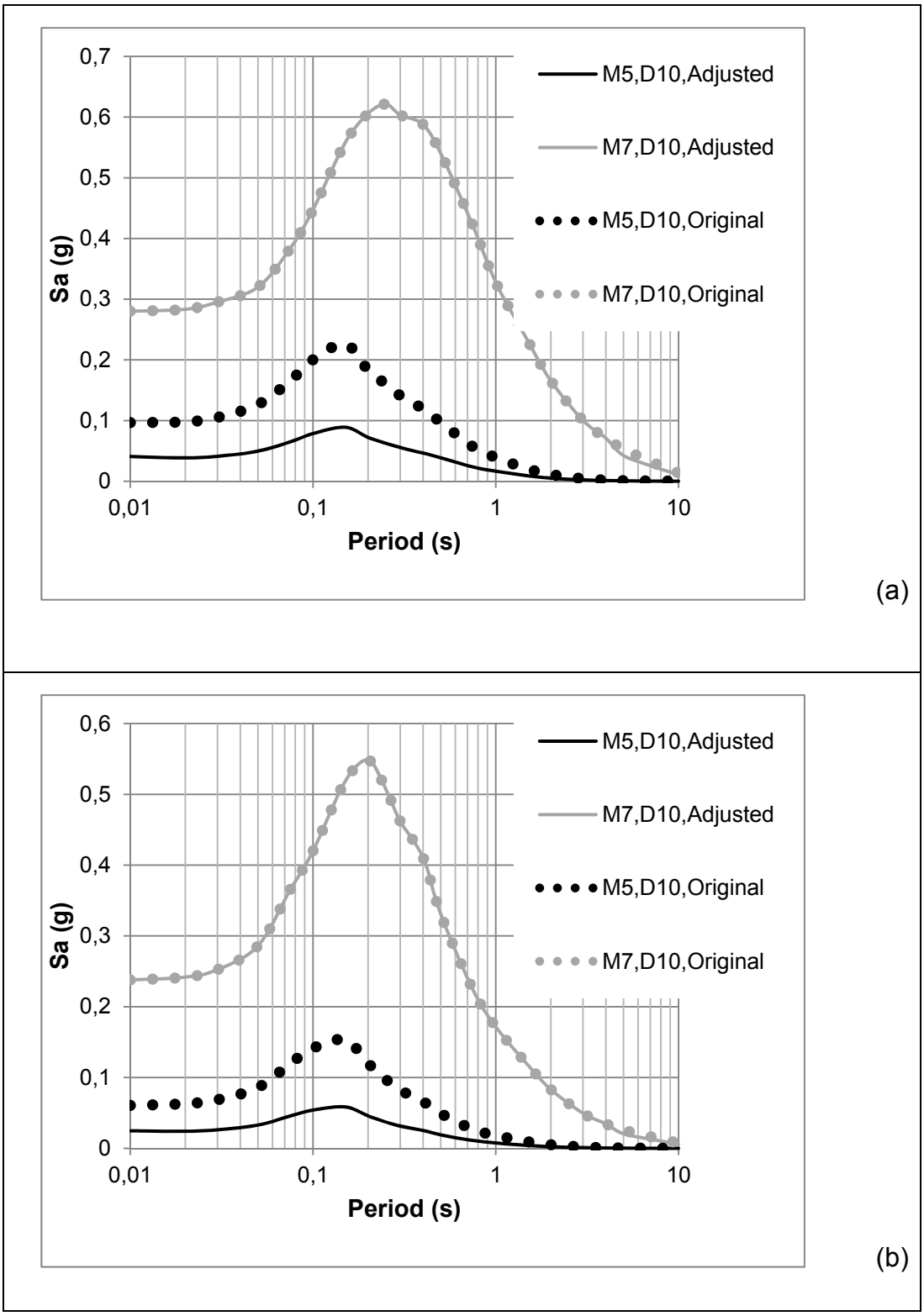

Figure 5.2 Turkey Adjusted and original BA08 model median predictions vs. Period for sites with a) V_{S30}=270 m/s, b) V_{S30}=760 m/s

Adjustment for CB08 model is conducted only for magnitude scaling term similar to BA08 model. Adjusted CB08 model is formulated as shown in Equation 5.8:

$$\ln \hat{Y} = f_{mag\_TA} + f_{dis} + f_{flt} + f_{hng} + f_{site} + f_{sed} \tag{5.8}$$

where f_{mag_TA} term is the magnitude scaling term of adjusted CB08 model. Magnitude scaling term is obtained by adding adjustment function to the original magnitude scaling term. Magnitude scaling term of adjusted model is given in Equation 5.9:

$$f_{mag\_TA} = f_{mag} + \begin{cases} c_{13} * (M - 6.50) \rightarrow for(M \leq 6.50) \\ 0 \rightarrow for(M > 6.50) \end{cases} \tag{5.9}$$

$$f_{mag} = \begin{cases} c_0 + c_1 M & M \leq 5.5 \\ c_0 + c_1 M + c_2(M - 5.5) & 5.5 < M \leq 6.5 \\ c_0 + c_1 M + c_2(M - 5.5) + c_3(M - 6.5) & M > 6.5 \end{cases} \tag{5.10}$$

where c_{13} is the new coefficient defined for adjusted CB08 model (See Table 4.2). Turkey adjusted CB08 model and original CB08 model median curves for magnitude 5 and magnitude 7 earthquakes at the rupture distance of 10 kilometers for V_{s30}=270 m/s and V_{s30}=760 m/s site conditions are presented in Figure 5.3. Again, Turkey adjusted model curves are shown with thick dash lines and original CB08 model is shown with thin solid lines. The characteristics for the adjusted BA08 model is observed in adjusted CB08 model since these two models are adjusted with the same modifications. Attenuation shape of the adjusted model shows similar aspects with original model, which signifies that applied modification did not create any distortion in the model.

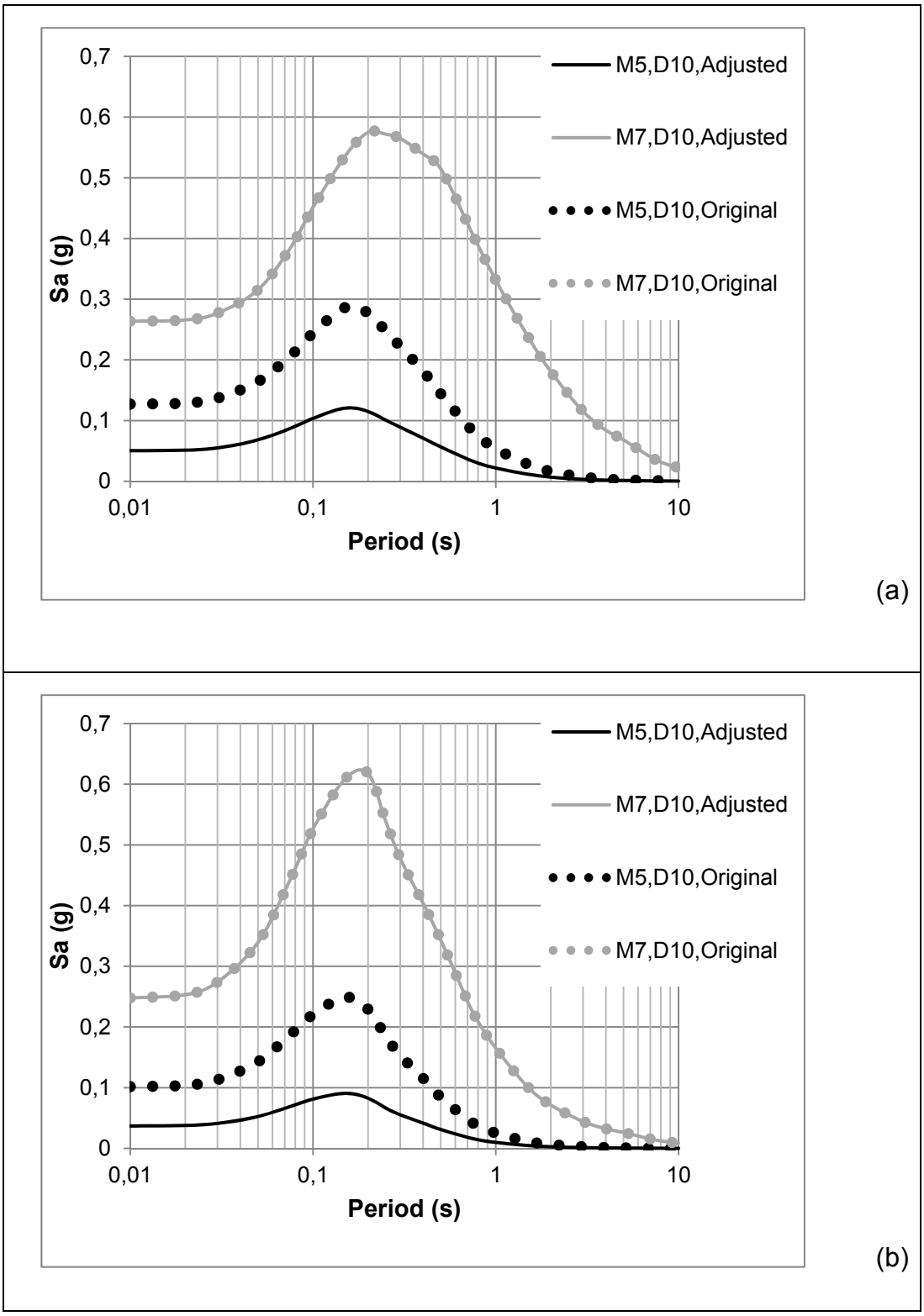

Figure 5.3 Turkey Adjusted and original CB08 model median predictions vs. Period for sites with a) V_{S30}=270 m/s, b) V_{S30}=760 m/s

Similar to AS08 model, adjustment functions were added to magnitude, distance and site effects terms of CY08 model. Median Turkey-Adjusted CY08 model is formulated as shown in Equation 5.11:

$$\ln(y_{ij}) = \ln\left(y_{ref_{ij}}\right) + \emptyset_1 * \min\left(\ln\left(\frac{V_{S30j}}{1130}\right), 0\right) + \emptyset_2\left(e^{\emptyset_3(\min(V_{S30j},1130)-360)} - e^{\emptyset_3(1130-360)}\right) * \ln\left(\frac{y_{ref_{ij}} e^{\eta_i+\emptyset_4}}{\emptyset_4}\right) + \emptyset_5\left(1 - \frac{1}{\cosh(\emptyset_6 * \max(0, Z_{1.0}-\emptyset_7))}\right) + \frac{\emptyset_8}{\cosh(0.15 * max(0, Z_{1.0}-15))} + \Delta f_{mag\_TA}(M) + \Delta\gamma + \Delta f_{site\_TA} \quad (5.11)$$

where $\Delta f_{mag\_TA}(M)$, $\Delta\gamma$ and Δf_{site_TA} are adjustment functions previously defined as:

$$\Delta f_{mag\_TA}(M) = \begin{cases} c_{ta}(M - 6.75) \rightarrow for(M \leq 6.75) \\ 0 \rightarrow for(M > 6.75) \end{cases} \quad (5.12)$$

$$\Delta\gamma = \begin{cases} 0 \rightarrow for(R_{rup} < 100) \\ c_{\gamma 4} * \left(R_{rup} - 100\right) \rightarrow for(R_{rup} \geq 100) \end{cases} \quad (5.13)$$

$$\Delta f_{site\_TA} = \begin{cases} 0 \rightarrow for(V_{S30} < V_{S30,hinge}(T)) \\ \phi_9 * ln(V_{S30}/V_{S30,hinge}(T)) \rightarrow for(V_{S30} \geq V_{S30,hinge}(T)) \end{cases} \quad (5.14)$$

where c_{ta}, $c_{\gamma 4}$, ϕ_9 and $V_{S30,hinge}(T)$ are new coefficients defined for adjusted CY08 model.

Turkey-adjusted CY08 model and original CY08 model median curves for magnitude 5 and magnitude 7 earthquakes at the rupture distance of 10 kilometers for V_{s30}=270 m/s and V_{s30}=760 m/s site conditions are presented in Figure 5.4. Turkey adjusted model curves are shown with thick dash lines and original CY08 model is shown with thin solid lines. Figure 5.4 shows that original and Turkey-adjusted curves are quite different in scenarios with magnitude 5. This result is expected since the magnitude adjustment is conducted up to the hinge magnitude of 6.75.

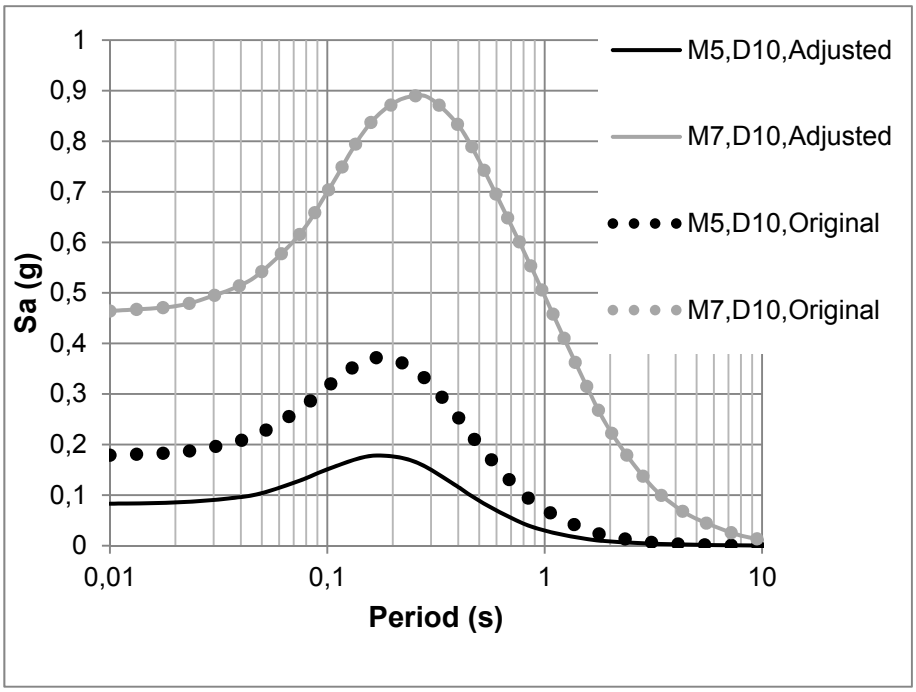

(a)

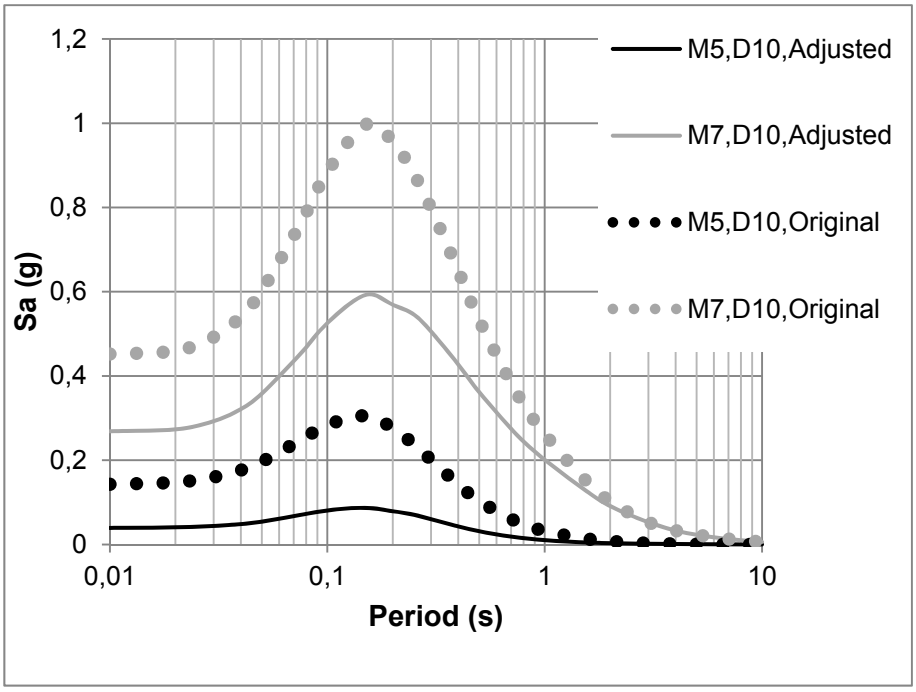

(b)

Figure 5.4 Turkey Adjusted and original CY08 model median predictions vs. Period for sites with a) V_{S30}=270 m/s, b) V_{S30}=760 m/s

For rock sites, original and Turkey-adjusted curves differ from each other for all scenarios due to the site effect term adjustment. Figure 5.4 implies that the Turkey-adjusted CY08 model has a similar spectral shape when compared to the original model which proves that the applied modifications did not create any distortion in the spectral shape.

Adjustment for ID08 model is conducted only for magnitude scaling term similar to BA08 and CB08 models. Adjusted ID08 model is formulated as shown in Equation 5.8:

$$\ln\big(PSA(T)\big) = \alpha_1(T) + \alpha_2(T)M - (\beta_1(T) + \beta_2(T)M)\ln\big(R_{rup} + 10\big) + \gamma(T)R_{rup} + \varphi(T)F + \Delta f_{mag\_TA} \quad (5.15)$$

where f_{mag_TA} term is the magnitude adjustment function previously defined as:

$$\Delta f_{mag\_TA} = \begin{cases} \alpha_3 * (M - 6.75) \rightarrow for(M \leq 6.75) \\ 0 \rightarrow for(M > 6.75) \end{cases} \quad (5.16)$$

where α_3 is new defined coefficient for adjusted ID08 model.

Turkey-adjusted ID08 model and original ID08 model median curves for magnitude 5 and magnitude 7 earthquakes at the rupture distance of 10 kilometers for V_{s30}=450 m/s and V_{s30}=760 m/s site conditions are presented in Figure 5.5. Turkey adjusted model curves are shown with thick dash lines and original ID08 model is shown with thin solid lines. It should be noted that, V_{S30} value is taken as 450 m/s for soil sites for this model, since Idriss (2008) restricted the applicability their model for V_{S30} ≥ 450 m/s. Again, the same observation with BA08 and CB08 models can be made for ID08 model since these models are adjusted to Turkish strong motion database using same modifications.

All Turkey adjusted NGA models are plotted on the same graph in Figure 5.6 for comparison.

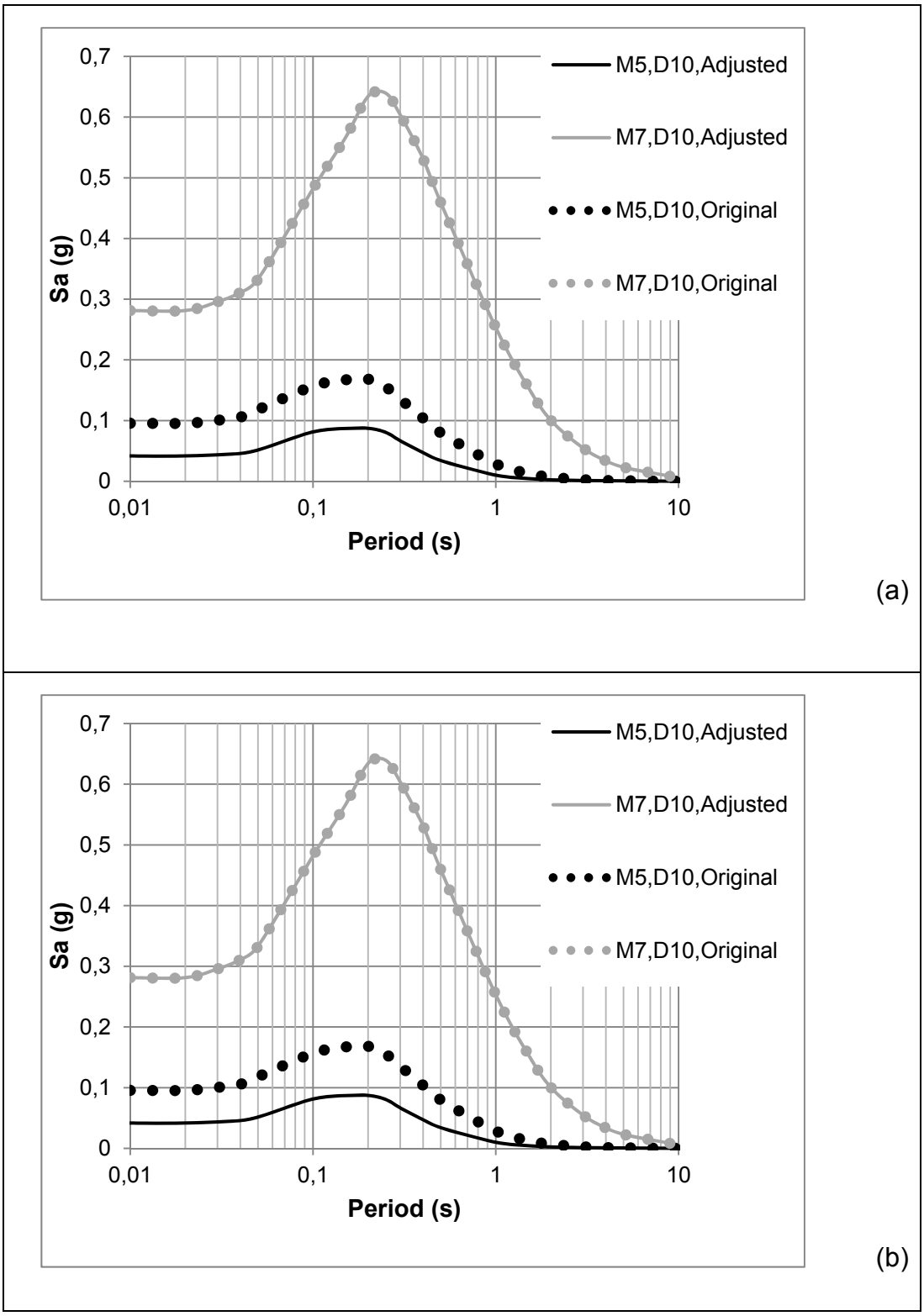

Figure 5.5 Turkey Adjusted and original ID08 model median predictions vs. Period for sites with a) V_{S30}=450 m/s, b) V_{S30}=760 m/s

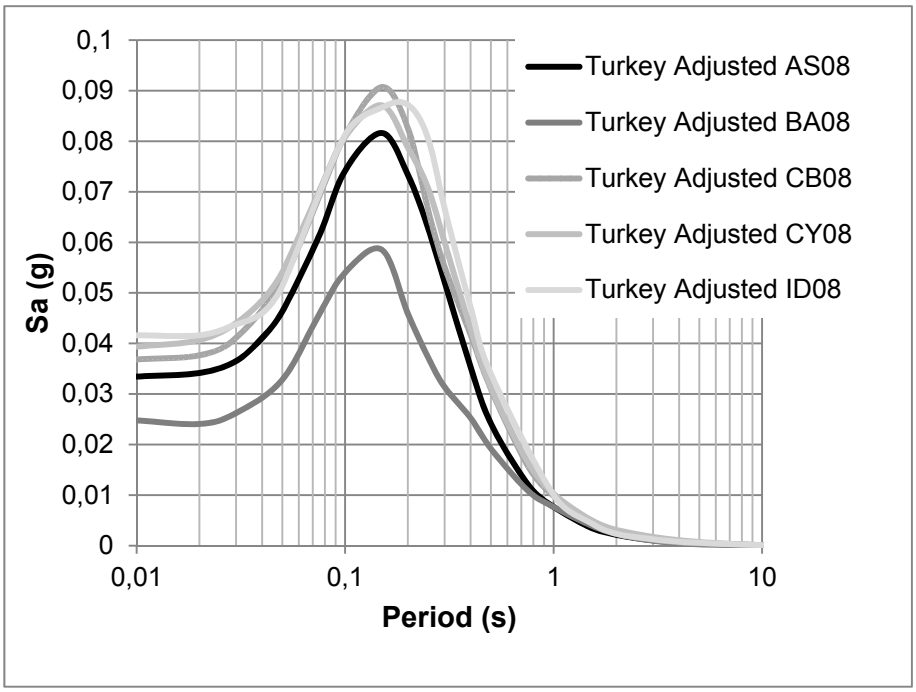

(a)

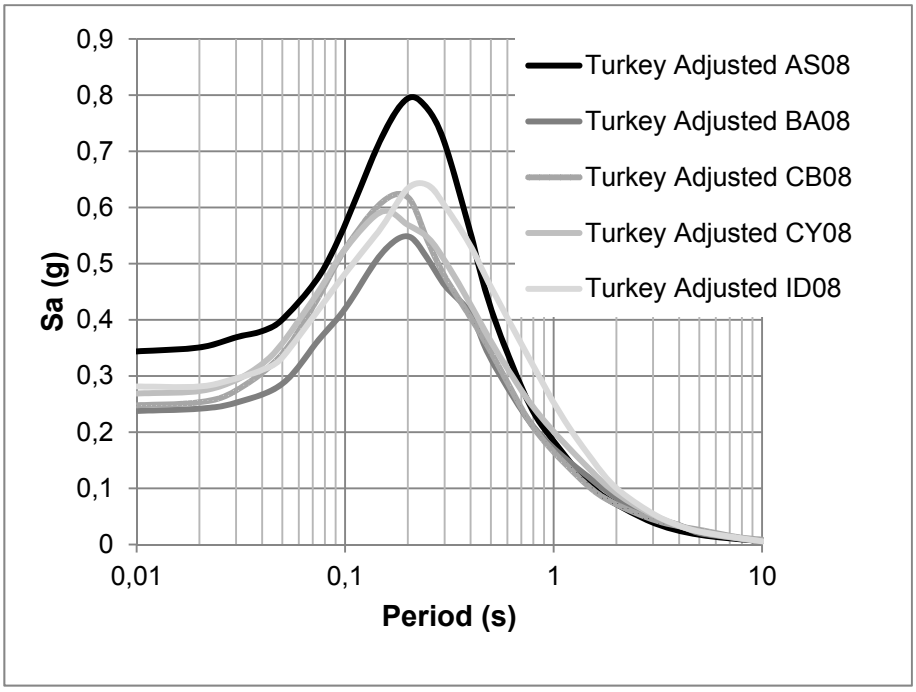

(b)

Figure 5.6 Turkey Adjusted NGA model median predictions vs. Period for scenarios with a) M=5.0; D=10 km; V_{S30}=270 m/s, b) M=7.0; D=10 km; V_{S30}=760 m/s

5.2 Comparison of Turkey Adjusted NGA-W1 Models with Turkish GMPEs

In this section, GMPEs proposed by Akkar and Çağnan (2010) (AC10) are compared with Turkey-Adjusted AS08 model and Kalkan and Gülkan (2004) (KG04) are compared with Turkey-Adjusted BA08 model since these models have similar functional forms. AC10 model is based on the TSMD database; therefore similar results are expected at small magnitudes and soft soil sites. Turkey-Adjusted AS08 model vs. AC10 model and Turkey-Adjusted BA08 model vs. KG04 model median curves for magnitude 5 and magnitude 7 earthquakes at the rupture distance of 10 kilometers for V_{s30}=270 m/s and V_{s30}=760 m/s site conditions are plotted in Figure 5.7 and 5.8, respectively. Turkey adjusted AS08 and BA08 model predictions are shown with solid lines and AC10 and KG04 model predictions are shown with dashed lines.

From Figure 5.7, it can be observed that for scenarios with M=5.0, two models gave almost the same spectral acceleration values. But same statement cannot be made for scenarios with M=7.0. For these scenarios, Turkey adjusted AS08 model gave significantly higher median spectral acceleration values from AC08 model. This difference is a result of magnitude correction we applied to NGA-W1 models. For all models, magnitude correction is conducted up to a hinge value which is at most M=6.75. Since there exist significantly low number of events at large magnitudes (only 2 events) and relatively low residuals with respect to small magnitudes, correction for large magnitude is not conducted. This application results in difference between two models at large magnitudes. Turkey adjusted BA08 model give similar spectral acceleration values with respect to KG04 model. But at small magnitude events, KG04 model overestimates the values significantly with respect to Turkey adjusted BA08 model.

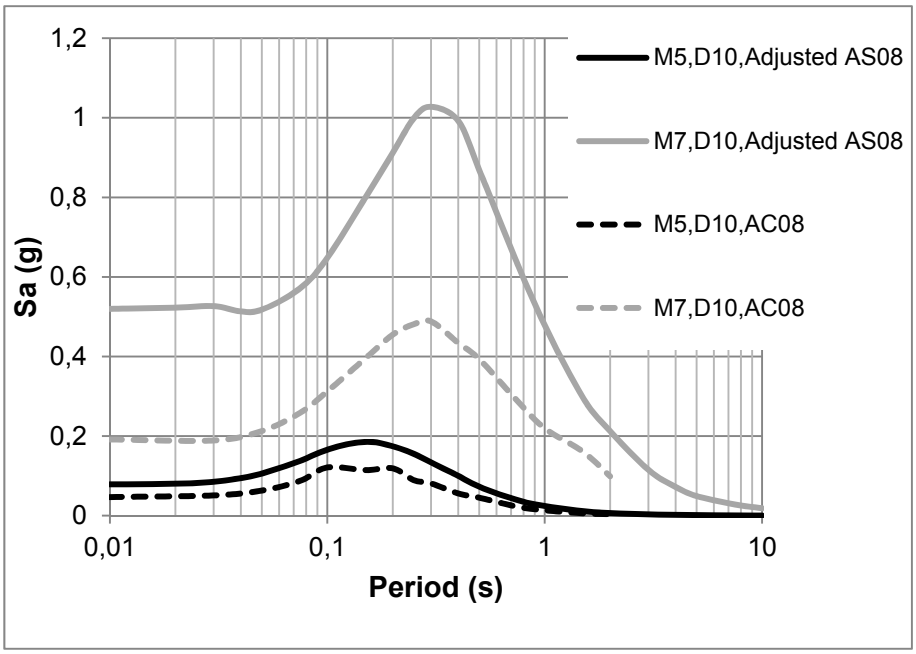

(a)

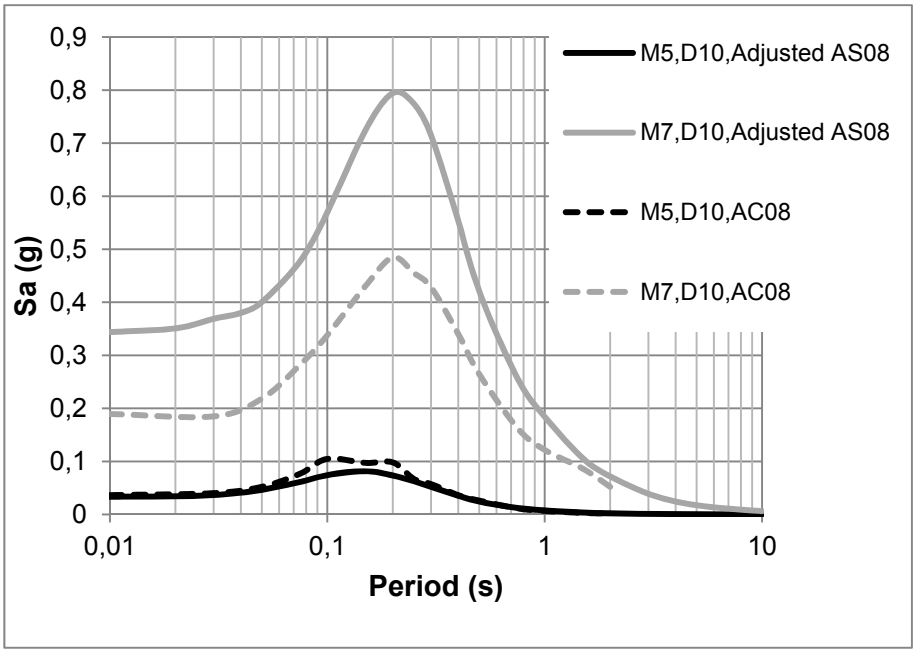

(b)

Figure 5.7 Turkey Adjusted AS08 and Akkar and Çağnan (2010) model median predictions vs. Period for sites with a) V_{S30}=270 m/s, b) V_{S30}=760 m/s

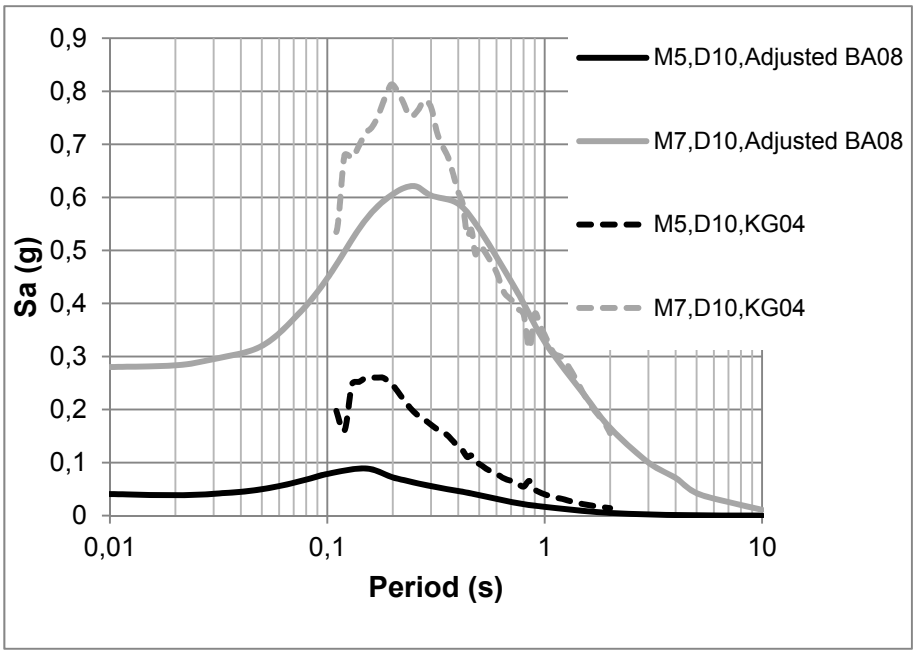

(a)

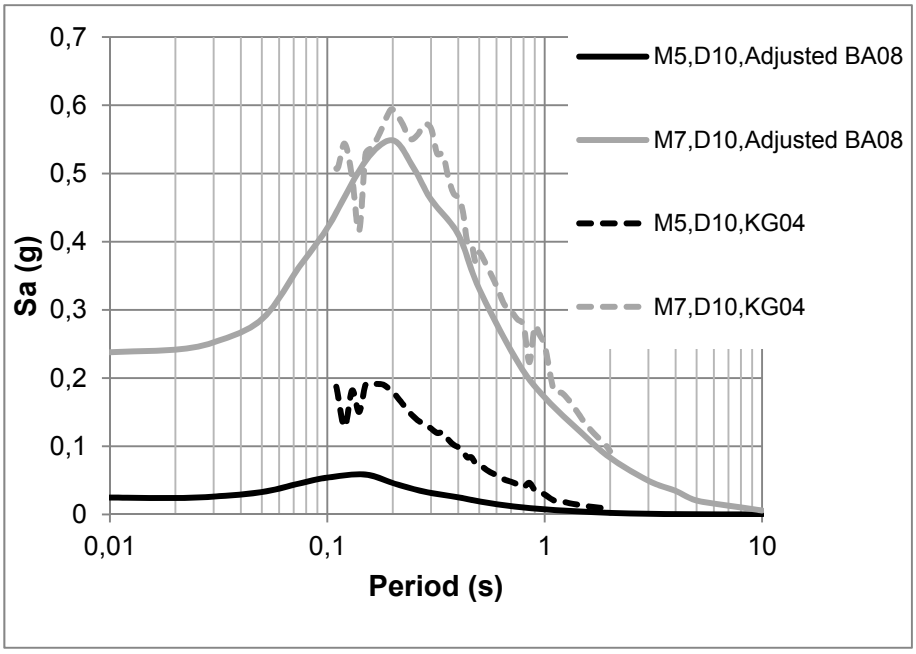

(b)

Figure 5.8 Turkey Adjusted AS08 and Kalkan and Gülkan (2004) model median predictions vs. Period for sites with a) V_{S30}=270 m/s, b) V_{S30}=760 m/s

5.3 Future Aspects

The work described here will be the first study that adjusts global GMPEs to Turkey. Considering the methodology applied for adjustment and the extent of conducted adjustments, it is also the first comprehensive worldwide on this particular issue. It is expected that this study will set a precedent for the adjustment works that will conducted for different tectonic regions.

Nevertheless, the most important missing aspect this study is the standard deviation values of the adjusted models to be used in PSHA. The standard deviations of the adjusted models are at the stage of calculation. Secondly, small magnitude earthquakes (M<4) and large distance recordings (R_{rup} >100) in the database might require additional adjustments. Also style of faulting effects is not inspected in this study as the majority of the events in the database consist of strike slip earthquakes (65-70%). Future earthquakes with different style of faulting may help the adjustment of style of faulting and hanging wall effects.

REFERENCES

Abrahamson, N. A., Youngs R. R. (1992). A stable algorithm for regression analyses using the random effects model, Bull. Seismol. Soc. Am. 82: 505–510.

Abrahamson, N. A., Silva, W. J. (1997). Empirical response spectral attenuation relations for shallow crustal earthquakes. *Seismological Research Letters*, 68:94–127.

Abrahamson, N. A., Silva, W. J. (2008). Summary of the Abrahamson and Silva NGA ground motion relations, Earthq. Spectra 24:67–97.

Abrahamson, N. A., Atkinson, G. M., Boore, D. M., Bozorgnia, Y., Campbell, K. W., Chiou, B., Idriss, I. M., Silva, W., and Youngs, R. (2008). Comparisons of the NGA ground-motion relations*, Earthquake Spectra,* 24:45–66.

Akkar, S., Bommer, J.J. (2006) Influence of long-period filter cut-off on elastic spectral displacements. Earthq. Eng. Struct. Dyn. 35:1145–1165

Akkar, S., & Çağnan, Z. 2010. A local ground-motion predictive model for Turkey and its comparison with other regional and global ground-motion models. *Bulletin of the Seismological Society of America*, 100(6), 2978–2995.

Akkar, S., Çağnan, Z., Yenier, E., Erdoğan, Ö., Sandıkkaya, A., Gülkan, P. (2010) The recently compiled Turkish strong motion database: preliminary investigation for seismological parameters, J. Seismol. 14:457– 479

Ambraseys, N., Durukal, E., Free, M. (1993) Re-evluation of strong-motion data in Tukey. ESEE research report, No. 93/2. Imperial College of Science, Technology and Medicine, Civil Engineering Department, London

Ambraseys, N., Smit, P., Berardi, R., Rinaldis, D., Cotton, F., Berge-Thierry, C. (2000) Dissemination of European strong-motion data. CD-ROM collection, European Commission, Directorate General XII, Science, Research and Development, Environment and Climate Programme, Bruxelles

Ambraseys, N., Douglas, J., Sigbjornsson, R., Berge-Thierry, C., Suhadolc, P., Costa, G., Smit, P.M. (2004) Dissemination of European strong motion data volume 2. In: Proceedings of 13th world conference on earthquake engineering, Vancouver, BC, Canada, 1–6 August 2004, paper no. 32

Anderson, J. G. (2003). Strong motion seismology, in *International Handbook of Earthquake and Engineering Seismology*, W. H. K. Lee, H. Kanamori, P. C. Jennings, and C. Kisslinger (Editors), Academic Press, New York, Part B, ch. 57, pp. 937-965.

Ateş, R.C., Bayülke, N. (1982) The 19 August 1976 Denizli, Turkey, earthquake: evaluation of the strong motion accelerograph record, *Bull. Seismol. Soc. Am.* 72:1635– 1649

Aydan O, Hasgür Z (1997) The characteristics of acceleration waves of Turkish earthquakes. *In: Proceedings of the 4th national confeernce on earthquake engineering, Ankara, Turkish National Committee of Earthquake Engineering*, pp 30–37 (in Turkish)

Baker, J. W., and Cornell, C. A., 2006. Which spectral acceleration are you using?, *Earthquake Spectra* **22**, 293–312.

Bolt, B. A., and Abrahamson, N. A., (2003). Estimation of strong seismic ground motions, in *International Handbook of Earthquake and Engineering Seismology*, W. H. K. Lee, H. Kanamori, P. C. Jennings, and C. Kisslinger (Editors), Academic Press, New York, Part B, ch. 59, pp. 983–1001.

Boore, D.M., Joyner, W.B., Fumal, T.E. (1997) Equations for estimating horizontal response spectra and peak acceleration from western North American earthquakes: a summary of recent work, *Seismol. Res. Lett.* 68: 128–153

Boore, D. M., and Bommer, J. J., (2005). Processing of strong-motion accelerograms: Needs, options and consequences, *Soil Dyn. Earthquake Eng.* **25**, 93–115.

Boore, D. M., Watson–Lamprey, J., Abrahamson, N. A. (2006). Orientation-independent measures of ground motion, *Bull. Seismol. Soc. Am*. 96, no. 4a, 1502–1511.

Boore, D. M., Atkinson, G. M. (2008). Ground motion prediction equations for the average horizontal component of PGA, PGV, and 5%- damped PSA at spectral periods between 0.01 and 10.0 s, *Earthq. Spectra* 24: 99–138.

Boore, D. M., Aida, A. S., Akkar, S. (2012) Using Pad-Stripped Acausally Filtered Strong-Motion Data

Brillinger, D. R., Preisler, H. K. (1984). An exploratory analysis of the Joyner-Boore attenuation data, *Bull. Seism. Soc. Am.* 74:1441-1450

Brillinger, D. R., Preisler, H. K. (1985). Further analysis of the Joyner-Boore attenuation data, *Bull. Seism. Soc. Am.* 75:611-614

Campbell, K.W. (1997) Empirical near-source attenuation relationships for horizontal and vertical components of peak ground acceleration, peak ground velocity, and pseudo-absolute acceleration response spectra, *Seismol. Res. Lett*. 68:154–179

Campbell, K. W., & Bozorgnia, Y. 2003a. Erratum: Updated near-source ground-motion (attenuation) relations for the horizontal and vertical components of peak ground acceleration and acceleration response spectra. *Bulletin of the Seismological Society of America*, 93(3), 1413.

Campbell, K. W., & Bozorgnia, Y. (2003b). Erratum: Updated near-source ground-motion (attenuation)relations for the horizontal and vertical components of peak ground accelerationand acceleration response spectra. *Bulletin of the Seismological Society of America*, 93(4), 1872.

Campbell, K. W., & Bozorgnia, Y. (2003c). Erratum: Updated near-source ground-motion (attenuation)relations for the horizontal and vertical components of peak ground accelerationand acceleration response spectra. *Bulletin of the Seismological Society of America*, 94(6), 2417.

Campbell, K. W., & Bozorgnia, Y. (2003d). Updated near-source ground-motion (attenuation)relations for the horizontal and vertical components of peak ground acceleration and accelerationresponse spectra. *Bulletin of the Seismological Society of America*, 93(1), 314–331.

Campbell, K. W., Bozorgnia, Y. (2008). NGA ground motion model for the geometric mean horizontal component of PGA, PGV, PGD, and 5%-damped linear elastic response spectra for periods ranging from 0.01 to 10 s, *Earthq. Spectra* 24:139–171.

Chiou, B., Darragh, R., Gregor, N., Silva, W. (2008) NGA project strong-motion database. *Earthq. Spectra* 24:23–44

Chiou, B. S. J., Youngs, R. R. (2008). An NGA model for the average horizontal component of peak ground motion and response spectra, *Earthq. Spectra* 24:173–215.

Converse, A. M., and A. G. Brady (1992). BAP: basic strong-motion accelerogram processing software, version 1.0, *U.S. Geol. Surv. Open-File Rept. 92-296A*, 174 pp.

Çelebi M, Akkar S, Gülerce U, S¸ anlı A, Bundock H, Salkın A (2001) Main shock and aftershock records of the 1999 ˙Izmit and Düzce, Turkey earthquakes. USGS/OFDA Project (USGS Project No.: 1-7460- 63170), USGS Open-File Report 01-163

Douglas, J. (2003) What is a poor quality strong-motion record? *Bull. Earthq. Eng.* 1:141–156

Durukal E, Alpay Y, Biro T, Mert A, Erdik M (1998) Analysis of strong motion data of the 1995 Dinar, Turkey earthquake, second Japan–Turkey workshop: earthquake disaster prevention research in Turkey, 23–25 February 1998, Technical University of ˙Istanbul

Erdik, M. (1984) Report on the Turkish earthquake of October 30, 1983. Earthq Spectra 1:151–172

Erdik M, Durukal E (2001) 1999 Kocaeli and Düzce, Turkey earthquakes: strong-ground motion, XV ICSMGE TC4 'Lessons learned from recent strong earthquakes, 25 August 2001, İstanbul, Turkey

Frohlich, C., Apperson, K.D. (1992) Earthquake focal mechanisms, moment tensors, and the consistency of seismic activity near plate boundaries, *Tectonics* 11: 279–296

Gardner, J. K. and L. Knopoff (1974). Is the sequence of earthquakes in southern California, with aftershocks removed, Poissonian? *Bull. Seism. Soc. Am.* 64, 1363-1367.

Gülkan, P. (2010) The Turkish national accelerometric network: 1973-2010, in Earthquake Data in Engineering Seismology, S. Akkar, P. Gülkan and T.V. Eck (editors), Springer, Netherlands, ch. 14, pp. 199-218.

Gulkan, P., & Kalkan, E. (2002). Attenuation modeling of recent earthquakes in Turkey. *Journal of Seismology*, 6(3), 397–409.

Idriss, I. M. (1993). Procedures for selecting earthquake ground motions at rock sites. *Tech. rept. NIST GCR 93-625. National Institute of Standards and Technology*.

Idriss, I. M. (2008). An NGA empirical model for estimating the horizontal spectral values generated by shallow crustal earthquakes, Earthq. Spectra 24:217–242.

Inan E., Çolakoğlu, Z., Koç, N., Bayülke, N., Çoruh, E. (1996) Earthquake catalogs with acceleration records from 1976 to 1996. General Directorate of Disaster Affairs, Earthquake Research Department, Ankara, Turkey, 98 pp (in Turkish)

Iwan, W.D., ed. (1978). *Strong-Motion Earthquake Arrays*. Proceedings of the International Workshop on Strong-Motion Arrays, May 2–5, 1978, Honolulu, Hawaii. Pasadena: California Institute of Technology.

Joyner, W. B., Boore, D. M., (1993) Methods for regression analysis of strong-motion data, Bull. Seismol. Soc. Am. 83:469–487

Kalkan, E., & Gulkan, P. (2004a). Empirical attenuation equations for vertical ground motion in Turkey. *Earthquake Spectra*, 20(3), 853–882.

Kalkan, E., & Gulkan, P. (2004b). Site-dependent spectra derived from ground motion records in Turkey. *Earthquake Spectra*, 20(4), 1111–1138.

Kalkan, E., & Gulkan, P. (2005). Erratum: Site-dependent spectra derived from ground motion records in Turkey. *Earthquake Spectra*, 21(1), 283.

Kramer, S. 1996. Geotechnical Earthquake Engineering. Prentice- Hall, Upper Saddle River, NJ, USA.

Lin, P., Lee, C., Chiou, B., Cheng, C., Chern, J., (2007). A study of applicability of NGA models in Taiwan, Taiwan Geosciences Assembly, May 15-18, 2007, Longtan

Ozbey, C., Sari, A., Manuel, L., Erdik, M., & Fahjan, Y. 2004. An empirical attenuation relationship for northwestern Turkey ground motion using a random effects approach. *Soil Dynamics and Earthquake Engineering*, 24(2), 115–125.

Power, M., Chiou, B., Abrahamson, N., Bozorgnia, Y., Shantz, T., and Roblee, C., 2008. An overview of the NGA project, *Earthquake Spectra* 24(1), 3–21.

Rathje EM, Stokoe KH II, Rosenblad BL (2003) Strongmotion station characterization and site effects during the 1999 earthquakes in Turkey. Earthq Spectra 19:653–676

Sadigh, K., Chang, C.Y., Egan, J.A., Makdisi, F., Youngs, R.R. (1997) Attenuation relationships for shallow crustal earthquakes based on California strong motion data, Seismol. Res. Lett. 68:180–189

Sandıkkaya, M.A. (2008) Site classification of national strong-motion recording sites. MSc thesis, Civil Engineering Department, Middle East Technical University, Ankara

Scasserra, G., Stewart, J. P., Bazzurro, P., Lanzo, G., and Mollaioli, F., 2009. A comparison of NGA ground motion prediction equations to Italian data, *Bulletin of the Seismological Society of Americ*a 99, 2961–2978.

Shoja-Taheri, J., Naserieh, S., and Ghofrani, H., 2010. A test of the applicability of NGA models to the strong ground motion data in the Iranian Plateau, *Journal of Earthquake Engineering* 14, 278–292.

Stafford, P. J., Strasser, F. O., Bommer, J. J (2008). An evaluation of the applicability of the NGA models to ground motion prediction in the Euro-Mediterranean region, *Bull. Earthq. Eng*. 6, 149–177.

Ulusay, R., Tuncay, E., Sonmez, H., & Gokceoglu, C. (2004). An attenuation relationship based on Turkish strong motion data and iso-acceleration map of Turkey. *Engineering Geology*, 74(3-4), 265–291.

Wells, D.L., Coppersmith, K.J. (1994) New empirical relationships among magnitude, rupture length, rupture width, rupture area, and surface displacement. Bull. Seismol. Soc. Am. 84:974–1002

Yılmaz, Ö., Savaşkan, E., Bakır, B.S., Yılmaz, M.T., Eser, M., Akkar, S., Tüzel, B., İravul, Y., Özmen, Ö.T., Denizlioğlu, A.Z., Alkan, A., Gürbüz, M. (2008) Shallow seismic and geotechnical site surveys at the Turkish national grid for strong-motion seismograph stations. In: *14th World Conference on Earthquake Engineering*, Beijing

Yunatcı, A. A. (2010). GIS based seismic hazard mapping of Turkey, Ph.D. Thesis, Middle East Technical University.

Zaré, M., Bard, P.Y. (2002) Strong motion dataset of Turkey: data processing and site classification. Soil. Dyn. Earthqu. Eng. 22:703–718